Ferdowsi University of Mashhad

ISSN 2008-9147
Numbers: 19

JCMR

Journal of Cell and Molecular Research

Volume 10, Number 1, Summer 2018

بسم الله الرحمن الرحيم

Issuance License No. 124/902-27.05.2008 from Ministry of Culture and Islamic Guidance
Scientific Research Issuance License No. 161675 from the Ministry of Science, Research and Technology, Iran

Journal of Cell and Molecular Research (JCMR)

Volume 10, Number 1, Summer 2018

Copyright and Publisher
Ferdowsi University of Mashhad

JCMR Office: Department of Biology, Faculty of Sciences, Ferdowsi University of Mashhad, Mashhad, Iran.
Postal Code: 9177948953
P.O. Box: 917751436
Tel: +98-513-8804063
Fax: +98-513-8795162
E-mail: jcmr@um.ac.ir
Online Submission: http://jcmr.fum.ac

Table of Contents

Evaluating the Effect of Eugenol on the Expression of Genes Involved in the Immunomodulatoty Potency of Mouse Mesenchymal Stem Cells In Vitro 1
Maryam Yazdani, Ali Bidmeshkipour, Sajjad Sisakhtnezhad

Polyurethane/Hydroxyapatite Induces MSCs towards Osteo-like Cells in a Similar Fashion to Demineralized Bone Matrix 11
Mostafa Shahrezaei, Mohamad Moosaee

Global Analysis of Gene Expression and Identification of Modules in Echinacea purpurea Using Systems Biology Approach 18
Ahmad Tahmasebi, Farzaneh Aram, Hassan Pakniyat, Ali Niazi, Elahe Tavakol, Esmaeil Ebrahimie

Investigation of coa Gene Polymorphism in Clinical Isolates of Staphylococcus aureus in North of Iran 27
Mohammad Reza Izadpanah, Leila Asadpour

Desaturase Genes Expression and Fatty Acid Composition of Pleurotus ostreatus in Response to Zinc and Iron 32
Kamran Safavi, Gholamreza Kavoosi, Roghayeh Siahbalaei

MicroRNA-mediated Resistance to Plant Viruses 40
Amir Ghaffar Shahriari, Aminallah Tahmasebi

A Novel Signal Peptide Derived from Bacillus Licheniformis α-Amylase Efficiently Targets Recombinant Human Activin A to the Periplasm of Escherichia coli 47
Zahra Hajihassan, Seyed kazem Hosseini, Alireza Zomorodipour

Journal of Cell and Molecular Research (2018) 10 (1), 1-10 DOI: 10.22067/jcmr.v10i1.70380

Research Article

Evaluating the Effect of Eugenol on the Expression of Genes Involved in the Immunomodulatoty Potency of Mouse Mesenchymal Stem Cells In Vitro

Maryam Yazdani, Ali Bidmeshkipour*, Sajjad Sisakhtnezhad*

Department of Biology, Faculty of Science, Razi University, Kermanshah, Iran

Received 21 January 2018 Accepted 1 September 2018

Abstract

The immunomodulatory ability of mesenchymal stem cells (MSCs) has attracted interest as a unique property that makes them interesting tools for the treatment of inflammatory and autoimmune diseases. Eugenol is a volatile compound from the phenylpropanoids class of chemical compounds. Despite extensive investigations on the biological and pharmacological properties of Eugenol, its effect on stem cells, especially, on MSCs remains to be clarified. Therefore, this study was designed to evaluate the effect of Eugenol on the expression of genes (*Tlr3*, *Tlr4*, *Ccl2,* and *Ccl3*) involved in immunomodulatory potency of mouse bone-marrow derived MSCs by quantitative real-time PCR (qRT-PCR). To do so, MSCs were isolated from 4-8 weeks old mouse bone marrow (BM). The effect of Eugenol on the viability of BM-MSCs was evaluated by MTT assay at 24, 48, and 72h after treatment. The results showed that Eugenol reduced the number of BM-MSCs in a dose- and time-dependent manner. In addition, the half maximum inhibitory concentration of Eugenol on MSCs was 400µg/ml at 24 and 48h and 200µg/ml at 72h after treatment. Moreover, about 90% of MSCs were alive at the concentration of 12.5µg/ml 24h after treatment. The qRT-PCR results indicated that *Tlr3*, *Tlr4*, and *Ccl3* genes were up-regulated 1.6-, 1.8-, and 2.2-fold, respectively, in Eugenol-treated BM-MSCs compared to untreated controls (Fold change > 1.5; P ≤0.05). In conclusion, we suggest that Eugenol may somewhat regulate the immunomodulatory potency of MSCs and thus this study provides a background for further studies on the effect of Eugenol on MSCs characteristics and functions, which may finally improve their potency for cell-based therapy applications.

***Keywords*:** Eugenol, Mesenchymal stem cells, Immunomodulatory potency, Mouse

Introduction

Mesenchymal stem cells, or MSCs, are multipotent stromal cells, which have received considerable attention in clinical cell-based therapies during the past decade. MSCs are easily isolated from various fetal and adult tissues (Hass et al., 2011; Huang et al., 2014; Savickiene et al., 2015; Wang et al., 2015). They have also remarkable self-renewal, migratory and immunomodulatory potentials and can differentiate into a variety of cell types (Zhao et al., 2016; Sisakhtnezhad et al., 2017). In addition to producing and secreting various factors, increasing evidence has also suggested that the main therapeutic potential of MSCs results from their immunomodulatory activity. Interestingly, MSCs show flexible immunomodulatory functions and they have two immunomodulatory phenotypes, pre-inflammatory (MSC1) or anti-inflammatory (MSC2) phenotypes, which have the immunoactivatory and immunosuppressive ability, respectively. MSCs can also switch from immunosuppressive to immunoactivatory phenotype (Zhao et al., 2016). Recent studies have been indicated that the immunomodulatory potency of MSCs is controlled by inflammatory factors in vivo (Ma et al., 2014). It has been shown that inflammatory environment induces or suppresses the expression of a large number of chemokines, cytokines, adhesion molecules and their correspondence receptors such as CXCRs ligands, CCRs ligands, intercellular adhesion molecule -1 (ICAM-1) and vascular cell adhesion molecule -1 (VCAM-1) (Ren et al., 2008; Ren et al., 2010). Renner et al., reported that low levels of inflammatory factors induce immunosuppressive properties of MSCs, while high levels of inflammation promote the immunoactivatory potential of MSCs (Renner et al., 2009). This conceptual change has crucial implications for the clinical applications of MSCs. Therefore, there is attention to new strategies to induce pre-inflammatory (MSC1) or anti-inflammatory phenotypes (MSC2) of MSCs to affect the immune system for treating human diseases, such as cancer

*Corresponding authors E-mail: abidmeshki@razi.ac.ir; s.sisakhtnezhad@razi.ac.ir

and autoimmune diseases. It also suggests that the immunomodulatory potency of MSCs may purposefully alter by adding the influential external factors in the cell culture medium.

Today, natural products, especially herbal active ingredients, as an alternative to chemical drugs have received considerable attention to prevent and treat a range of human diseases. Eugenol is a volatile compound in the essential oils of some plants. Some in vitro and in vivo studies have demonstrated the widespread pharmacological effects of Eugenol. In this regard, it was reported that Eugenol has a wide range of anti-microbial, anti-oxidant, anti-inflammatory, immunomodulatory, anti-nociceptive, anti-tumourigenic, anti-genotoxic and neuroprotective effects (Ito et al., 2005; Raghavenra et al., 2006; Singh et al., 2007; Bachiega et al., 2012; Kamatou et al., 2012). Despite the well-known biological and pharmacological capabilities of Eugenol, its effect on the characteristics and function of stem cells, especially MSCs, remains to be studied and clarified. Given the importance of immunomodulatory potency of MSCs in cell-based therapy applications and extensive biological and pharmaceutical effects of Eugenol, this study, for the first time, was aimed to evaluate the effect of Eugenol on the expression of genes involved in the immunomodulatory potency of the mouse BM-derived MSCs in vitro.

Materials and Methods

Isolation and culture of mouse BM-MSCs

For the derivation of mouse MSCs, 4-8 weeks old NMRI mice were obtained from the Laboratory of Cell & Developmental Biology at Razi University (Kermanshah, Iran). Isolation of MSCs from mouse bone marrow (BM) was carried out under the approval (permit number 395-1-111) and the bioethics guidelines of the Deputy Research of Razi University. In the current study, cervical dislocation method was used to kill mice. Consequently, BM was isolated and collected from the tibias and femurs of mice. The BM from one animal were cultured in a T25 flask in the presence of Dulbecco's modified Eagle's medium (DMEM) (Gibco, Scotland) containing 15% (v/v) fetal bovine serum (FBS) (Gibco, Scotland), 2mM L-glutamine, and 1x penicillin-streptomycin (Pen-Strep) (Bioidea, Iran) at 37ºC and 5% CO_2. After 72h, the cell culture medium was replaced to remove unattached cells. The cultured cells of BM were reached to confluency after 7-10 days. The confluent primary culture of BM cells was then trypsinised by trypsin-EDTA (0.25%-1mM) (Bioidea, Iran) and the sub-cultured cells were incubated under previous conditions. Finally, the obtained cells in passage 3 were used for following studies.

Characterization of BM-MSCs

Phenotypic characterisation of MSCs by Flow-cytometry

The BM-MSCs were detached by 0.25% trypsin-1mM EDTA. After centrifugation, result pellet was solved in phosphate-buffered saline (PBS) and then 1×10^6 cells were used for flow-cytometry analysis. The phenotypic characterization of cells was carried out on a FACS Caliber for the presence of mesenchymal stem cell markers CD44, CD90, CD105 and hematopoietic marker CD45 and CD34.

Differentiation of MSCs to adipocytes in vitro

MSCs at third passage were cultured in an adipogenic medium composed of DMEM supplemented with 10% FBS, vitamin C (50 µg/ml) (Sigma, Germany), dexamethasone (1×10^{-3} µmol/ml) (Osvah, Iran), indomethacin (50 µg/ml) (Sigma, Germany) and 0.1 x Pen-Strep. After 21 days, the differentiation of MSCs into adipocytes was confirmed by Oil-red O (Acros, USA) staining.

Differentiation of MSCs to osteoblasts in vitro

To induce differentiation of BM-MSCs to osteoblasts, cells were cultured in an osteogenic medium containing DMEM supplemented with 10% FBS, vitamin C (50 µg/ml), dexamethasone (1×10^{-3} µmol/ml), β-sodium glycerolphosphate (10 mM) (Sigma, Germany) and 0.1 x Pen-Strep for 21 days. Consequently, the differentiation of MSCs into osteoblasts was investigated by Alizarin-red S (Acros, USA) staining.

The effect of Eugenol on BM-MSCs viability

BM-MSCs were cultured in 96-well plates at 8×10^3 cells per well and incubated at 37ºC and 5% CO_2 overnight. Consequently, Eugenol at concentrations of 12.5, 25, 50, 100, 200, 400, 800, 1600, 3200 µg/ml was added to each well. To evaluate the cytotoxicity effect of Eugenol, the tetrazolium-based colourimetric assay was used at 24, 48, and 72h after treatments. To do so, 3-(4,5-Dimethylthiazol-2-yl)-2,5-diphenyltetrazolium bromide (MTT) (Sigma, Germany) solution at the concentration of 5 mg/ml was added to each well and incubated at 37ºC and 5% CO_2 for 4h. The MTT salt was cleaved by mitochondrial enzymes of metabolically active cells and produced purple formazan crystals. The resulting crystals were

solubilised with 150 µl of dimethyl sulfoxide (DMSO) and the absorption of the solution was then measured at 570 nm in an ELISA reader. MTT assay was carried out at least in triplicate and the percentages of living cells against the controls were calculated by the following equation for each treatment:

Cell viability (%) = The mean absorbance of Eugenol-treated cells in each well / The mean absorbance of control cells × 100

Morphological evaluation

BM-MSCs in passage 3 were cultured in 6-well plates at 0.5×10^6 cells per well and incubated at 37ºC and 5% CO_2 overnight. Cells were then treated with different concentrations of Eugenol and morphological changes were evaluated under an inverted microscope 24h after treatments.

Gene expression analysis

The effect of Eugenol on the immunomodulatory potential of MSCs was investigated by evaluating the expression of *Tlr3*, *Tlr4*, *Ccl2,* and *Ccl3* genes using real-time PCR. To evaluate the effect of Eugenol on the expression of the genes in BM-MSCs, first, the half maximal inhibitory concentration (IC_{50}) of Eugenol was determined 24h after treatment. BM-MSCs were then treated with Eugenol at IC_{50} for 24h. Consequently, total RNA was extracted from the Eugenol-treated and control BM-MSCs using RNX-Plus reagent (SinaClon, Iran). The RNA samples were then treated with RNase-free DNase I (Fermentas, Germany) according to the manufactures' instruction. Finally, 1 µg of the DNase-treated total RNA was converted into cDNA using reverse transcription (RT)-enzyme (Fermentas, Germany) at 42ºC for 60 min. In this study, Allele ID (version 6) software was used to design primers (Table 1) for the gene expression analysis by quantitative RT-PCR. To assess and compare the expression of genes in the Eugenol-treated BM-MSCs relative to untreated control cells, quantitative gene expression analysis was performed in duplicates using specific primers and SYBR Green PCR master kit (Takara, Japan) in a real-time PCR instrument. The real-time PCR reactions were carried out in a 10 µl reaction volume using the two-step time and temperature program, including 10 sec at 95ºC and 30 sec at 60ºC for 40 cycles. The beta-actin (*β-actin*) gene was considered as housekeeping gene and the expression of interesting genes (*Tlr3*, *Tlr4*, *Ccl2,* and *Ccl3*) were normalised to the *β-actin* expression. Quantitative real-time PCR (qRT-PCR) reactions were performed in duplicates and each experiment was repeated three times. The standard deviations were calculated for the expression of each gene. The comparative C_t method was used to calculate the relative quantification of the gene expression in the Eugenol-treated BM-MSCs relative to untreated control cells (Livak & Schmittgen 2001). Finally, the fold-change more than or equal to 1.5 was considered as significant to identify differentially expressed genes in the Eugenol-treated BM-MSCs in comparison to untreated control cells.

Statistical analysis

Data analysis was carried out using the SPSS software package (version 21.0) for Windows through a Student's *t*-test. Data were also expressed as mean value ± standard deviation and differences were also considered significant when the P-value was 0.05 or less.

Results

Culture of BM-MSCs

The mouse bone marrow tissue was cultured and cells from the BM tissue were started to attach on the surface of the flask. After 72h, the cell culture medium was replaced and, thereby unattached cells

Table 1: Nucleotide sequences of the primers used for the gene expression analysis by qRT-PCR.

Gene	Accession number	Primer	Sequence
Tlr3	NM_126166	Forward	5′-GCCACCAGCGAGAGCACTTTC-3′
		Reverse	5′-GAGAAGGAACCGTTGCCGACATC-3′
Tlr4	NM_021297	Forward	5′-TGGGAGGGAAGAGGCAGGTG-3′
		Reverse	5′-TGGTGTCAGGCAGGAGAAGAAC-3′
Ccl2	NM_011333	Forward	5′-AGAGAGCCAGACGGGAGGAAG-3′
		Reverse	5′-TGAATGAGTAGCAGCAGGTGAGTG-3′
Ccl3	NM_011337	Forward	5′-ACACCAGAAGGATACAAGCAGCAG-3′
		Reverse	5′-GTAGGAGAAGCAGCAGGCAGTC-3′
B-actin	NM_007393	Forward	5′-GGCTGTATTCCCCTCCATCG-3′
		Reverse	5′-CCAGTTGGTAACAATGCCATGT-3′

were removed from the primary culture. The primary culture was reached to confluency after 7-10 days and, therefore, it trypsinised and sub-cultured to new flasks. Finally, the purified BM-MSCs in passage 3 were used for following studies. The mouse bone marrow-derived primary cell culture and the purified BM-MSCs are shown in Figure 1A & B, respectively.

Flow-cytometry analysis

Phenotypic characterization of cells was achieved using flow-cytometry analysis. Results indicated that although cells derived from mouse BM were positive for the MSCs markers CD44, CD90, CD105, they were also negative for hematopoietic markers CD45 and CD34 (Figure 2).

Adipogenesis potential of BM-MSCs

Results of differentiation assay showed that the adipogenic medium induced the conversion of BM-MSCs into adipocytes. Twenty-one days after the culture of BM-MSCs with the osteogenic medium, the Oil-red O staining and microscopic observations of cells demonstrated distinguishable primary lipid droplets in cells (Figure 3A). Results also indicated that lipid droplets were not detectable in untreated BM-MSCs (Figure 3B).

Osteogenesis potential of BM-MSCs

Twenty-one days after treatment of BM-MSCs with the osteogenic medium, Alizarin-red S staining was used to evaluate osteogenesis in the cells. The differentiated cells displayed a red colour

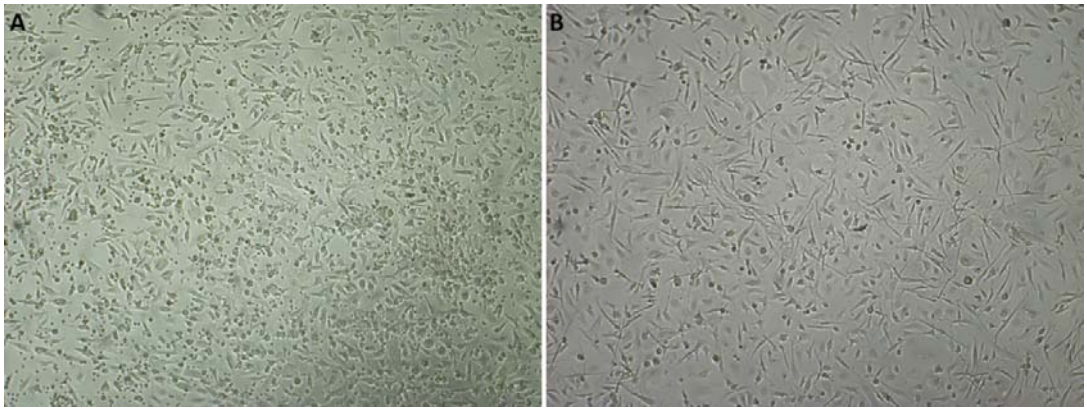

Figure 1. Mouse bone marrow-derived cell cultures. The primary cell culture derived from BM tissue (A) and the BM-derived MSCs in passage 3 (B).

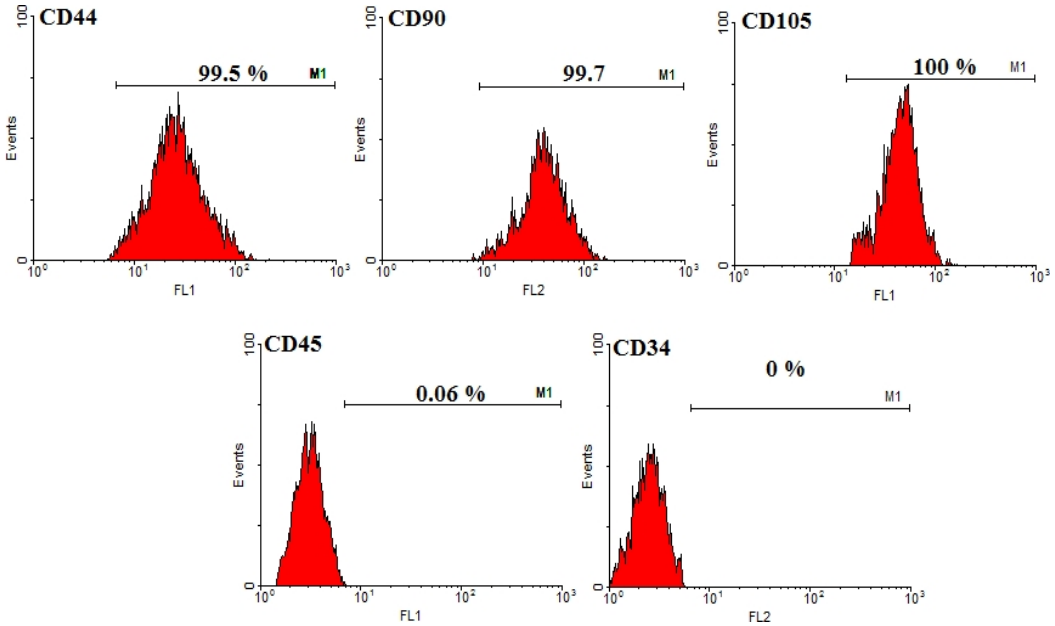

Figure 2. Phenotypic characterization of BM-MSCs by Flow-cytometry. Results showed that the mouse BM-MSCs were positive for CD44, CD90 and CD105, but they were negative for hematopoietic cell markers CD45 and CD34.

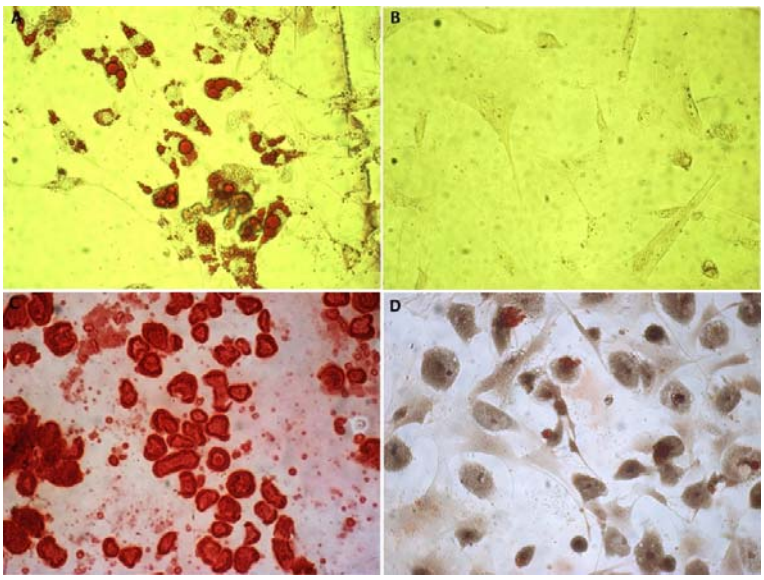

Figure 3. Differentiation potency of BM-MSCs. Oil-red O staining demonstrated that lipid-rich vacuoles formed in the BM-MSCs after 3 weeks of adipogenic induction (A); untreated BM-MSCs were considered as negative control (B). Alizarin-red S staining showed that mineralised nodules formed in the BM-MSCs after 3 weeks under the osteogenic induction. After 3 weeks of osteogenic induction, alizarin-red S staining indicated the osteocyte formation (C), while untreated BM-MSCs were negative for osteogenesis (D).

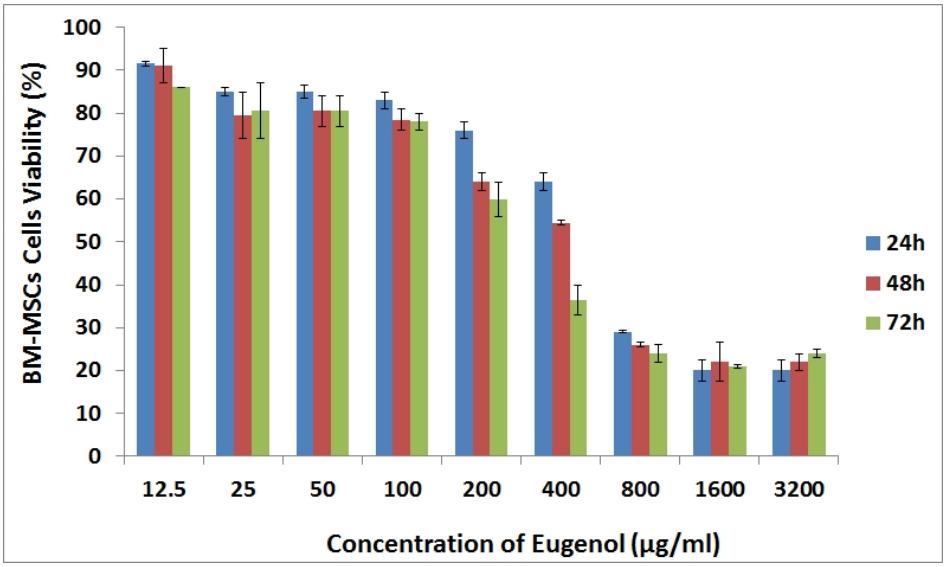

Figure 4. The cytotoxic effect of Eugenol was evaluated on BM-MSCs by MTT assay at 24, 48, and 72h after treatment.

after staining (Figure 3C), while this phenomenon was not observed in untreated BM-MSCs (Figure 3D).

Cytotoxic effect of Eugenol on MSCs

The cytotoxic effect of Eugenol was evaluated on BM-MSCs by MTT assay at 24, 48, and 72h after treatment. Results demonstrated that Eugenol reduced the viability of BM-MSCs in a dose- and time-dependent manner and the IC_{50} values for Eugenol were 400 µg/ml after 24 and 48h, and 200 µg/ml after 72h. Moreover, the results of the MTT assay showed about 90% cell viability at the concentration of 12.5 µg/ml 24h after treatment (Figure 4).

Morphological changes

Microscopic observations demonstrated that Eugenol affects the shape of the BM-MSCs in a dose-dependent manner and prominent morphological alterations were common 24h after treatments. The morphological changes of BM-

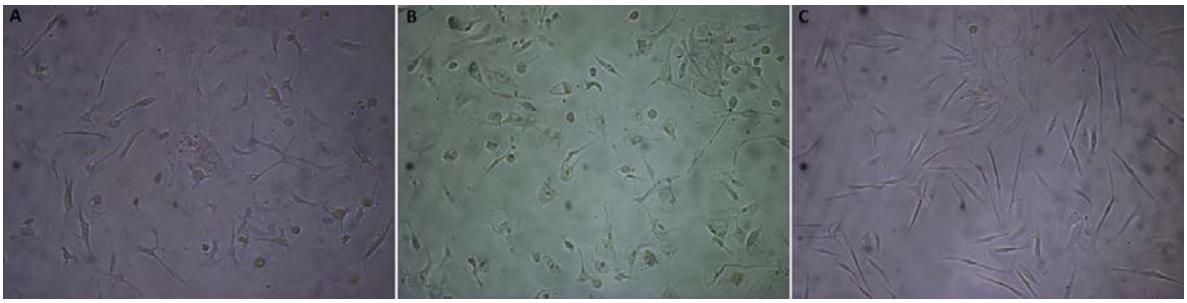

Figure 5. The effect of Eugenol on the morphology of BM-MSCs. Microscopic observations demonstrated the morphological alterations in the mouse BM-MSCs treated with 100 (A) and 300 µg/ml (B) of Eugenol, while untreated BM-MSCs were not showing the morphological changes (C).

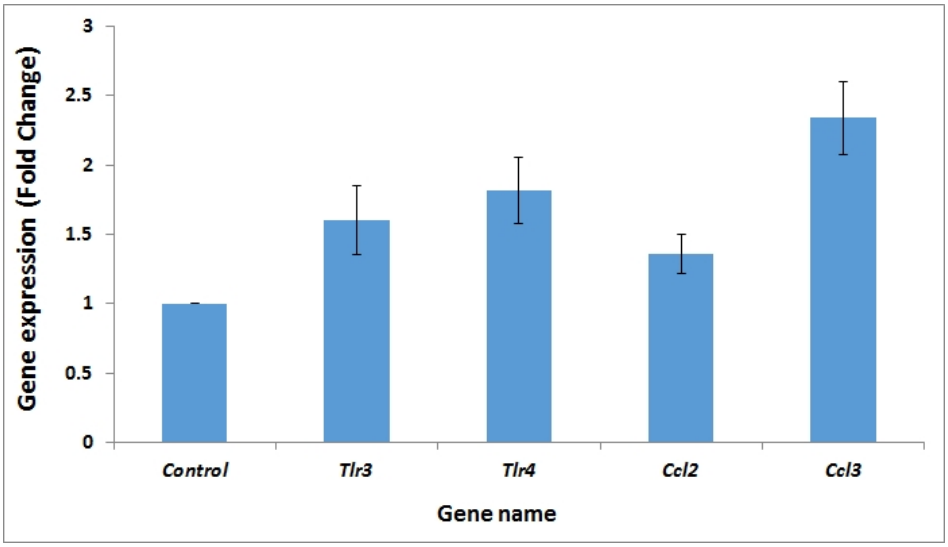

Figure 6. qRT-PCR for *Tlr3*, *Tlr4*, *Ccl2,* and *Ccl3*. The gene expression analysis showed that *Tlr3*, *Tlr4*, *Ccl2,* and *Ccl3* genes were over-expressed in the Eugenol-treated BM-MSCs in comparison to untreated control cells. However, results indicated that *Tlr3*, *Tlr4*, and *Ccl3* have 1.6, 1.8 and 2.2-fold change of expression, respectively, in Eugenol-treated mouse BM-MSCs relative to untreated cells.

MSCs treated with 100 and 300 µg/ml of Eugenol are shown in Figure 5A & B. To note, the morphological alterations were not detectable in untreated BM-MSCs (Figure 5C).

Gene expression analysis of the Eugenol-treated BM-MSCs

The effect of Eugenol on the expression of genes involved in the immunomodulatory potency of BM-MSCs, including *Tlr3*, *Tlr4*, *Ccl2,* and *Ccl3*, was evaluated at transcript level by qRT-PCR method. The results of the gene expression analysis showed that *Tlr3*, *Tlr4*, *Ccl2,* and *Ccl3* genes were up-regulated 1.6-, 1.8-, 1.3-, 2.2-fold, respectively, in the Eugenol-treated MSCs compared to untreated control cells (Figure 6). These findings indicated that *Tlr3*, *Tlr4*, and *Ccl3* have the fold change of expression more than 1.5 in Eugenol-treated BM-MSCs relative to untreated cells. Moreover, *Ccl3* and *Ccl2* had the highest and the lowest levels of expression in the Eugenol-treated cells.

Discussion

Immunomodulatory potency is a unique property of MSCs and, therefore, it makes them interesting tools for the treatment of inflammatory and autoimmune diseases. Scientists have tried to find the influential factors that influence the immunomodulatory properties of MSCs in vitro. Eugenol is a volatile compound from the phenylpropanoids class of chemical compounds, which has widespread biological and pharmacological properties. Despite extensive investigations on the biological and pharmacological effects of Eugenol (Ito et al., 2005; Raghavenra et al., 2006; Singh et al., 2007;

Bachiega et al., 2012; Kamatou et al., 2012), its effect on MSCs remains to be clarified. Therefore, in the current study, we investigated the effect of Eugenol on the expression of genes, including *Tlr3*, *Tlr4*, *Ccl2,* and *Ccl3*, involved in the MSCs immunomodulatory potency. The results of qRT-PCR showed that Eugenol influence the expression of *Tlr3*, *Tlr4*, and *Ccl3* genes in BM-MSCs. Interestingly, MSCs can be polarised into two anti-inflammatory (MSC1) or a pro-inflammatory (MSC2) phenotype through activation of different Toll-like receptors (TLRs) (Waterman et al., 2010). It has been found that MSCs express different types of TLRs, including TLRs-1, 2, 3, 4, 5, 6, 7, 8 and 9 (Najar et al., 2017). The role of TLR3 and TLR4 in regulating the function of MSCs has been shown in different studies. Waterman et al. demonstrated that MSCs polarisation process toward MSC1 or MSC2 phenotype may occur depending on the type of TLR activated. They found that MSC1 and MSC2 phenotype express TLR4 and TLR3, respectively (Waterman et al., 2010). Interestingly, TLRs signalling pathways induced MSC migration and immunomodulatory factor secretion (Tomchuck et al., 2008; Hwang et al., 2014). For example, activation of TLR3 amplifies MSCs multifunctional trophic factors and enhances therapeutic potency (Mastri et al., 2012). Activation of TLR3 enhances the therapeutic potential of MSCs by stimulating the expression and secretion of interleukin-6 (IL-6), IL-8 IFNγ, STO-1, hepatic growth factor (HGF), and vascular endothelial growth factor (VEGF) (Tomchuck et al., 2008; Mastri et al., 2012; O'Neill et al., 2013). Activation of TLR4 increases the production and secretion of IL-6 and IL-8 by of MSCs, as well (Tomchuck et al., 2008). The therapeutic advantages of TLR3 and TLR4 activation are not only limited to secretion of trophic factors but also to its immunoregulatory response (Delarosa et al., 2012). A recent study revealed that stimulation of TLR3 signalling by RNA mimetic polyinosinic-polycytidylic acid [Poly(I:C)], enhanced the immunosuppressive ability of human umbilical cord-derived MSCs (UC-MSCs) through microRNA-143 inhibition (Zhao et al., 2014). Moreover, Zhang et al., demonstrated that the activation of TLR3 and TLR4 in human UC-MSCs stimulates the expression of inflammatory markers (Zhang et al., 2015). A study by Rashedi et al., also showed that activation of TLR3 or TLR4 in MSCs increases Treg induction via the Notch pathway (Rashedi et al., 2017). Mechanistically, it has been found that stimulation of TLR3 and TLR4 by lipopolysaccharide and Poly-IC, respectively, resulted in enhanced phospho-IKKα/β and phospho-MAPK and thus activation of NF-kB and/or MAPK signalling in MSCs. Significantly, TLR3 induced the expression of stem cell markers and inhibited the differentiation potential of UC-MSCs into osteocytes. On the other hand, TLR4 inhibited the expression of stem cell markers and, therefore, increased the osteogenic differentiation of UC-MSCs (Zhang et al., 2015). Eugenol exhibits anti-inflammatory and immunomodulatory activities through inhibiting the activity of enzymes such as COX-1/2, 15-LOX, 5-LOX manganese prostaglandin H synthase (Mn-PHS) and NF-KB signalling pathway. It induces the production of free radicals, like tyrosyl, and lipid peroxidation, and also preventing the production of inflammatory mediators such as prostaglandin (PGE2) and leukotrienes (LTC-4) (Ito et al., 2005; Raghavenra et al., 2006; Singh et al., 2007; Bachiega et al., 2012). Generally, it has been found that the anti-oxidant and anti-inflammatory activity of Eugenol is achieved at low concentrations, while at higher concentrations it acts as a pro-oxidant, which leading to tissue damage by increasing the production of free radicals (Kabuto & Yamanushi 2011; Kamatou et al., 2012). The protective effects of Eugenol on immune cells have also been proven in a few studies. Our quantitative gene expression analysis also showed that Eugenol at 10 µg/ml somewhat enhanced the expression of *Tlr3* and *Tlr4* genes in BM-MSCs. Therefore, we propose that Eugenol can also influence on MSCs characteristics in vitro. Moreover, although Eugenol slightly over-expressed *Tlr3* or *Tlr4* in BM-MSCs, more experimental studies will be necessary to confirm the effect of Eugenol on the immunomodulatoty potency of MSCs.

In addition to TLRs, the pro-inflammatory chemokine (C-C motif) ligands (CCLs) are important regulators of the immunomodulatory properties of MSCs. Collectively, different studies revealed that MSCs exhibit changes in gene expression indicative of a pro-inflammatory phenotype, with increased expression of CCL2, CCL3, CCL4, CCL5, CCL7, CCL20, CXCL6, CXCL10, CXCL12 and IL-8 mRNA (Anton et al., 2012; Pyo et al., 2015; Lee et al., 2017). Functionally, the secretion of pro-inflammatory chemokine (C-C motif) ligands, including CCL2, CCL3 and CCL12 by MSCs stimulates the migration of immune cells such as monocytes and T cells and recruits them into inflamed tissues to induce wound repair at the site of injury (Le Blanc & Davies 2015; Lee et al., 2017). Mechanistically, it was also elucidated that CCL2 increases the

duration of the MSC–T cell contacts through enhancing the expression of VCAM-1 in T cells (Pyo et al., 2015; Lee et al., 2017). In the present study, we also found that Eugenol significantly up-regulated the expression of *Ccl3* in BM-MSCs. Therefore, we suggest that Eugenol may enhance the immunomodulatory potency of BM-MSCs through activation of *Ccl3* expression. However, the exact mechanisms and the roles of this regulation are needed to be elucidated in further study.

In this study, we investigated the effect of Eugenol on the mouse BM-MSCs through evaluation of the expression of *Tlr3*, *Tlr4*, *Ccl2,* and *Ccl3*, which are involved in the immunomodulatory potency of MSCs. Our findings showed that Eugenol somewhat affects the expression of *Tlr3*, *Tlr4*, and *Ccl3* in BM-MSCs. Therefore, we declare that Eugenol can influence on MSCs characteristics. This study also provides a background for further studies on the effect of Eugenol on MSCs characteristics and functions, especially their immunomodulatory potency, which may finally improve their potency for cell-based therapy of the human inflammatory and autoimmune diseases.

Acknowledgements

The authors would like to thank Dr. Azadbakht Lab. for generously providing the mice. The authors are thankful to Ms. Elham Alimoradi and Ms. Mojdeh Heidari for their great assistance.

References

1. Abdi R., Fiorina P., Adra C. N., Atkinson M. and Sayegh M. H. (2008) Immunomodulation by mesenchymal stem cells: a potential therapeutic strategy for type 1 diabetes. Diabetes 57: 1759-1767.
2. Bachiega T. F., de Sousa J. P., Bastos J. K. and Sforcin J. M. (2012) Clove and eugenol in noncytotoxic concentrations exert immunomodulatory/anti-inflammatory action on cytokine production by murine macrophages. The Journal of Pharmacy and Pharmacology 64: 610-616.
3. Delarosa O., Dalemans W. and Lombardo E. (2012) Toll-like receptors as modulators of mesenchymal stem cells. Frontiers in Immunology. 3: 182.
4. Hass R., Kasper C., Böhm S. and Jacobs R. (2011) Different populations and sources of human mesenchymal stem cells (MSC): a comparison of adult and neonatal tissue-derived MSC. Cell Communication and Signaling 9: 1.
5. Huang C. E., Hu F. W., Yu C. H., Tsai L. L., Lee T. H., Chou M. Y. and Yu C. C. (2014) Concurrent expression of Oct4 and Nanog maintains mesenchymal stem-like property of human dental pulp cells. International Journal of Molecular Sciences 15: 18623-18639.
6. Hwang S. H., Cho H. K., Park S. H., Lee W., Lee H. J., Lee D. C., Oh J. H., Kim T. G., Sohn H. J., Kang J. M. and Kim S. W. (2014) Toll like receptor 3 & 4 responses of human turbinate derived mesenchymal stem cells: stimulation by double stranded RNA and lipopolysaccharide. PloS one. 9, e101558.
7. Ito M., Murakami K. and Yoshino M. (2005) Antioxidant action of eugenol compounds: role of metal ion in the inhibition of lipid peroxidation. Food and Chemical Toxicology 43: 461-466.
8. Kabuto H. and Yamanushi T. T. (2011) Effects of zingerone [4-(4-hydroxy-3-methoxyphenyl)-2-butanone] and eugenol [2-methoxy-4-(2-propenyl)phenol] on the pathological progress in the 6-hydroxydopamine-induced Parkinson's disease mouse model. Neurochemical Research 36: 2244-2249.
9. Kamatou G. P., Vermaak I. and Viljoen A. M. (2012) Eugenol--from the remote Maluku Islands to the international market place: a review of a remarkable and versatile molecule. Molecules 17: 6953-6981.
10. Le Blanc K. and Davies L. C. (2015) Mesenchymal stromal cells and the innate immune response. Immunology Letters 168: 140-146.
11. Lee H. K., Kim H. S., Kim J. S., Kim Y. G., Park K. H., Lee J. H., Kim K. H., Chang I. Y., Bae S. C., Kim Y., Hong J. T., Kehrl J. H. and Han S. B. (2017) CCL2 deficient mesenchymal stem cells fail to establish long-lasting contact with T cells and no longer ameliorate lupus symptoms. Scientific Reports 7: 41258.
12. Livak K. J. and Schmittgen T. D. (2001) Analysis of relative gene expression data using real-time quantitative PCR and the 2(-Delta Delta C(T)) Method. Methods 25: 402-408.
13. Ma S., Xie N., Li W., Yuan B., Shi Y. and Wang Y. (2014) Immunobiology of

mesenchymal stem cells. Cell Death and Differentiation 21: 216-225.
14. Mastri M., Shah Z., McLaughlin T., Greene C. J., Baum L., Suzuki G. and Lee T. (2012) Activation of Toll-like receptor 3 amplifies mesenchymal stem cell trophic factors and enhances therapeutic potency. American Journal of Physiology. Cell Physiology 303: C1021-1033.
15. Najar M., Krayem M., Meuleman N., Bron D. and Lagneaux L. (2017) Mesenchymal Stromal Cells and Toll-Like Receptor Priming: A Critical Review. Immune Network 17: 89-102.
16. O'Neill L. A., Golenbock D. and Bowie A. G. (2013) The history of Toll-like receptors - redefining innate immunity. Nature Reviews. Immunology 13: 453-460.
17. Pyo M., Lee H. K., Uhm J., Ryu H. S., Hong J. T., Kim Y. and Han S. B. (2015) Time-lapse imaging of contact dynamics between mesenchymal stem cells and T cells (THER5P. 913)ed^eds): Am Assoc Immnol.
18. Raghavenra H., Diwakr B. T., Lokesh B. R. and Naidu K. A. (2006) Eugenol--the active principle from cloves inhibits 5-lipoxygenase activity and leukotriene-C4 in human PMNL cells. Prostaglandins, Leukotrienes, and Essential Fatty Acids 74: 23-27.
19. Rashedi I., Gomez-Aristizabal A., Wang X. H., Viswanathan S. and Keating A. (2017) TLR3 or TLR4 Activation Enhances Mesenchymal Stromal Cell-Mediated Treg Induction via Notch Signaling. Stem Cells 35: 265-275.
20. Ren G., Zhang L., Zhao X., Xu G., Zhang Y., Roberts A. I., Zhao R. C. nad Shi Y. (2008) Mesenchymal stem cell-mediated immunosuppression occurs via concerted action of chemokines and nitric oxide. Cell Stem Cell 2: 141-150.
21. Ren G., Zhao X., Zhang L., Zhang J., L'Huillier A., Ling W., Roberts A. I., Le A. D., Shi S., Shao C. and Shi Y. (2010) Inflammatory cytokine-induced intercellular adhesion molecule-1 and vascular cell adhesion molecule-1 in mesenchymal stem cells are critical for immunosuppression. Journal of Immunology 184: 2321-2328.
22. Renner P., Eggenhofer E., Rosenauer A., Popp F. C., Steinmann J. F., Slowik P., Geissler E. K., Piso P., Schlitt H. J. and Dahlke M. H. (2009) Mesenchymal stem cells require a sufficient, ongoing immune response to exert their immunosuppressive function. Transplantation Proceedings 41: 2607-2611.
23. Savickiene J., Treigyte G., Baronaite S., Valiuliene G., Kaupinis A., Valius M., Arlauskiene A. and Navakauskiene R. (2015) Human amniotic fluid mesenchymal stem cells from second-and third-trimester amniocentesis: Differentiation potential, molecular signature, and proteome analysis. Stem Cells Intternational 2015.
24. Singh G., Maurya S., DeLampasona M. P. and Catalan C. A. (2007) A comparison of chemical, antioxidant and antimicrobial studies of cinnamon leaf and bark volatile oils, oleoresins and their constituents. Food and Chemical Toxicology 45: 1650-1661.
25. Sisakhtnezhad S., Alimoradi E. and Akrami H. (2017) External factors influencing mesenchymal stem cell fate in vitro. European Journal of Cell Biology 96: 13-33.
26. Tomchuck S. L., Zwezdaryk K. J., Coffelt S. B., Waterman R. S., Danka E. S. and Scandurro A. B. (2008) Toll-like receptors on human mesenchymal stem cells drive their migration and immunomodulating responses. Stem Cells 26: 99-107.
27. Wang J., Zhao Y., Wu X., Yin S., Chuai Y. and Wang A. (2015) The utility of human fallopian tube mucosa as a novel source of multipotent stem cells for the treatment of autologous reproductive tract injury. Stem Cell Research & Therapy 6: 98.
28. Waterman R. S., Tomchuck S. L., Henkle S. L. and Betancourt A. M. (2010) A new mesenchymal stem cell (MSC) paradigm: polarization into a pro-inflammatory MSC1 or an Immunosuppressive MSC2 phenotype. PloS One 5: e10088.
29. Zhang L., Liu D., Pu D., Wang Y., Li L., He Y., Li Y., Qiu Z., Zhao S. and Li W. (2015) The role of Toll-like receptor 3 and 4 in regulating the function of mesenchymal stem cells isolated from umbilical cord. International Journal of Molecular Medicine 35: 1003-1010.
30. Zhao Q., Ren H. and Han Z. (2016). Mesenchymal stem cells: Immunomodulatory capability and clinical potential in immune diseases. Journal of Cellular Immunotherapy 2: 3-20.
31. Zhao X., Liu D., Gong W., Zhao G., Liu L.,

Yang L. and Hou Y. (2014) The toll-like receptor 3 ligand, poly(I:C), improves immunosuppressive function and therapeutic effect of mesenchymal stem cells on sepsis via inhibiting MiR-143. Stem Cells 32: 521-533.

Journal of Cell and Molecular Research (2018) 10 (1), 11-17 DOI: 10.22067/jcmr.v10i1.71261

Research Article

Polyurethane/Hydroxyapatite Induces MSCs towards Osteo-like Cells in a Similar Fashion to Demineralized Bone Matrix

Mostafa Shahrezaei, Mohamad Moosaee*

Department of Orthopedic Surgery, AJA University of Medical Sciences, Tehran, Iran

Received 26 February 2018 Accepted 19 June 2018

Abstract

Osteoarthritis (OA) is the single most prevalent disorder in older adults having a predicted value of 130 million patients in 2050. Several clinical chemotherapeutic approaches are being applied to treat early or late osteoarthritis. It has been recommended that autologous mesenchymal stem cells (MSCs) from OA patients could be the gold standard to treat OA as these cells have high proliferation and chondrocyte lineage differentiation potential. In this work, human MSCs, derived from adipose tissue (Ad-MSCs), loaded on Polyurethane/Hydroxyapatite (PUHA) and Demineralized Bone Matrix (DBM) and their proliferation, differentiation capabilities were determined by MTT assay and Alizarin Red S staining and the expression of mRNA into osteoblast lineage were determined using Real Time PCR . The result showed that MSCs were more viable on PUHA when compared with DBM and the expression of lineage specific markers showed that differentiation potential of PUHA and DBM was not much different. The osteoblast lineage cells were stained positively with Alizarin Red S in completely similar in both groups. Electron microscopy analysis indicated attachment of Ad-MSCs when cultured on the PUHA and DBM. It was concluded that PUHA can be used in clinics as Osteo-inductive scaffold to treat OA easily, however further investigations are required before moving to clinical studies.

***Keywords*:** Demineralized Bone Matrix, Osteoarthritis, Osteo-like Cells, Polyurethane/Hydroxyapatite

Introduction

Osteoarthritis (OA) is a long-term chronic degenerative disorder with undiscovered origin that identified by the atrophy of cartilage in joints. The main symptoms of OA are rigidity, pain and restricted movements when bones rubbed together. OA has been known as a most common disease with a worldwide distribution (Baharvand et al., 2004). According to the United Nations, people aged over 60 will account for more than 20 percent of the world's population by 2050 which are the prime victims of OA rising a danger of 130 million OA patients of whom 40 million will be disordered by the severity of disease (Bahrami et al., 2011). There are several therapeutic approaches including physical activity, surgery, medication etc. but recently stem cells especially mesenchymal stem cells (MSCs) have emerged as promising agents to treat OA because of their excessive proliferation and multilineage differentiation capability (Brodie and Humes, 2005, Caplon, 2005). Their clinical trials and promising results with enhanced healing and improved joints recovery have resulted in the applications of these cells in comparison with other cells to treat various osteo-diseases(Chakkalakal et al., 2001, Dexheimer et al., 2011). These cells can be isolated from approximately all parts of body including skin, blood, pancreas, adipose, liver, brain, lungs, heart, umbilical cord blood and kidneys. Among these issues, adipose tissue is the most common source of these kinds of stem cells with limited oncogenicity, which could be derived from the lipoasparate in routine liposuction (Friedenstein et al., 1987, García-Álvarez et al., 2011, Ghannam et al., 2010).

In comparison to the misconception that OA is easily a "wear and tear" disease, it is now obvious that pro-inflammatory cytokines and moderators are involved in the onset and advancement of this disease (Hare et al., 2009). In this regard, the potential effect of inflammatory cytokines exist in the joint space must be thought when estimating stem cell-based therapies and a good scaffold can induce precise differentiation for bone healing and recovering the damages (Hofmann et al., 2008). Scaffold based engineering may result in the generation of tissues resistant to inflammations, a major challenge in tissue engineering. Considering the importance of a scaffold, demineralized bone

*Corresponding author E-mail: Drmoosaee@gmail.com

graft (DBG) that is derived from the bone tissue, have been applied by researchers for bone healing and treatment of OA (Hosea Blewett, 2008).. Mineralized bone matrices with osteoconductive and osteoinductive properties (Hsieh et al., 2015, Jiang et al., 2002), have been utilized widely for the most of bone disorders with non-union characteristics (Labusca et al., 2012, Lee et al., 2008, Levenberg et al., 2003). Demineralized bone matrix is constituted of native compositions of ECM, which enhance its osteoinductive characteristics. Osteoconductive features of DBM are consequence of its collagenous network (Maetzel et al., 2004). Efficient alternatives to DBM remained a challenging step in stem cell-based treatment of osteo-diseases and it has been considered that natural derivatives could be the ideal agents for cellular seeding to induce towards osteo-like cells (Maniatopoulos et al., 1988). In this work, PUHA as a combination of PU (Polyurethane) and HA (Hydroxyapatite) has been used to seed the cells and to study cellular behavior on it. Cellular behavior has been studied and compared with DBM as a current gold standard in tissue engineering and transcriptional based approaches have been applied to find out the molecular switching (*RUNX2*, *COL1A1*, *BGLAP* and *SPARC*) of seeded MSCs on PUHA and DBM.

Materials and Methods

Isolation and characterization of Adipose MSCs

Human adipose-derived mesenchymal stem cells (Ad-MSCs) were extracted from adipose tissue as previously mentioned (Martin et al., 1999, Mulliken et al., 1981, Murphy et al., 2002, Polo-Corrales et al., 2014). Adipose tissues were isolated from three patients using liposuction surgery with written agreement at Razavi Hospital (Mashhad, Iran). Cells were separated using collagenase type I (Gibco, Australia) and MSCs were subsequently derived by centrifugation and cultured in Dulbecco's Modified Eagle's Medium-Low Glucose (DMEM-LG; Gibco, Australia) supplementary with 10% fetal bovine serum (FBS; Gibco, Australia), 100 µg/ml streptomycin and 100 U/ml penicillin (Biowest, UK). The recognition of extracted human Ad-MSCs was affirmed by their expression of particular cell surface antigens as explained before (Martin et al., 1999).

Culturing of MSCs on Scaffold

Ad-MSCs in passage three were applied for culturing on the scaffolds. Cells were separated from culture plates with trypsin/EDTA (Gibco, Australia) then added into each well. A seeding density of 1×10^6 cells was applied for both PUHA and DBM (TRC, Iran) scaffolds and 2D culture of Ad-MSCs was used as control group. In order to loading the cells in scaffolds, Ad-MSCs were resuspended in FBS. Then, all samples were incubated at 37ºC under 5% of CO_2 conditions for 15 min, after which, 1 ml of DMEM-LG supplemented with 10% FBS was added to each well. After 48h incubation, the matrices were cultured in induction media (DMEM-LG supplemented with 10% FBS, 100 µg/ml streptomycin and 100 U/mL penicillin plus 0.1 µM dexamethasone,10 mM β-glycerophosphate, and 10 mM ascorbic acid) for 21 days.

Cell Viability Assay

Cell viability assay was applied to estimate the rate of Ad-MSCs proliferation and viability. Cell-seeded on DBM and PUHA scaffolds in 12-well tissue culture plates were cultured in osteogenic induction medium for 14 and 21 days. The mitochondrial activity of ADSCs into the DBM and PUHA scaffolds can be determined by the conversion of 3-(4,5-dimethylthiazolyl-2)-2,5-diphenyltetrazolium bromide (Sigma, USA) to formazan crystals. Cells were incubated in the existence of 0.5 mg/mL 3-(4,5-Dimethylthiazol-2-yl)-2,5-diphenyltetrazoliumbromide (MTT) for 3 hours. The optical densities (OD) of the formazan were read with a spectrophotometer at a wavelength of 570 nm. This absorbance was caused by Ad-MSCs seeded in DBM and PUHA for 14 and 21 days after culture.

Alizarin Red staining

Scaffolds were fixed with 4% paraformaldehyde, incubated with Alizarin Red S solution for 20 min. The samples were washed with distilled water and in order to quantitative analysis the scaffolds were detained in 10% acetic acid. The concentration of dye in solution was measured with the spectrophotometer at 405 nm.

Gene Expression Analysis

Total RNAs were isolated from all three groups of MSCs cultured on DBM, PUHA and control group after 21 days and cDNAs were synthesized and subjected to reverse transcription polymerase chain reaction (RT-PCR) to observe the expression of *RUNX2, BGLAP, SPARC* and *COL1A1* using specific primers as shown in Table 1. The relative expressions of osteo-lineage markers were determined using real time quantitative RT-PCR. For this purpose, synthesized cDNAs were mixed with 2x SYBR® Green Real Time PCR Master Mix (Parstous, Iran) in 8-strip tubes (Gunster Biotech,

Table 1. List of primers used for mRNA expression analysis using real time quantitative RT-PCR. *SPARC*: secreted protein acidic and rich in cysteine or osteonectin, *COL1A1*: Collagen, Type I, Alpha 1, *BGLAP*: Bone gamma-carboxyglutamate (Gla) protein or osteocalcin, *RUNX2*: Runt-related transcription factor 2, *TBP*: TATA binding protein gene.

Name of Gene	Forward Primer	Reverse Primer	Length of Primer
SPARC	CTGTATTCTGGTGTTCTCTTCTAC	AATGACTGAATGAGCCAATGC	170 bp
COL1A1	GACGAAGACATCCCACCAAT	CGTCATCGCACAACACCTT	124 bp
BGLAP	CTCACACTCCTCGCCCTATTG	CTCTTCACTACCTCGCTGCC	134 bp
RUNX2	CTCACTGCCTCTCACTTG	ATGTATTAACCTGGATTCTGG	163 bp
TBP	TTGTGAGAAGATGGATGTTG	AGATAGCAGCACGGTATG	151 bp

Taiwan). and the mixture was subject to CFX96 Touch Real-Time PCR Detection System (Bio-Rad, USA) using following parameters: initial denaturation at 94°C for 10 minutes, 40 cycles of 94°C for 15 seconds, 60°C for 30 seconds and 72°C for 30 seconds, followed by a final extension at 72°C for 2 minutes.

Electron Microscopy

One sample from each category was set with 2.5% glutaraldehyde solution (Sigma) for 4 hours at room temperature in order to scanning electron microscopic (SEM) analyses. After dehydration in a gradient series of ethanol (50%, 70%, 90%, 100%, for 10 min in each one), specimens were dried, coated with gold and analyzed by SEM (LEO, Germany).

Statistical Analysis

Statistical analyses were carried out by SPSS and applying one-way ANOVA test. Results are exhibited as mean values ± standard deviation. A significance value of $p < 0.05$ was approved as statistically significant.

Results

Characterization of Ad-MSCs

Flow cytometry analysis was carried out to characterize Ad-MSCs. We used 6 different antibodies against CD90, CD105, CD44, CD45, CD34 and CD11b. Majority of these cells express CD90, CD105 and CD44 markers, whereas CD45, CD34 and CD11b are expressed in low percentage of the cells (data not shown).

Cell viability

MTT assay was used in order to evaluate the rate of Ad-MSCs proliferation and viability. The cells seeded on DBM and PUHA scaffolds in osteogenic induction medium for 14 and 21 days. The OD of the formazan product produced by Ad-MSCs seeded in DBM and PUHA 14 days after culture were similar. On day 21, the viability of the cells in two types of scaffolds and control groups was similar although in PUHA group was increased, slightly (Figure 1).

Alizarin Red staining

In order to analyze calcium crystals in cells or matrix fibers, alizarin red staining carried out. The Ad-MSCs seeded on DBM and PUHA scaffolds for 21 days with osteogenic induction medium. The Alizarin Red staining of the cells culture in the two types of scaffolds was the same, as analyzed by absorbance of the solvent as shown in Figure 2.

Expression of Osteogenic genes in Ad-MSCs seeded on scaffold

At day 21, in order to examine the expression of osteogenic-related genes in the Ad-MSCs seeded in DBM, real time quantitative RT-PCRwas performed. The expressions of Runt-related transcription factor 2 (*RUNX2*), Collagen, Type I, Alpha 1 (*COL1A1*), Bone gamma-carboxyglutamate (Gla) protein or osteocalcin (*BGLAP*) and secreted protein acidic and rich in cysteine or osteonectin (*SPARC*) in relation to TATA binding protein (*TBP*) gene are shown in Figure 3. The expression of *RUNX2*, *SPARC* and *COL1A1* was increased in the Ad-MSCs seeded on DBM in presence of the induction medium, significantly. However, expression of *BGLAP* was similar in Ad-MSCs loaded on DBM and PUHA.

Electron microscopy analysis

Significant integration of cells to the DBM and PUHA scaffolds were also affirmed by SEM images.

Ad-MSCs attached and proliferated into well in the DBM and PUHA (Figure 4). In DBM and PUHA groups, Ad-MSCs were directly injected in the scaffolds, the cells would attach into the scaffold holes and its surface. In these groups, Ad-MSCs adhere on the scaffolds via pseudopodia. SEM was shown PUHA was better than demineralized bone graft.

Discussion

Stem cell-based tissue-engineering approaches are currently being investigated at high pace and are setting up a new era of learning that how to control the body's constitutional capacity to repair and renew skeletal tissues. For this purpose, MSCs are being introduced as reparative cells to the disorder site to fill the injury and to promote the body's self-repair by managing its intrinsically self-renewal capacity by its unmatched paracrine effects (Rosenthal et al., 1999).

Covering the challenge of autologous stem cell treatment demand, MSCs are being taken from young, healthy donors exhibiting enhanced expansion and differentiation potential for OA patients as it was hypothesized that onset of OA may decrease the chondrogenic potential of stem cells (Supronowicz et al., 2013). Studies approved that MSCs from OA patients can be derived, amplified, and differentiated into the chondrocyte lineage and then transplanted again (Thibault et al., 2009, Tran et al., 2009). However, raised age and obesity are both critical risk factors for OA and may influence the characteristic of stem cells (Hare et al., 2009, Upton et al., 1984).

Many of conventional cell culture investigations for clinical purpose have been applied in 2-dimensional (2D) culture systems; nevertheless, these culture systems are significantly limited in simulation of cell fortune in native tissues (Vilalta et al., 2008). Therefore, three-dimensional (3D) culture systems have been improved as a strategy to overcome this challenge and cells are being cultured using different scaffolds to reduce the variations in cell morphology, migration, signaling and adherence (Wang et al., 2009, Yang et al., 2015) and steps have been taken to generate a natural microenvironment *in vitro* which is more proper for investigation of cell interactions with ECM constituents (Yang et al., 2011). Biomaterial scaffolds indicated to operate as supporting structures to osteogenic cells playing a crucial role in bone tissue engineering (Yoon et al., 2007). Various types of adopted chitosan have been performed as 3D scaffolds including chitosan hydrogel and chitosan sponges to study their potential to induce MSCs towards osteo-lineage and to keep cells viable in culturing systems (Zotarelli Filho et al., 2013).

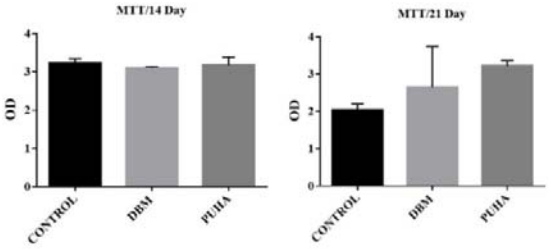

Figure 1. The proliferation and viability of adipose derived mesenchymal stem cell cultured on the PUHA and DBM (*P<0.05*).

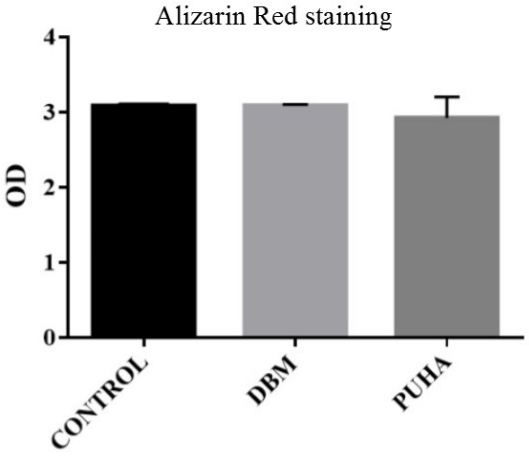

Figure 2. Alizarin Red S staining of adipose derived mesenchymal stem cell cultured on the PUHA and DBM for 14 and 21 days (*P<0.05*).

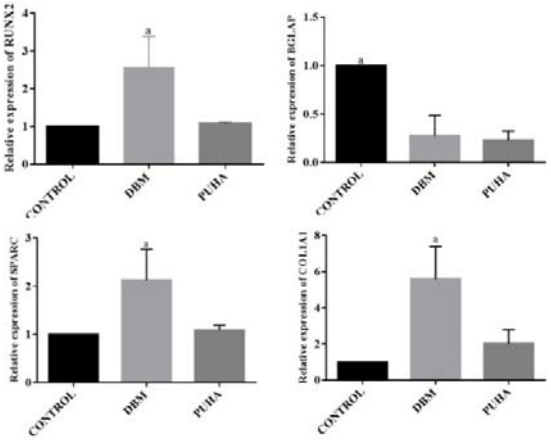

Figure 3. Gene expression of adipose derived mesenchymal stem cell cultured on PUHA and DBM (*P<0.05*).

DBM have been known as the ideal scaffold for osteo-lineage induction of stem cells but the

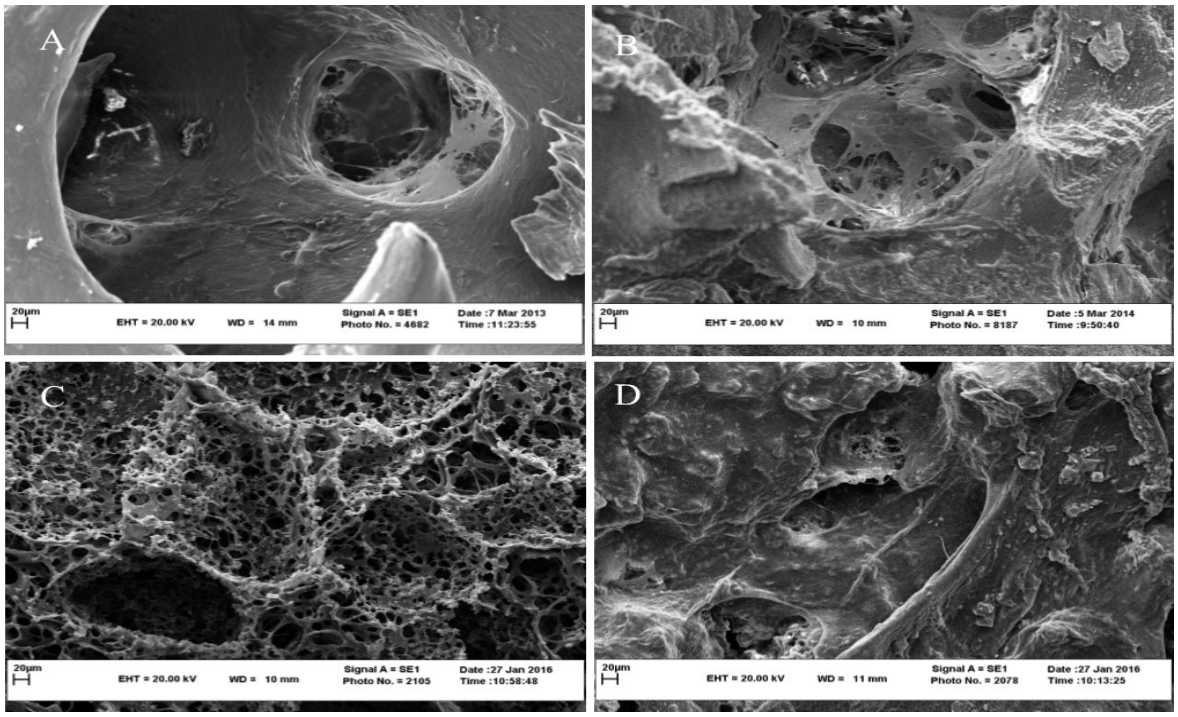

Figure 4. Scanning electron microscopy of PUHA and DBM. A & B) Ad-MSCs cultured on the DBM, A) in the day of seeding (500X), B) 21 days after culture in induction medium (500X), C &D) Ad-MSCs cultured on the PUHA, C) in the day of seeding (500X), D) 21 days after culture in induction medium (500X).

availability of DBM depends upon the existence of dead bone, a major challenge in the scaffold preparation (Hosea Blewett, 2008). PUHA, an ideal conjugation of PU (Polyurethane) and HA (Hydroxyl Appetite) have emerged as an ideal candidate to generate *in vitro* microenvironment as PUHA provides more vitality to cells as compared to other available scaffold matrices (Yoon et al., 2007) and an excellent three-dimensional structure for bone tissue ingrowth and cell migration and hopefully could be used as an substitute to DBM in near future for bone tissue regeneration (Zuk et al., 2002).. It has been shown that this 3D co-culture system could supply a novel foundation for the improvement of complex tissue engineered constructs with high regeneration ability (Zuk et al., 2001).. In current study, we used Ad-MSCs and studied their viability while cultured on DBM and PUHA. It was observed that PUHA is much more viable scaffold as compared to DBM for ad-MSCs whereas both scaffolds showed equal amount of osteogenic differentiation as determined by MTT and Alizan red assay respectively, as shown in Figure 1 and 2. Results obtained by qRT-PCR, confirmed the consistency of our
previously mentioned reports regarding their osteogenic differentiation (Figure 3). Considering the challenges in deriving DBM and advantages of PUHA, it can be concluded from the current work that PUHA could be used as a novel scaffold for bone tissue engineering as there was no significant difference in cell viability, differentiation, molecular expression and electron microscopic morphology, when we compared both scaffold.

Acknowledgements

The authors would like to thank the AJA University of Medical Sciences.

References

1. Baharvand, H., Hashemi, S.M., Ashtiani, S.K., and Farrokhi, A. (2004). Differentiation of human embryonic stem cells into hepatocytes in 2D and 3D culture systems in vitro. Int J Dev Biol 50: 645-52.
2. Bahrami, A.R., Ebrahimi, M., Matin, M.M., Neshati, Z., Almohaddesin, M.R., Aghdami, N., and Bidkhori, H.R. (2011). Comparative analysis of chemokine receptor's expression in mesenchymal stem cells derived from human bone marrow and adipose tissue. J Mol Neurosci 44: 178-85.
3. Brodie, J.C., and Humes, H.D. (2005). Stem cell approaches for the treatment of renal

failure. Pharmacol Rev 57: 299-313.
4. Caplon, A. (2005). Mesenchymal stem cells: Cell based reconstructive therapy in orthopedics. Tissue Eng 11: 1198-211.
5. Chakkalakal, D.A., Strates, B.S., Garvin, K.L., Novak, J.R., Fritz, E.D., Mollner, T.J., and McGuire, M.H. (2001). Demineralized bone matrix as a biological scaffold for bone repair. Tissue Eng 7: 161-77.
6. Dexheimer, V., Mueller, S., Braatz, F., and Richter, W. (2011). Reduced reactivation from dormancy but maintained lineage choice of human mesenchymal stem cells with donor age. PloS one 6: e22980.
7. Friedenstein, A., Chailakhyan, R., and Gerasimov, U. (1987). Bone marrow osteogenic stem cells: in vitro cultivation and transplantation in diffusion chambers. Cell Tissue Kinet 20: 263-72.
8. García-Álvarez, F., Alegre-Aguarón, E., Desportes, P., Royo-Cañas, M., Castiella, T., Larrad, L., and Martínez-Lorenzo, M.J. (2011). Chondrogenic differentiation in femoral bone marrow-derived mesenchymal cells (MSC) from elderly patients suffering osteoarthritis or femoral fracture. Arch Gerontol Geriatr 52: 239-42.
9. Ghannam, S., Bouffi, C., Djouad, F., Jorgensen, C., and Noël, D. (2010). Immunosuppression by mesenchymal stem cells: mechanisms and clinical applications. Stem Cell Res Ther 1:1.
10. Hare, J.M., Traverse, J.H., Henry, T.D., Dib, N., Strumpf, R.K., Schulman, S.P., Gerstenblith, G., DeMaria, A.N., Denktas, A.E., and Gammon, R.S. (2009). A randomized, double-blind, placebo-controlled, dose-escalation study of intravenous adult human mesenchymal stem cells (prochymal) after acute myocardial infarction. J Am Coll Cardiol 54: 2277-86.
11. Hofmann, A., Ritz, U., Verrier, S., Eglin, D., Alini, M., Fuchs, S., Kirkpatrick, C.J., and Rommens, P.M. (2008). The effect of human osteoblasts on proliferation and neo-vessel formation of human umbilical vein endothelial cells in a long-term 3D co-culture on polyurethane scaffolds. Biomaterials 29: 4217-26.
12. Hosea Blewett, H.J. (2008). Exploring the mechanisms behind S-adenosylmethionine (SAMe) in the treatment of osteoarthritis. Crit Rev Food Sci Nutr 48: 458-63.
13. Hsieh, W.-C., Liau, J.-J., and Li, Y.-J. (2015). Characterization and cell culture of a grafted chitosan scaffold for tissue engineering. International Journal of Polymer Science 2015.
14. Jiang, Y., Jahagirdar, B.N., Reinhardt, R.L., Schwartz, R.E., Keene, C.D., Ortiz-Gonzalez, X.R., Reyes, M., Lenvik, T., Lund, T., and Blackstad, M. (2002). Pluripotency of mesenchymal stem cells derived from adult marrow. Nature 418: 41-49.
15. Labusca, L., Zugun-Eloae, F., Shaw, G., Botez, P., Barry, F., and Mashayekhi, K. (2012). Isolation and phenotypic characterisation of stem cells from late stage osteoarthritic mesenchymal tissues. Curr Stem Cell Res Ther7: 319-28.
16. Lee, J., Cuddihy, M.J., and Kotov, N.A. (2008). Three-dimensional cell culture matrices: state of the art. Tissue Eng Part B Rev14: 61-86.
17. Levenberg, S., Huang, N.F., Lavik, E., Rogers, A.B., Itskovitz-Eldor, J., and Langer, R. (2003). Differentiation of human embryonic stem cells on three-dimensional polymer scaffolds. PANS 100: 12741-6.
18. Maetzel, A., Li, L., Pencharz, J., Tomlinson, G., and Bombardier, C. (2004). The economic burden associated with osteoarthritis, rheumatoid arthritis, and hypertension: a comparative study. Ann Rheum Dis 63: 395-401.
19. Maniatopoulos, C., Sodek, J., and Melcher, A. (1988). Bone formation in vitro by stromal cells obtained from bone marrow of young adult rats. Cell Tissue Res 254: 317-30.
20. Martin, G.J., Jr., Boden, S.D., Titus, L., and Scarborough, N.L. (1999). New formulations of demineralized bone matrix as a more effective graft alternative in experimental posterolateral lumbar spine arthrodesis. Spine 24: 637-45.
21. Mulliken, J.B., Glowacki, J., Kaban, L.B., Folkman, J., and Murray, J.E. (1981). Use of demineralized allogeneic bone implants for the correction of maxillocraniofacial deformities. Ann Surg 194: 366-72.
22. Murphy, J.M., Dixon, K., Beck, S., Fabian, D., Feldman, A., and Barry, F. (2002). Reduced chondrogenic and adipogenic activity of mesenchymal stem cells from patients with advanced osteoarthritis. Arthritis Rheum 46: 704-13.
23. Polo-Corrales, L., Latorre-Esteves, M., and Ramirez-Vick, J.E. (2014). Scaffold design

for bone regeneration. J Nanosci Nanotechnol 14: 15-56.
24. Rosenthal, R.K., Folkman, J., and Glowacki, J. (1999). Demineralized bone implants for nonunion fractures, bone cysts, and fibrous lesions. Clin Orthop Relat Res 364: 61-9.
25. Supronowicz, P., Gill, E., Trujillo, A., Thula, T., Zhukauskas, R., Perry, R., and Cobb, R.R. (2013). Multipotent adult progenitor cell-loaded demineralized bone matrix for bone tissue engineering. J Tissue Eng Regen Med 10: 275-83.
26. Thibault, R.A., Scott Baggett, L., Mikos, A.G., and Kasper, F.K. (2009). Osteogenic differentiation of mesenchymal stem cells on pregenerated extracellular matrix scaffolds in the absence of osteogenic cell culture supplements. Tissue Eng Part A 16: 431-40.
27. Tran, C., Ouk, S., Clegg, N.J., Chen, Y., Watson, P.A., Arora, V., Wongvipat, J., Smith-Jones, P.M., Yoo, D., and Kwon, A. (2009). Development of a second-generation antiandrogen for treatment of advanced prostate cancer. Science 324: 787-90.
28. Upton, J., Boyajian, M., Mulliken, J.B., and Glowacki, J. (1984). The use of demineralized xenogeneic bone implants to correct phalangeal defects: a case report. J Hand Surg Am 9: 388-91.
29. Vilalta, M., Dégano, I.R., Bagó, J., Gould, D., Santos, M., García-Arranz, M., Ayats, R., Fuster, C., Chernajovsky, Y., and García-Olmo, D. (2008). Biodistribution, long-term survival, and safety of human adipose tissue-derived mesenchymal stem cells transplanted in nude mice by high sensitivity non-invasive bioluminescence imaging. Stem Cells Dev 17: 993-1004.
30. Wang, L., Li, Y., Zuo, Y., Zhang, L., Zou, Q., Cheng, L., and Jiang, H. (2009). Porous bioactive scaffold of aliphatic polyurethane and hydroxyapatite for tissue regeneration. Biomed Mater 4: 025003.
31. Yang, W., Both, S.K., Zuo, Y., Birgani, Z.T., Habibovic, P., Li, Y., Jansen, J.A., and Yang, F. (2015). Biological evaluation of porous aliphatic polyurethane/hydroxyapatite composite scaffolds for bone tissue engineering. J Biomed Mater Res A 103: 2251-59.
32. Yang, Z., Wu, Y., Li, C., Zhang, T., Zou, Y., Hui, J.H., Ge, Z., and Lee, E.H. (2011). Improved mesenchymal stem cells attachment and in vitro cartilage tissue formation on chitosan-modified poly (L-lactide-co-epsilon-caprolactone) scaffold. Tissue Eng Part A 18: 242-51.
33. Yoon, E., Dhar, S., Chun, D.E., Gharibjanian, N.A., and Evans, G.R. (2007). In vivo osteogenic potential of human adipose-derived stem cells/poly lactide-co-glycolic acid constructs for bone regeneration in a rat critical-sized calvarial defect model. Tissue Eng 13: 619-27.
34. Zotarelli Filho, I.J., Frascino, L.F., Greco, O.T., de Araújo, J.D., Bilaqui, A., Kassis, E.N., Ardito, R.V., and Bonilla-Rodriguez, G.O. (2013). Chitosan-collagen scaffolds can regulate the biological activities of adipose mesenchymal stem cells for tissue engineering. journal of Regenerative Medicine and Tissue Engineering 2: 12.
35. Zuk, P.A., Zhu, M., Ashjian, P., De Ugarte, D.A., Huang, J.I., Mizuno, H., Alfonso, Z.C., Fraser, J.K., Benhaim, P., and Hedrick, M.H. (2002). Human adipose tissue is a source of multipotent stem cells. Mol Biol Cell 13: 4279-95.
36. Zuk, P.A., Zhu, M., Mizuno, H., Huang, J., Futrell, J.W., Katz, A.J., Benhaim, P., Lorenz, H.P., and Hedrick, M.H. (2001). Multilineage cells from human adipose tissue: implications for cell-based therapies. Tissue Eng 7: 211-28.

Journal of Cell and Molecular Research (2018) 10 (1), 18-26 DOI: 10.22067/jcmr.v10i1.67357

Research Article

Global Analysis of Gene Expression and Identification of Modules in *Echinacea purpurea* Using Systems Biology Approach

Ahmad Tahmasebi[1], Farzaneh Aram[2], Hassan Pakniyat[1], Ali Niazi[2], Elahe Tavakol[1], Esmaeil Ebrahimie[2,3,4,5*]

[1] *Department of Crop Production and Plant Breeding, College of Agriculture, Shiraz University, Shiraz, Iran*
[2] *Institute of Biotechnology, Shiraz University, Shiraz, Iran*
[3] *School of Medicine, The University of Adelaide, Adelaide, Australia*
[4] *School of Information Technology and Mathematical Sciences, Division of Information Technology, Engineering and the Environment, University of South Australia, Adelaide, Australia*
[5] *School of Biological Sciences, Faculty of Science and Engineering, Flinders University, Adelaide, Australia*

Received 10 September 2017 Accepted 25 November 2017

Abstract

Co-expression analysis is a useful tool to analysis data and detection of genes that act in the same pathway or biological process. *Echinacea purpurea* is one of the most important medicinal plant of the Asteraceae family that is known as antioxidative and antiviral agent. Despite medicinal importance of *E. purpurea*, very few reports are available for metabolic mechanisms in this plant. With the aim to elucidate the gene expression profiling and identification of modules in *E. purpurea*, we performed a systems biology analysis on publicly available transcriptome data. Gene ontology and KEGG pathway enrichment analysis revealed that the unigenes were highly related to the cellular process, primary metabolic process, carbon metabolism and biosynthesis of antibiotics. The co-expression networks divided genes into multiple modules. Of these, module M2 associated with secondary metabolic process. Moreover, a total of 47 transcription factor families such as bHLH, bZIP, C2H2, MYB and WRKY in modules were identified. These findings can provide an overall picture for better understanding the gene expression patterns and common transcriptional mechanisms in *E. purpurea*.

Keywords**:** *Co-expression analysis, Echinacea purpurea, Transcriptomics data*

Introduction

The emergence of sequencing technology and bioinformatics tools provide an opportunity for study important aspects of metabolic processes and complexity of transcriptome in non-model plant species. Gene co-expression analyses can uncover the functional interaction between genes. A co-expression network represents pairwise interactions among genes which based on these relationships, it is possible to find gene clusters (modules) that involved in common biological pathways (Guo et al., 2014; Lee et al., 2010). Currently, availability of transcriptomics data for various medicinal plants also can be used as tools to explore transcriptome information and molecular mechanisms, specifically related to the secondary metabolites. The biosynthesis of secondary metabolites is a complex process and regulate by transcriptional, translational and post-translational mechanisms. The accumulation and synthesis of these metabolites affect by different factors. Transcriptome analysis can facilitate identification of key genes and regulators associated with such bioactive compounds (Graham et al., 2010; Xiao et al., 2013). Investigation of the network controlling the biosynthesis, transportation, accumulation of secondary metabolites will be helpful for production of these metabolites. Engineering biosynthetic pathways can be considered as an approach but is still limited, partially due to complexity of biosynthesis pathways (Yang et al., 2012). Identification and annotation of transcription factors as regulatory proteins of gene expression can assist greatly in this regard.

Echinacea purpurea is an important medicinal plant which belongs to Asteraceae family. The roots, flowers and aerial parts are used mainly for medicinal purposes. In recent years, *E. purpurea* has been considered for high medicinal value and industrial applications in pharmaceutical and food industries. It has antioxidant, anti-inflammatory and immuno-stimulating properties and is used for treating viral and inflammatory diseases. Nowadays, numerous photochemical constituents include polysaccharides, caffeic acid derivatives and

* Corresponding author E-mail: esmaeil.ebrahimie@adelaide.edu.au

alkylamides; have been identified from *E. purpurea* (Pellati et al., 2004; Tsai et al., 2012). Despite the importance of this plant, mechanism and regulation of biosynthesis of metabolites have been rarely investigated. In this study, by using transcriptome data and gene co-expression network analysis, we provide global expression patterns of genes and detected pathways, modules and transcription factors to achieve insights into particularly molecular mechanisms of secondary metabolism-related genes in *E. purpurea*.

Materials and Methods

Data collection and functional annotation analysis

The raw expression data of different tissues of *E. purpurea* were obtained from the Medicinal Plant Genomics Resource database (MPGR, http://medicinalplantgenomics.msu.edu/) (Góngora-Castillo et al., 2012). All expressed transcripts were searched against the Arabidopsis Information Resource (TAIR) (http://www. Arabidopsis.org) using the BLASTX.

GO enrichment analysis of the transcripts was performed using Gene Ontology (GO, http://wego.genomics.org.cn/cgi-bin/wego/index.pl) database for categories of biological process (BP), molecular function (MF) and cellular components (CC). DAVID database (Dennis et al., 2003) was carried out to find important pathways according to the KEGG pathway database. Significantly enriched pathways were determined using a Benjamini test (*P* value <0.05).

Co-expressed gene network analysis

A Co-expression analysis was conducted with the Weighted Gene Co-expression Network Analysis (WGCNA) (Langfelder and Horvath, 2008). First, transcripts with low expression were filtered out, then expression matrix was used to cluster groups of highly co-expressed genes. The pairwise gene correlation matrix was transformed into a weighted matrix with a soft thresholding power of 10 to calculate a topological overlap matrix (TOM) and creating a hierarchical cluster tree. Finally, the modules were identified with minimum module size of 100, the power of 8 and TOMType of signed.

Enrichment analysis of modules

To interpret of functional characterization of modules that were identified by the WGCNA analysis, a separate enrichment analysis was performed to transcript list of modules using agriGO (Du et al., 2010). Moreover, to identify and classify transcription factors (TFs) corresponding to each module, transcripts were aligned to AtTFDB database (http://arabidopsis.med.ohio-state.edu/AtTFDB/) using BLASTX with a cut-off E-value ≤ 10−5.

Results and Discussion

Gene ontology (GO) and KEGG pathway analysis

To obtain insight into functions and characterize the *E. purpurea* transcriptome, all unigenes from different tissues were annotated using BLASTX searches against the TAIR database. A total of 73,643 unigenes (69.74%) were matched to TAIR database. GO analysis was used to predict the function of unigenes by classifying them into three major functional categories (biological process, cellular component and molecular function) (Figure 1). In the category of molecular function, catalytic activity (GO:0003824) with 4,168, binding (GO:0005488) with 2,421 and transporter activity (GO:0005215) with 1,071 transcripts were predominant. In the biological process group, unique sequences related to cellular process (GO:0009987) with 4056, primary metabolic process (GO:0044238) with 3872, localization (GO:0051179) with 1408, and cellular component organization (GO:0071840) with 999 transcripts were found. Moreover, secondary metabolic process (GO:0019748) was one of most common categories. In the cellular component domain, cell part (GO:0044464), organelle (GO:0043226), and macromolecular complex (GO:0032991) were shown to be the top 3 clusters.

KEGG pathway enrichment analysis of unigenes was also carried out in web-based DAVID. Of the 15,085 unigenes, 2,129 genes were categorized into 41 pathways which 7 pathways include carbon metabolism, biosynthesis of antibiotics, glycolysis/gluconeogenesis, peroxisome, glycerolipid metabolism, endocytosis and fatty acid degradation, were significantly enriched (Table 1).

Identification of the genes associated with phenylpropanoid biosynthesis

In plants, phenylpropanoid pathway is a source of metabolites and starting point for the generation of secondary metabolites such as phenolic volatiles, flavonoids and lignans (Fraser and Chapple, 2011; Vogt, 2010). The phenylpropanoids and their derivatives play also key roles in plant responses to biotic and abiotic stresses. In this study, a total of 491 unigenes were obtained that related to

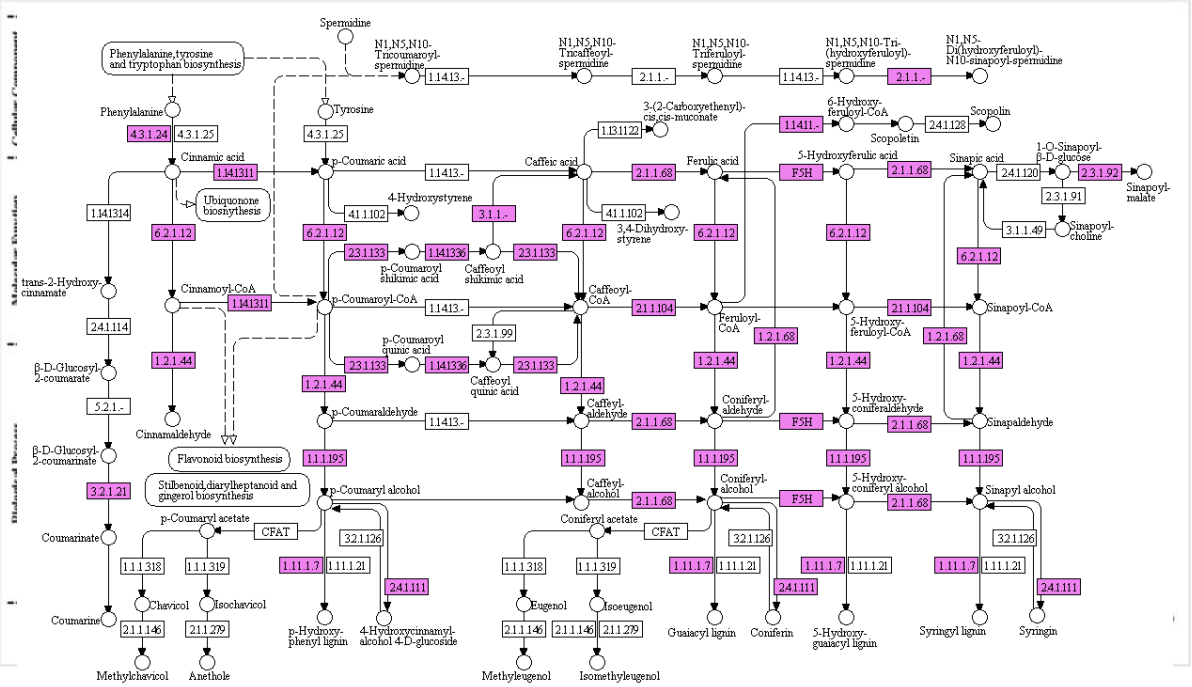

Figure 2. Pathway classification of the unigenes into five major categories. Colored boxes indicate the molecular functional identified genes.

Table 1. The KEGG pathway enrichment analysis of the total unigenes.

Term	Gene count*	Percentage	p-value
Carbon metabolism	217	1.5	0.000
Biosynthesis of antibiotics	353	2.4	0.000
Glycolysis / Gluconeogenesis	97	0.6	0.009
Peroxisome	76	0.5	0.013
Glycerolipid metabolism	48	0.3	0.013
Endocytosis	117	0.8	0.026
Fatty acid degradation	38	0.3	0.040

* The number and percentage of genes in each pathway.

phenylpropanoid biosynthesis pathway (Figure 2). Several key enzymes such as phenylalanine ammonia-lyase [EC:4.3.1.24], peroxidase [EC:1.11.1.7] and caffeoyl-CoA O-methyltransferase [EC:2.1.1.104] that involved in phenylpropanoid biosynthesis were expressed. Phenolic compounds are derived from phenylalanine through the phenylpropanoid pathway. The pathway is initiated by ammonia-lyase (PAL) and cinnamate-4-hydroxylase (C4H), which their activities are positively correlated to phenylpropanoid product accumulation (Ali and McNear, 2014; Lee and Scagel, 2010). The enhancement of PAL and C4H activities was accompanied with an increase in the cichoric acid content in *E.purpurea.* In addition, previous studies have reported that enzyme activity of PAL changes by application of GA3 that has resulted in accumulation of flavonoids, lignin and starch (Abbasi et al., 2012).

Gene co-expression network analysis

To detect networks of co-expressed genes in *E. purpurea*, systems biology approach was performed by weighted gene correlation network analysis (WGCNA). WGCNA clusters genes based on gene expression similarity into modules. After low expression filtering, a FPKM (fragments per kilobase of transcript per million fragments mapped) matrix of different tissues include 21,363

transcripts were obtained for construct gene co-

expression networks. The genes were clustered based on similar patterns. A dendrogram and correlation heat map was generated to visualize topological overlap values between genes in the modules (Figure 3). In total, 25 modules were identified which ranged in size from 1,783 members to 245 members and tagged with different colors. Turquoise (containing 1,783 genes), blue (1,495 genes), brown (1,472 genes), yellow (1,326 genes) and green (1,310 genes) were five major modules. Based on the eigengenes and a minimum cut height (0.5), modules grouped in seven distinct clades (Figure 4). Subsequently, the MEtur and MEsalmon modules had very similar expression profiles, thus these modules were merged and renamed as M1. Similarly, MEdarkturquoise and MEpink were merged and renamed as M2, whereas MEcyan, MEgreen, MEbrown and MEmidnightblue were merged and renamed as M3. MEdarkgreen, MEred, MElightgreen and MEyellow were renamed as M4. MEmagenta, MEturquoise, MEroyalblue and MEtan were renamed as M5. MEgrey60, MEorange, MEdarkred, MElightyellow, MEblack and MEgreenyellow were merged and renamed as M6. MElightcyan, MEdarkgrey and MEpurple were renamed as M7.

Functional annotation of modules

To find the biological functions associated with modules, the modules were submitted to enrichment analysis. A FDR<0.01 was used to define significantly enriched terms. All of the modules were significantly enriched for at least one GO term. The biological process GO terms of each module are presented in Additional file. Module M1 was associated with aspects of the cellular process according to gene ontology, and the module was highly enriched for cellular component organization (GO:0016043), reproductive process (GO:0022414), reproduction (GO:0000003), metabolic process (GO:0008152) and response to stimulus (GO:0050896) terms that are related to the immune system (Table S1). Also, 583 genes were identified from this module that were involved in primary metabolic process. Module M2 enriched for functions related to metabolic process. The module also was associated with several GO terms that involved in developmental process (GO:0032502) and multicellular organismal process (GO:0032501). Interestingly, 37 and 20 genes were associated with secondary metabolic process (GO:0019748) and pigment metabolic process (GO:0042440), respectively (Table S2). Module M3 linked to localization (GO:0051179), immune system process (GO:0002376), response to stimulus (GO:0050896) and growth (GO:0040007).

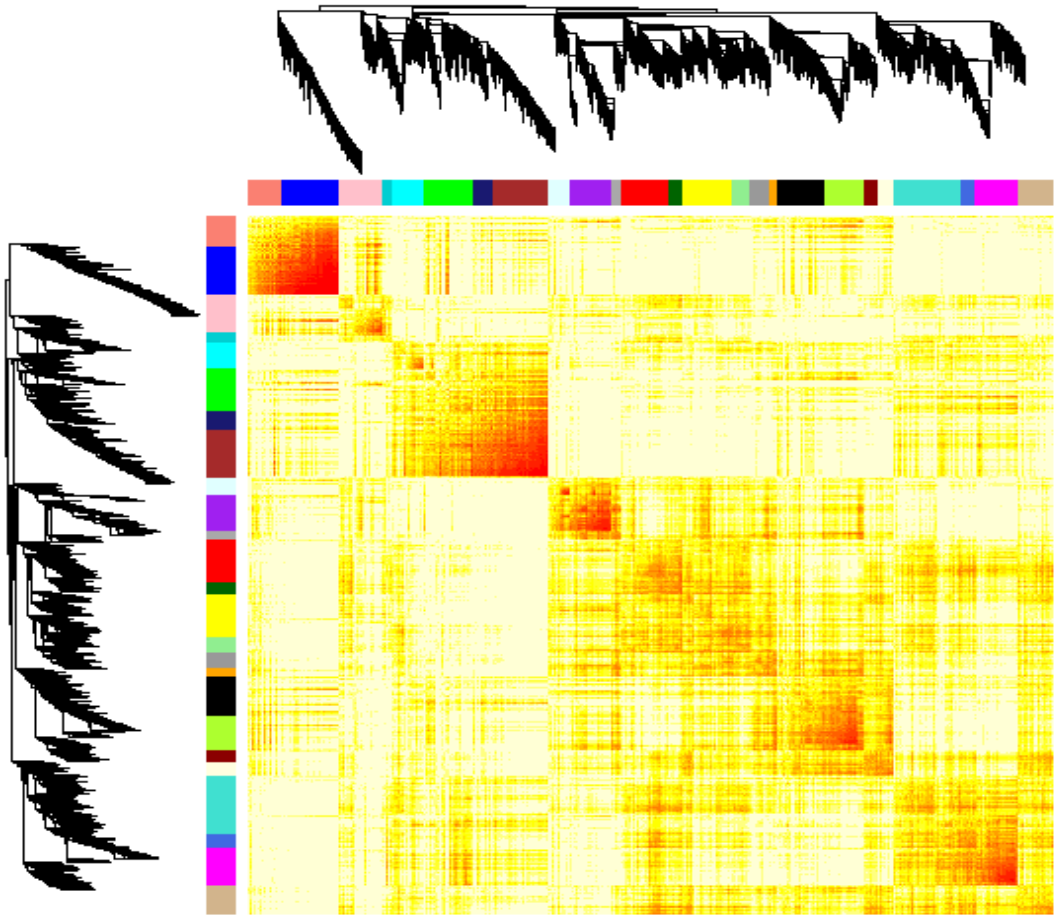

Figure 3. Topological overlap matrix plot (TOMplot) for all WGCNA modules. Modules are illustrated by different colors. Red color in the heat map represents the genes that showed high correlation.

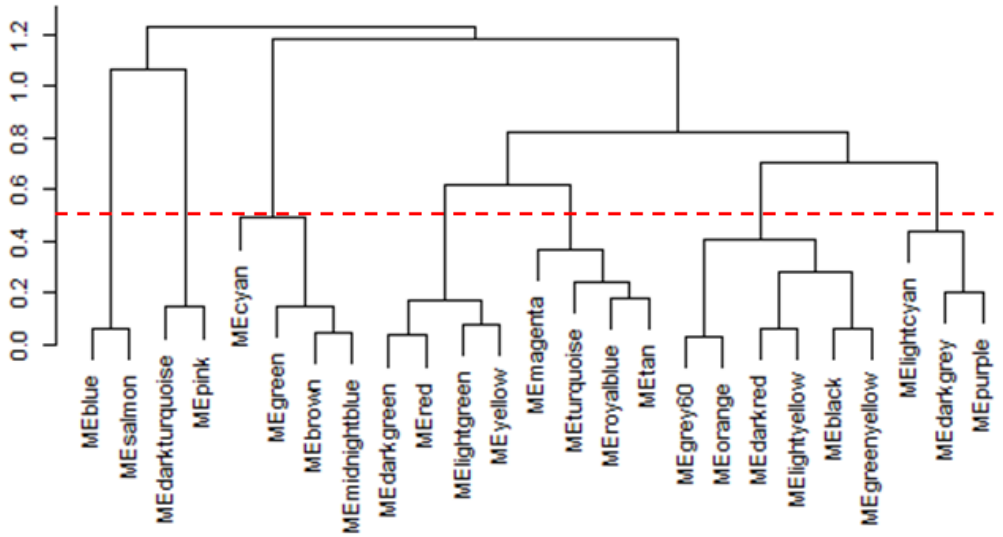

Figure 4. Clustering dendrogram of modules. The horizontal line showing merge cut height of 0.5.

Under biological regulation, 205 genes also were associated with regulation of primary metabolic process (GO:0080090). For the response to stimulus, 51 genes were associated with the response to auxin stimulus (GO:0009733) (Table S3). Module M4 was related to reproductive process (GO:0022414), primary metabolic process (GO:0044238) and macromolecule metabolic process (GO:0043170). Moreover, genes that are involved in organ development (GO:0048513) were in this module (Table S4). Likewise, in module M5, M6 and M7, enriched for functions related to chromatin organization multicellular organismal process (GO:0032501), developmental process (GO:0032502) and reproduction (GO:0000003) (Table S5, S6 and S7). The results showed that these modules involved in various biological processes.

In functional annotation observed that some genes of module M2 involved in secondary metabolic process. To evaluate details of metabolites related to module M2, metabolome data of *E. purpurea* available at PMR database (PMR; http://metnetdb.org/PMR/) (Hur et al., 2013) was used. The genes present in module M2 were searched against correlation data of metabolomes to determine metabolites synthesized by module M2. The results indicated that module M2 was significantly correlated with biosynthesis of monoterpenoids, fatty acid derivatives, isoflavonoids and anthocyanidins.

Identification of transcription factors association with modules

Transcription factors (TFs) are key set of proteins that regulate gene expression and function as central regulators in many important biological processes such as growth, development and secondary metabolism (Mitsuda and Ohme-Takagi, 2009; Patra et al., 2013). To assess the regulatory mechanisms of detected modules, unigene sequences of first five WGCNA modules were searched against AtTFDB database. Based on BLASTX, TFs were assigned to different modules and classified into different families. Generally, 47 TF families such as AP2/ERF-ERF, bHLH, bZIP, C2H2, MYB and WRKY were identified in all five modules (Table 2). The turquoise module was enriched in bHLH, HB-HD-ZIP, bZIP, TUB and WRKY TF families. The blue module also included C2H2, AP2/ERF-ERF and bHLH TF families which associated with gibberellic acid mediated signaling pathway. The brown module displayed the largest number of GRAS, AP2/ERF-ERF and WRKY TF families. The yellow and green modules were particularly enriched for AP2/ERF-ERF, WRKY and bHLH.

The different TF families were also reported to regulate anthocyanin and flavonoid biosynthesis. The anthocyanin biosynthesis starts from amino acid phenylalanine. Most of the structural genes in the pathway are coordinately regulated by the MBW complex, which is composed of the MYB, bHLH and WDR proteins. TFs belonging to these three groups are functionally conserved among plant species. In Arabidopsis, early genes of anthocyanin pathway are positively regulated by MYB TF family, MYB11, MYB12 and MYB111, however late pathway genes are regulated by MBW complex. However, the MYB (phMYB27) negatively regulates anthocyanin biosynthesis in Petunia. The phMYB27 is up-regulated in shadow-grown leaves and is repressed under high light. Light-induced expression pattern of TFs as activator or repressor in Arabidopsis and Petunia is similar that suggest the conserved controlling mechanism of anthocyanin synthesis in vegetative tissues (Patra et al., 2013). In Arabidopsis, over-expression of the MYB TF (AtPAp1) Led to up-regulation of PAL, CHS and DER genes that subsequently enhanced production of lignin (Deluc et al., 2006). Additionally, NAC TF family has transcriptional activation effect on anthocyanin pathway genes in high light condition (Patra et al., 2013).This TF family especially present in brown and green modules. AP2/ERF-ERF and WRKY TF families present in all modules. These TF families act as regulatory proteins of major indole alkaloids pathway (Patra et al., 2013). C2H2 TF, as a member of Zinc-finger proteins (ZFPs) transcription factor family, is involved in controlling various abiotic stress and phytohormone responses, floral development (Wu et al., 2008), secondary metabolism and cell wall structure (Liu et al., 2015). In *Aspergillus nidulans*, C2H2 TF (MtfA) have been identified that regulate the secondary metabolism (Ramamoorthy et al., 2013). GRAS proteins are an important TF family that play key regulatory role in the development, abiotic stress and phytochrome signaling (Hirsch and Oldroyd, 2009). According to our data, GRAS TF family was strongly enriched in brown, yellow and green modules, this result suggests that this TF might associate with secondary metabolite production. Moreover, GRAS proteins function as regulator in GA3 signaling and biosynthesis. In *E. purpurea*, GA3 treatment resulted in higher production of caftaric acid, cichoric acid and anthocyanins. We propose GRAS TF family has the potential to secondary metabolic engineering in *E. purpurea*.

In conclusion, this study, using systems biology approach, provides a transcriptional overview of *E. purpurea*. The analysis also highlights several

Table 2. List of TF families in the first five modules

Turquoise		Blue		Brown		Yellow		Green	
TF family	N*	TF family	N	TF family	N	TF family	N	TF family	N
bHLH	5	C2H2	5	GRAS	15	GRAS	10	AP2/ERF-ERF	8
HB-HD-ZIP	5	AP2/ERF-ERF	3	AP2/ERF-ERF	14	AP2/ERF-ERF	7	WRKY	7
bZIP	4	bHLH	3	WRKY	14	MADS-MIKC	6	bHLH	6
TUB	4	MYB-related	2	C2H2	13	C2H2	6	HSF	5
WRKY	4	Trihelix	2	bHLH	9	MYB-related	6	MYB-related	5
AP2/ERF-ERF	3	C2C2-CO-like	2	NAC	8	bZIP	4	bZIP	5
B3	3	C3H	1	Tify	6	Trihelix	4	NAC	5
GARP-G2-like	3	MYB	1	MYB	5	C3H	4	GARP-G2-like	4
HB-other	2	TCP	1	HSF	4	HB-HD-ZIP	3	GRAS	4
MYB-related	2	bZIP	1	B3	3	bHLH	3	HB-HD-ZIP	3
NAC	2	FAR1	1	FAR1	3	TCP	3	HB-other	2
FAR1	2	NAC	1	bZIP	3	LOB	2	B3	2
PLATZ	2	WRKY	1	C3H	3	NAC	2	MYB	2
C2H2	2	CSD	1	DBP	2	C2C2-Dof	2	HB-BELL	2
C3H	2	GARP-G2-like	1	MYB-related	2	HB-other	2	zf-HD	2
GRAS	2	OFP	1	C2C2-GATA	2	SBP	2	C2C2-Dof	1
AP2/ERF-AP2	1	HB-BELL	1	GARP-G2-like	2	FAR1	2	RWP-RK	1
E2F-DP	1	SBP	1	C2C2-Dof	1	MYB	2	B3-ARF	1
TCP	1			HB-HD-ZIP	1	SRS	2	C2H2	1
EIL	1			TUB	1	GARP-G2-like	2	C2C2-GATA	1
Tify	1			MADS-MIKC	1	CSD	1	Trihelix	1
C2C2-GATA	1			NF-YB	1	B3	1	FAR1	1
HB-BELL	1			BES1	1	DBB	1	NF-YA	1
B3-ARF	1			C2C2-CO-like	1	NF-YB	1	C3H	1
HSF	1			LOB	1	WRKY	1		
RWP-RK	1			NF-YC	1	B3-ARF	1		
ULT	1			zf-HD	1	C2C2-GATA	1		
SRS	1			HB-other	1	E2F-DP	1		
BES1	1					HB-KNOX	1		
LOB	1					MADS-M-type	1		
						BBR-BPC	1		
						HB-BELL	1		

important TFs which their function as regulatory elements involved in secondary metabolism and stress responses. Although, some pathways have not yet been identified for *E. purpurea*, these TFs such as GRAS, AP2/ERF-ERF, bHLH, bZIP, C2H2, MYB and WRKY can be considered as promising candidates for pathway studies and manipulation toward accumulation of valuable products.

References

1. Abbasi BH., Stiles AR., Saxena PK. and Liu C-Z. (2012) Gibberellic acid increases secondary metabolite production in Echinacea purpurea hairy roots. Applied biochemistry and biotechnology 168: 2057-2066.
2. Ali MB. and McNear DH. (2014) Induced transcriptional profiling of phenylpropanoid pathway genes increased flavonoid and lignin content in Arabidopsis leaves in response to microbial products. BMC plant biology 14: 84.
3. Deluc L., Barrieu F., Marchive C.,

Lauvergeat V., Decendit A., Richard T., Carde J-P., Mérillon J-M. and Hamdi S. (2006) Characterization of a grapevine R2R3-MYB transcription factor that regulates the phenylpropanoid pathway. Plant physiology 140: 499-511.
4. Dennis G., Sherman BT., Hosack DA., Yang J., Gao W., Lane HC. and Lempicki RA. (2003) DAVID: database for annotation, visualization, and integrated discovery. Genome biology 4: R60.
5. Du Z., Zhou X., Ling Y., Zhang Z. and Su Z. (2010) agriGO: a GO analysis toolkit for the agricultural community. Nucleic acids research 38: W64-W70.
6. Fraser CM. and Chapple C. (2011) The phenylpropanoid pathway in Arabidopsis. The Arabidopsis Book, e0152.
7. Góngora-Castillo E., Childs KL., Fedewa G., Hamilton JP., Liscombe DK., Magallanes-Lundback M., Mandadi KK., Nims E., Runguphan W. and Vaillancourt B. (2012) Development of transcriptomic resources for interrogating the biosynthesis of monoterpene indole alkaloids in medicinal plant species. PloS one 7: e52506.
8. Graham IA., Besser K., Blumer S., Branigan CA., Czechowski T., Elias L., Guterman I., Harvey D., Isaac PG. and Khan AM. (2010) The genetic map of Artemisia annua L. identifies loci affecting yield of the antimalarial drug artemisinin. science 327: 328-331.
9. Guo K., Zou W., Feng Y., Zhang M., Zhang J., Tu F., Xie G., Wang L., Wang Y. and Klie S. (2014) An integrated genomic and metabolomic framework for cell wall biology in rice. BMC genomics 15: 596.
10. Hirsch S. and Oldroyd GE. (2009) GRAS-domain transcription factors that regulate plant development. Plant signaling & behavior 4: 698-700.
11. Hur M., Campbell AA., Almeida-de-Macedo M., Li L., Ransom N., Jose A., Crispin M., Nikolau BJ. and Wurtele ES. (2013) A global approach to analysis and interpretation of metabolic data for plant natural product discovery. Natural product reports 30: 565-583.
12. Langfelder P. and Horvath S. (2008) WGCNA: an R package for weighted correlation network analysis. BMC bioinformatics 9: 559.
13. Lee I., Ambaru B., Thakkar P., Marcotte EM. and Rhee SY. (2010) Rational association of genes with traits using a genome-scale gene network for Arabidopsis thaliana. Nature biotechnology 28: 149-156.
14. Lee J. and Scagel CF. (2010) Chicoric acid levels in commercial basil (Ocimum basilicum) and Echinacea purpurea products. Journal of functional foods 2: 77-84.
15. Liu Q., Wang Z., Xu X., Zhang H. and Li C. (2015) Genome-wide analysis of C2H2 zinc-finger family transcription factors and their responses to abiotic stresses in poplar (Populus trichocarpa). PloS one 10: e0134753.
16. Mitsuda N. and Ohme-Takagi M. (2009) Functional analysis of transcription factors in Arabidopsis. Plant and Cell Physiology 50: 1232-1248.
17. Patra B., Schluttenhofer C., Wu Y., Pattanaik S. and Yuan L. (2013) Transcriptional regulation of secondary metabolite biosynthesis in plants. Biochimica et Biophysica Acta (BBA)-Gene Regulatory Mechanisms 1829: 1236-1247.
18. Pellati F., Benvenuti S., Magro L., Melegari M. and Soragni F. (2004) Analysis of phenolic compounds and radical scavenging activity of Echinacea spp. Journal of Pharmaceutical and Biomedical Analysis 35: 289-301.
19. Ramamoorthy V., Dhingra S., Kincaid A., Shantappa S., Feng X. and Calvo AM. (2013) The putative C2H2 transcription factor MtfA is a novel regulator of secondary metabolism and morphogenesis in Aspergillus nidulans. PLoS One 8: e74122.
20. Tsai Y-L., Chiu C-C., Chen JY-F., Chan K-C. and Lin S-D. (2012) Cytotoxic effects of Echinacea purpurea flower extracts and cichoric acid on human colon cancer cells through induction of apoptosis. Journal of ethnopharmacology 143: 914-919.
21. Vogt T. (2010) Phenylpropanoid biosynthesis. Molecular plant 3: 2-20.
22. Wu C., You C., Li C., Long T., Chen G., Byrne ME. and Zhang Q. (2008) RID1, encoding a Cys2/His2-type zinc finger transcription factor, acts as a master switch from vegetative to floral development in rice. Proceedings of the National Academy of Sciences 105: 12915-12920.
23. Xiao M., Zhang Y., Chen X., Lee E-J., Barber CJ., Chakrabarty R., Desgagné-

Penix I., Haslam TM., Kim Y-B. and Liu E. (2013) Transcriptome analysis based on next-generation sequencing of non-model plants producing specialized metabolites of biotechnological interest. Journal of biotechnology 166: 122-134.

24. Yang CQ., Fang X., Wu XM., Mao YB., Wang LJ. and Chen XY. (2012) Transcriptional regulation of plant secondary metabolism. Journal of integrative plant biology 54: 703-712.

Research Article

Investigation of coa Gene Polymorphism in Clinical Isolates of Staphylococcus aureus in North of Iran

Mohammad Reza Izadpanah, Leila Asadpour*

Department of Biology, Rasht Branch, Islamic Azad University, Rasht, Iran

Received 3 January 2016 Accepted 24 September 2018

Abstract

Staphylococcus aureus is a common pathogen potentially able to cause a wide range of infectious diseases in human and animals and coagulase enzyme is one of the important virulence factors of this bacterium. Polymorphism of the coagulase encoding gene (*coa*) is one of the molecular-based typing methods of *S. aureus* isolates. In this study, the polymorphism of the coagulase gene among MRSA and MSSA isolates were investigated using PCR-RFLP analysis. To perform coagulase gene typing, the repeated units encoding hypervariable regions of coagulase gene of 30 clinical isolates of *S. aureus* were amplified by the PCR technique; this was followed by *Alu*I restriction enzyme digestion and analysis of restriction fragment length polymorphism (RFLP) patterns. In total two amplicons (680 bp and 750 bp) and four distinct RFLP banding patterns (280+400, 340+340, 280+470, and no digested amplicon of 750 bp) were observed. Genotype with PCR-RFLP patterns of 280+400 bp was predominated. The results indicated polymorphism in the investigated regions of coagulase gene. This polymorphism can be used for identification of *S. aureus* isolates and showing the epidemiological relationship among them.

***Keywords*:** *Staphylococcus aureus*, *coa* gene, PCR-RFLP, Polymorphism

Introduction

Staphylococcus aureus is a common pathogen potentially able to cause a wide range of infectious diseases, including skin and soft tissue infections, urinary tract infections, sepsis, endocarditis, pneumonia, deep abscess formation and osteomyelitis in both community and hospitals (Daum, 2007, Muder et al., 2006). In addition, *S. aureus* is responsible for toxin-mediated diseases, such as toxic shock syndrome (Dinges et al., 2000). The emergence of hypervirulent strains and the rise in antibiotic resistance increased public health concern of *S. aureus* (Shorr et al., 2006). Several cell wall associated components and extracellular proteins of *S. aureus* act as pathogenicity factors (Foster, 2005). Staphylocoagulase is an important virulence factor during *S. aureus* infection process, causes the clotting of host plasma and is required for abscess formation, bacterial persistence in host tissues and *S. aureus* lethal bacteremia (Cheng et al., 2010, McAdow et al., 2012). The biological activity of coagulase is caused by prothrombin binding domain. At the 3' end of coagulase encoding gene, 81 bp heterogenic tandem repeats encoding repeated 27 amino acid sequences have been recognized which are polymorphic in both number and sequence. Clotting occurs independently of the repeats but polymorphism of this region can be used for differentiation of *S. aureus* isolates and investigating the epidemiological relationship among them (Mahmoudi et al., 2017, McAdow et al., 2012). Because of diversity in size and sequence, PCR amplification of 3' end of the *coa* gene from different *S. aureus* species may yield amplicons of different sizes and different restriction sites. PCR products of the *coa* gene can be digested by *Alu*I, *Cfo*I, *Hae*III (Janwithayanuchit et al., 2006). *Alu*I appears to yield the highest RFLP in restriction enzyme analysis and allows a greater discriminatory power than others. So *coa* gene PCR- and *Alu*I RFLP-based typing can be used as a simple and effective method for typing of *S. aureus* clinical isolates (Schwarzkopf et al., 1994).

The present study was aimed to investigate *coa* gene polymorphism in clinical isolates of methicillin resistant and methicillin sensitive *Staphylococcus aureus* from various infection sources in Rasht, the north of Iran, using PCR and *Alu*I restriction fragment length polymorphism.

Materials and Methods

Bacterial isolates

A total of 30 *S. aureus* isolated from various sources including urine (n=17), skin (n=6), blood

* Corresponding author E-mail: Asadpour@iaurasht.ac.ir

(n=3) and synovial fluid (n=2) were identified using several tests such as gram staining, catalase test, growth onto MSA, haemolysis onto blood agar and tube coagulase test. A single isolate from individual patients was subjected to this study and all *S. aureus* isolates were screened for methicillin resistance by disc diffusion (6 µg/ml oxacillin) on Mueller Hinton agar with 2% NaCL.

DNA extraction and Ribotyping

The bacterial genomic DNA was extracted using Kit for the isolation of DNA from gram positive bacteria (Cinnagen, Iran). All the isolates were confirmed as *S. aureus* as described previously (Izadpanah & Asadpour, 2015) .

***Coa* gene amplification**

The *coa* gene was amplified by using Forward primer: 5′ ATAGAGATGCTGGTACAGG 3′ and reverse primer: 5′ GCTTCCGATTGTTCGATGC 3′ as described previously (Anggraini et al., 2017) with a thermal cycling program of 94°C for 5 min, followed by 30 cycles of 95°C for 30 sec, 55°C for 45 sec and 72°C for 2 min. The final elongation step was 10 minutes at 72^{0C}. PCR products were electrophoresed on a 1.5 % agarose gel, stained with gel red DNA stain and visualized under UV light. The 100-bp marker (MBI Fermentas) was used as a size standard for the calculation of the sizes of the *coa* gene.

RFLP of *Coa* gene amplicon

The *coa* gene restriction analysis was carried out by using *Alu*I (MBI Fermentas). 10µl of *coa* gene PCR products were digested with 10U of *Alu*I restriction enzyme in a 20 µL reaction mixture and incubated at 37ºC for 16 hours.

PCR- RFLP reproducibility was tested by twice submitting PCR products to *AluI* digestion. The generated restricted fragments were separated on 1.5 % agarose gel.

Results

In total 30 *S. aureus* strains were isolated from clinical samples using conventional biochemical test. 21 isolates (70%) phenotypically recognized as MRSA. PCR amplification of *coa* gene of the isolates resulted in two different size fragments including 680 bp (17 isolates) and 750 bp (13 isolates). All the PCR products were digested with *Alu I* enzyme and four different RFLP patterns were observed. Digestion of 680 bp amplicons in 13 isolates produced two fragments of 400 bp and 280 bp (pattern 1) and in 6 isolates only one fragment of 340bp was obtained (pattern 2). For 4 isolates *Alu*I digestion produced two size fragments of 470 bp and 280 bp (pattern 3) and in 7 isolates *Alu*I had no restriction site on the amplicon (pattern 4). Some of the obtained results are shown in figures 1and 2.

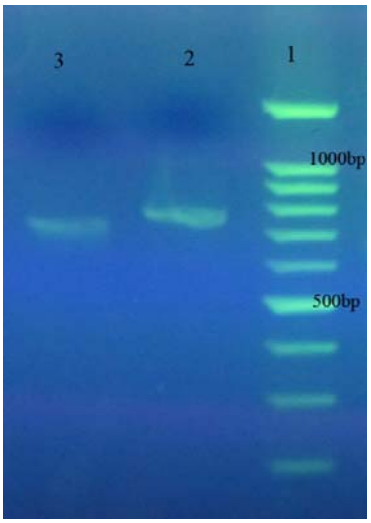

Figure 1. Polymorphism in *coa* gene PCR amplicons. Lane 1: 100bp DNA marker, Lane 2: 750 bp PCR amplicon, Lane 3: 680 bp amplicon.

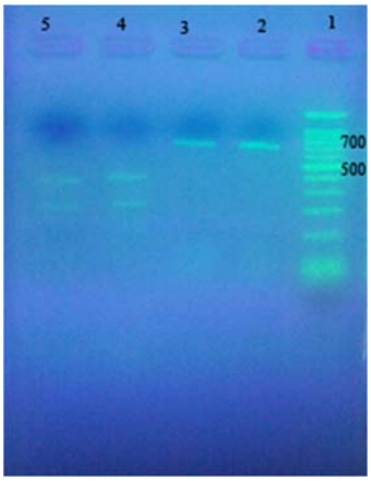

Figure 2. RFLP patterns obtained from *Alu*I digestion of *coa* gene amplicons. Lane 1: 100bp DNA marker, Lane 2: pattern 4 (750 bp PCR product without digestion), Lane 4: pattern 1 (two size fragments of 400 bp and 280 bp).

Out of 21, 7 MRSA isolates (33%) showed restriction pattern 1, 5 isolates (23%) showed restriction pattern 2. In addition, pattern 3 and 4 were observed in 4 (19%) and 5 (23%) isolates, respectively.

Discussion

In the present study, the polymorphism existing in *coa* gene of 30 *S. aureus* strains including MRSA and MSSA isolated from clinical samples in Rasht city, north of Iran, was investigated. The result of PCR-based RFLP on *coa* gene of the test bacteria showed 2 *coa* PCR type and 4 different RFLP pattern. In different studies, the *coa* gene polymorphism has been used as a simple and accurate method for molecular typing of *S. aureus* strains. In a study conducted by Babu et al, the PCR-RFLP results of 14 coagulase positive *S. aureus* gave two different sets of amplicons and 5 different *Alu*I digestion patterns (Babu et al., 2014). Ishino et al (2007) classified 678 *S. aureus* isolates into 8 classes and the sizes of the PCR products of *coa* gene ranged from 350 to 917 bp. Sanjiv et al (2008) found three types of *coa* gene products of 600, 680 or 850 bp size and three distinct RFLP patterns in 20 *S. aureus* isolates. Talebi-Satlou et al (2012) determined 4 classes of PCR amplicons ranging from 410-790 bp and 6 distinct *Hea*III RFLP patterns in the 3' end of *coa* gene in 26 *S. aureus* isolates associated with skin and urinary tract infections in Urmia, Iran.

In our research, amplified products with an approximate size of 680 bp and 750 bp were obtained. This variation in the size of amplicons indicates the presence of only one more 81 bp repeat in strains with 750 bp PCR product. *Alu*I digestion of *coa* gene PCR products lead to 4 distinct patterns. Pattern 1, the most common pattern (43% isolates), includes two fragments of 400 bp and 280 bp. The pattern 2 with two fragments of 340 bp from 680 bp amplicon suggested that the amplicon was cut into two equal halves of 340 bp by *Alu*I. Single fragment pattern of digestion was also obtained by Sanjiv et al (2008) when *S. aureus coa* gene amplicon of 600 bp was digested with *Alu*I. *Alu*I digestion of 750 bp amplicon in 4 isolates produced two size fragments 470 bp and 280 bp (pattern 3) and 750 bp amplicons without *Alu*I digestion (in 7 isolates) designated as pattern 4. Lack of enzyme restriction sites amongst the amplicons has been previously reported by Sarvari et al, 2014. According to the results, MRSA isolates were found in each of the four patterns without discrimination. Similar results were obtained by Himabindu et al (2009) who found that *coa* PCR-RFLP typing method cannot be used to distinguish MRSA and MSSA. Also, we found no discriminative pattern to distinguish between various microbial sources including urine and skin. These results are contrary to those of Talebi-Satlou et al (2012) who reported tissue-specific tendency of some genotypes.

The results of this study demonstrated genetic diversity in *S. aureus* clinical isolates in Rasht. The variation in the size of PCR amplicons indicates the variation in the *coa* gene lengths and differences in the RFLP patterns reflects the presence of VNTRs in the *coa* gene of *S. aureus* isolates. These *coa* gene variants are different from those reported in the previous studies in Iran (Afrough et al., 2013, Mahmoudi et al., 2017, Rezaee et al., 2016, Saei et al., 2009, Sajadi et al., 2017, Talebi-Satlou et al., 2012). So the presence of many variants of *S. aureus* in the country is concluded.

Acknowledgements

This manuscript is prepared from MSc thesis at Islamic Azad University, Rasht Branch, Rasht, Iran. We are grateful to the Islamic Azad University, Rasht Branch for support.

References

1. Afrough P., Pourmand M. R., Sarajian A. A. and Saki, M. (2013) Molecular investigation of Staphylococcus aureus, *coa* and *spa* genes in Ahvaz hospitals, staff nose compared with patients' clinical samples. Jundishapur Journal of Microbiology *6*(4): 1-7.
2. Anggraini A. D., Koendhori E. B., Pramono H. and Wahyono D. D. (2017) Polymorphism analysis of the *coA* (Coagulase) gene in isolates of methicillin-resistant *Staphylococcus aureus* with *AluI* restriction sites. Health Science Journal of Indonesia 8(1):1-6.
3. Babu N. R., Shree G. B., Rekha L. and Karthiga, P. (2014) Molecular Analysis of Coagulase (*coa*) gene polymorphism in clinical isolates of *Staphylococcus aureus* by PCR-RFLP. Int J Innov Res Sci Eng Technol 3: 8163-8.
4. Cheng A. G., McAdow M., Kim H. K., Bae T., Missiakas D. M. and Schneewind O. (2010) Contribution of coagulases towards Staphylococcus aureus disease and protective immunity. PLoS pathogens 6(8): e1001036.
5. Daum R. S. (2007) Skin and soft-tissue infections caused by methicillin-resistant *Staphylococcus aureus*. New England Journal of Medicine 357(4): 380-390.

6. Dinges M. M., Orwin P. M. and Schlievert P. M. (2000) Exotoxins of *Staphylococcus aureus*. Clinical microbiology reviews 13(1): 16-34.
7. Foster T. J. (2005) Immune evasion by staphylococci. Nature reviews microbiology 3(12): 948–958.
8. Himabindu M., Muthamilselvan D. S., Bishi D. K. and Verma, R. S. (2009) Molecular analysis of coagulase gene polymorphism in clinical isolates of methicillin resistant *Staphylococcus aureus* by restriction fragment length polymorphism based genotyping. Am J Infect Dis 5: 170-176.
9. Izadpanah M. R. and Asadpour L. (2015) Molecular identification and antibacterial drug resistance pattern of *Staphylococcus aureus* isolated in Rasht, Iran. *Mljgoums 9*(3): 40-6.
10. Ishino K., Tsuchizaki N., Ishikawa J. and Hotta K. (2007) Usefulness of PCR-restriction fragment length polymorphism typing of the coagulase gene to discriminate arbekacin-resistant methicillin-resistant *Staphylococcus aureus* strains. Journal of clinical microbiology 45(2): 607-609.
11. Janwithayanuchit I., Ngam-Ululert S., Paungmoung P. and Rangsipanuratn, W. (2006) Epidemiologic study of methicillin-resistant *Staphylococcus aureus* by coagulase gene polymorphism. Science Asia 32: 127-132.
12. Mahmoudi H., Arabestani M. R., Mousavi S. F. and Alikhani M. Y. (2017) Molecular analysis of the coagulase gene in clinical and nasal carrier isolates of methicillin-resistant *Staphylococcus aureus* by restriction fragment length polymorphism. Journal of global antimicrobial resistance 8: 41-45.
13. McAdow M., Missiakas D. M. and Schneewind O. (2012) *Staphylococcus aureus* secretes coagulase and von Willebrand factor binding protein to modify the coagulation cascade and establish host infections. Journal of innate immunity 4(2): 141-148.
14. Muder R. R., Brennen C., Rihs J. D., Wagener M. M., Obman A., Obman A. and Yu V. L. (2006) Isolation of *Staphylococcus aureus* from the urinary tract: association of isolation with symptomatic urinary tract infection and subsequent staphylococcal bacteremia. Clinical infectious diseases 42(1): 46-50.
15. Rezaee M. A., Mirkarimi S. F., Hasani A., Sheikhalizadeh V., Soroush M. H. and Abdinia B. (2016) Molecular typing of *Staphylococcus aureus* isolated from clinical specimens during an eight-year period (2005-2012) in Tabriz, Iran. Archives of Pediatric Infectious Diseases 4(2): e35563.
16. Saei H. D., Ahmadi M., Mardani K. and Batavani R. A. (2009) Molecular typing of *Staphylococcus aureus* isolated from bovine mastitis based on polymorphism of the coagulase gene in the north west of Iran. Veterinary microbiology 137(1-2):202-206.
17. Sajadi S. N., Kaboosi H. and Ghadikolii F. P. (2017) Relationship between antibiotic resistance patterns and coagulase in clinical isolates of *Staphylococcus aureus* in Nowshahr and Chalous. Zahedan Journal of Research in Medical Sciences 19(11): e55079
18. Sanjiv K., Kataria A. K., Sharma R. and Singh G. (2008) Epidemiological typing of *Staphylococcus aureus* by DNA restriction fragment length polymorphism of *coa* gene. Veterinarski arhiv 78(1): 31-38.
19. Sarvari J., Bazargani A., Kandekar-Ghahraman M. R., Nazari-Alam A. and Motamedifar M. (2014) Molecular typing of methicillin-resistant and methicillin-susceptible *Staphylococcus aureus* isolates from Shiraz teaching hospitals by PCR-RFLP of coagulase gene. Iranian journal of microbiology 6(4): 246-252.
20. Schwarzkopf A. and Karch H. (1994) Genetic variation in Staphylococcus aureus coagulase genes: potential and limits for use as epidemiological marker. Journal of Clinical Microbiology 32(10): 2407-2412.
21. Shorr A. F., Jackson W. L. and Lipman J. (2006) Making the wrong choice: Consequences for patients with infections due to methicillin-resistant *Staphylococcus aureus*. Critical care medicine 34(8): 2239-2241.
22. Talebi-Satlou R., Ahmadi M. and Saei H.D. (2012) Restriction fragment length polymorphism genotyping of Human *Staphylococcus aureus* isolates from two hospitals in Urmia region of Iran using the *coa* gene. Jundishapur Journal of Microbiology 5(2):416-20.

Open Access Statement:

Journal of Cell and Molecular Research (2018) 10 (1), 32-39 DOI: 10.22067/jcmr.v10i1.73844

Research Article

Desaturase Genes Expression and Fatty Acid Composition of *Pleurotus ostreatus* in Response to Zinc and Iron

Kamran Safavi, Gholamreza Kavoosi*, Roghayeh Siahbalaei

Institute of Biotechnology, Shiraz University, Shiraz, Iran

Received 1 July 2018 Accepted 6 September 2018

Abstract

The influence of $ZnSO_4$, $FeSO_4$, ZnO, and Fe_2O_3 at 80 µM on the expression of desaturase genes and fatty acid composition of *Pleurotus ostreatus* was investigated. Fatty acid was extracted by lipid extraction and methylation procedure using acidic methanol: normal saline: hexane solution followed by gas chromatography-mass spectrometry (GC-MS). The most prominent fatty acids in *P. ostreatus* were linoleic acid (44.7%), palmitic acid (8.6%), oleic acid (8.5%), stearic acid (2.9%), pentadecanoic acid (2.6%) and heptadecanoic acid (2.3%). ZnO strongly and Fe_2O_3 slightly lead a decrease in unsaturated fatty acid (UFA), polyunsaturated fatty acid (PUFA) and omega-6 and an increase in the monounsaturated fatty acid (MUFA), omega-7 and omega-9 content. Accordingly, our results considerably confirmed the different effects of $ZnSO_4$ and ZnO on fatty acid content. These differential effects for $FeSO_4$ and Fe_2O_3 were not significant. Δ9-desaturase and Δ12-desaturase expression but not Δ15-desaturase were upregulated in the seeds cultured in media containing ZnO and Fe_2O_3.

Keywords**:** *Pleurotus ostreatus,* essential fatty acid, desaturase

Introduction

In recent years, mushrooms have been appreciated for texture, flavor, nutritional and medical applications. They have been reported as therapeutic food in preventing diseases such as hypertension, hypercholesterolemia, atherosclerosis, diabetes mellitus and cancer. They presented potent cholesterol-lowering, glucose-lowering, antitumor, antiviral, antithrombic and immunomodulating effects (Rathore et al., 2017; Roncero-Ramos and Delgado-Andrade, 2017). Biological and functional characteristics of mushroom are mainly due to their chemical composition, since they are characterized as a useful source of carbohydrates, fibers, proteins, essential amino acids, non-essential amino acids, lipids, unsaturated fatty acids, essential fatty acids, vitamins, vitamin precursors, minerals and a large variety of secondary metabolites like organic acid, alkaloids, terpenoids, steroids and phenolic compounds (Stephan et al., 2018; Zhang et al., 2017).

Fatty acids, especially unsaturated fatty acids and essential fatty acids, are used as indicators of nutritional, medicinal and pharmacological purposes of foodstuff. Linoleic and linolenic acids are essential fatty acids for synthesis of other polyunsaturated fatty acids during biological pathways in mammals. They are building blocks of cell membranes; support the defensive barrier and also are involved in cholesterol metabolism. Moreover, it has been shown that essential fatty acids can reduce the rate of cancer colony formation, prevent breast cancer, regulate blood pressure, decrease the level of cholesterol, improve diabetes, and ameliorate the body's immunological resistance against antigens (Freitas et al., 2017; Zarate et al., 2017).

Among mushrooms, *Pleurotus ostreatus* is a culinary and medicinal mushroom with beneficial biological and medicinal properties. *P. ostreatus,* as a nutritional and therapeutic mushroom, is a valuable source of carbohydrates, vegetable proteins and amino acids, fibers, vitamins and vitamin precursors, minerals, organic acids, phenolic and flavonoid compounds and low levels of lipid and essential fatty acids with low calories (Poniedziałek et al., 2017; Gasecka, et al., 2016). Unlike plants, mushrooms do not require agricultural land, and their resulting metabolite profile could be manipulated and changed substantially by simply varying their growth conditions. In this study, we decided to evaluate the influence of $ZnSO_4$, $FeSO_4$, ZnO, and Fe_2O_3 on the expression of desaturase genes and fatty acids profiling in *P. ostreatus*.

*Corresponding author E-mail: ghkavoosi@shirazu.ac.ir

Materials and Methods

Materials

Glucose (CID: 79025), $ZnSO_4$ (CID: 24424), $FeSO_4$ (CID: 24393), ZnO (CID:14806), Fe_2O_3 (CID:14833), KH_2PO_4 (CID:516951), $MgSO_4$ (CID: 24083), NaCl (CID: 5234), 2,2 Dimethoxypropane (CID: 6495), Methanol CID: 887, Sulfuric acid (CID: 1118), Hexane (CID: 8900), Formic acid.

Mushroom Strain and Preparation of Seed Culture

P. ostreatus edible-medicinal mushroom was obtained through Arian's Mushrooms Research Company (Tehran, Iran). The seeds were grown in 200 mL of basal medium (glucose 50.0 g/L, yeast extract 10.0 g/L, casein hydrolysate 10.0 g/L, KH_2PO_4 1.0 g/L, distilled water 1 L, and pH 6.0) in 500 mL Erlenmeyer flask at 25°C, on a rotary shaker, at 110 rev/min for 7 days. The obtained seed culture was used for inoculation (Turlo et al., 2010).

Preparation of Basal Liquid Media Containing $ZnSO_4$, $FeSO_4$, ZnO, and Fe_2O_3

The composition of the basal liquid medium for mycelium cultivation was beet molasses 50 g/L (beet sugar factory, Isfahan, Iran), soybean flour 5 g/L (IPP company, Isfahan, Iran), KH_2PO_4 1 g/L, $MgSO_4 \cdot 7H_2O$ 1 g/L (Merck, Germany) and distilled water 1 L with initial pH 6.0. The liquid media was enriched with 0.08 mM of $ZnSO_4$, $FeSO_4$, ZnO, and Fe_2O_3. All liquid culture media were sterilized by autoclaving at 121°C for 20 min. After cooling, cultivation had been carried out in polypropylene containers containing 95 mL of liquid medium and inoculated with five mL of the seed culture (Poursaeid et al., 2015).

Biochemical Analysis

The total lipid content was quantified by sulphuric acid-phosphoric acid-vanillin reagent using sesame oil (1mg/mL in ethanol) as standard and monitoring light absorbance at 530 nm. Briefly, 100 mg of powder carefully was suspended in 500 µL of ethanol. 1 mL of concentrated sulfuric acid (98%) was added to the samples and then heated at 100°C for 10 min. After cooling in room temperature (25-27°C), 1 mL phosphoric acid-vanillin reagent (0.6 g vanillin in 100 mL deionized water and 400 mL concentrated phosphoric acid) was added and the sample incubated for 15 min at room temperature (Mishra et al., 2014).

Fatty Acids Methylester Profiling by GC-MS

Mushroom powder (200 mg) was put into extraction glass test tubes. Then 1.0 mL of acidic methanol (methanol: sulfuric acid in 85:15 v/v) was added to glass tubes. The tubes were placed in shaking water bath at 80°C for 120 min. Next, tubes were placed in the vortex until they come to room temperature. 1.0 mL of normal saline was added to tubes and vortexed for 5 min. Afterward, 1.0 mL of hexane was added to tubes, and vortexed for 5 min then centrifuged for 20 min at 3000g. The upper phase (hexane phase) was extracted and transferred to gas chromatography vials for gas chromatography - mass spectrometry (GC-MS) (Agilent 7890B GC 7955A MSD) analysis according to manual instruction (Woldegiorgis et al., 2015).

Real-Time Quantitative PCR Analysis

P. ostreatus that were grown in different liquid media were frozen in liquid nitrogen and then stored at -70°C for RNA isolation. Total RNA was extracted from 100 mg of mushroom using the RNX-Plus buffer (Cinnagen, Tehran, Iran) according to the manufacturer's instructions. Quantification of total RNA was performed with a Nano Drop ND 1000 spectrophotometer at 260 nm (Thermo Fisher Scientific, Wilmington, DE, USA). DNase treatment was carried out using a Fermentas DNase Kit (Fermentas, Hanover, MD, Germany) using the manufacturer's protocol. The integrity of RNA was checked by visual observation of 28S rRNA and 18S rRNA bands on an agarose gel electrophoresis before real-time PCR analysis (Figure S1 in the supplemental file). 5 µg of DNase-treated RNA was converted to cDNA with a Revert Aid First Strand cDNA Synthesis Kit (Thermo Scientific, Fermentas) using the manufacturer's protocol in a 20 µL final volume.

Primers for the target (D9-desaturase, D12-desaturase, D15-desaturase) and internal control (beta-actin) genes were designed using Allele ID 7 software (Table 1). Primers for the PCR reactions were designed to have a melting temperature of about 55°C to 65°C and to give a PCR product between 100 and 200 bp. Real-time PCR was performed using a line Gene K Thermal cycler (Bioer Technology Co, Hangzhou, China). The cDNA samples were diluted 1:5 by using nuclease-free water, and 5 µL of cDNA was used for real-time PCR. The final volume for relative real-time PCR was 20 µL containing 4 pmol of each primer, 5 µL (diluted) of the first-strand cDNA and 1x SYBR Premix Ex Taq TM II (Takara, Japan). The initial denaturing time was 5 min., followed by 40

Table 1. Primer used in this study

Genes	Primer sequence	TM	Length
Δ9 Desaturase F	TCATTGCCTTGTGTAACTTCA	62	21
Δ9 Desaturase R	TGTCTCTGCCTCCTTCTG	62	18
Δ12 Desaturase F	TGGGTCAACCAyTGGCT	57	17
Δ12 Desaturase R	TCAATACCAGAGTCGCTGG	57	19
Δ15 Desaturase F	TGGATTTTGGCyCATGAATG	57	20
Δ15 Desaturase R	ATGGCCAGTAGCTTTATGATG	57	21
18S rRNA F	CAGCGAAATGCGATAAGTAAT	55	21
18S rRNA R	CCAACAATCCAAACATCACAA	55	21

Primers for target genes and internal control gene were designed using Allele ID 7 software.

PCR cycles consisting of 94 °C for 10 s, annealing temperatures of each primer 15 s, and 72 °C for 30 s. A melting curve was recorded after the PCR cycles followed by heating from 50 to 95 °C. A Proper control reaction was carried out without the reverse transcriptase treatment. For each sample, the subsequent real-time PCR reactions were performed in twice under identical conditions.

For real-time data analysis, the relative expression of the target gene in each sample was compared with the control sample, and was determined with the delta-delta Ct method. The Ct for each sample was calculated using the Line-gene K software (fqdpcr ver. 4.2.00), where Ct refers to the threshold cycle determined for each gene in the exponential phase of PCR amplification. In this analysis method, the relative expression of the target gene in the control sample was equal to one (2^0) by definition (Livak and Schmittgen, 2001).

Results and Discussion

Fatty Acid Composition

Biochemical analysis of *P. ostreatus* cultivated in beet molasses, and soybean flour using sulfuric acid-phosphoric acid vanillin (SPV) as chromogen confirmed a total fatty acid content of 5660 mg/100 g dried weight (Table 2). Our experimental analysis clearly demonstrated that $ZnSO_4$ and ZnO or $FeSO_4$ and Fe_2O_3 had no significant effects on the total fatty acid content but GC-MS analysis revealed a significant difference between the qualities of the fatty acid composition. It has been shown that cultivation of *Mortierella ramanniana* mushroom in the presence of dextrose-yeast extract with $FeCl_2$ and $ZnSO_4$ lead to a significant increase and decrease in the biomass, respectively (Dyal et al., 2005). Tan et al. (2017) reported that metal ions such as $ZnSO_4$ and $FeCl_3$ increased biomass and lipid content in Mortierella. Sajbidor et al. (1992) examined the effects of various concentrations of calcium, magnesium, manganese and iron ions on lipid synthesize by Mortierella. Based on the results, all above-mentioned ions exception manganese inhibit lipid accumulation and arachidonic acid production. Moreover, iron had an inhibitory effect on arachidonic acid production by Mortierella. Hansson and Distalek (1988) indicated that Cu_2^+ and Zn_2^+ have positive effects on lipid accumulation and gamma-linolenic acid production by Mortierella. Accordingly, there are various reports in the literature for the stimulatory effects of metal ions on the production of biomass or lipid content in the mushroom. The difference may be related to mushroom species, basal medium composition, inoculation condition, type of metal ion salts (for example; $ZnSO_4$, ZnO, FeCl2, $FeCl_3$, $FeSO_4$, FeO, Fe_2O_3).

GC-MS analyzed of *P. ostreatus* indicated different components in the mushroom including fatty acids (73%) and other metabolites (27%) including limonene, organic acid, and phenol compounds (Table 3). $FeSO_4$ and $ZnSO_4$ had not a significant effect on total fatty acid content while ZnO and Fe_2O_3 significantly reduced fatty acid content. Fe_2O_3 significantly increased while ZnO significantly reduced secondary metabolite of *P. ostreatus* while $FeSO_4$ and $ZnSO_4$ did not display significant effect. The most prominent fatty acids in *P. ostreatus* were linoleic acid (44.7%), palmitic acid (8.6%), oleic acid (8.5%) stearic acid (2.9%), pentadecanoic acid (2.6%) and heptadecanoic acid (2.3%) (Table 3). The most prominent fatty acid in $ZnSO_4$ enriched *P. ostreatus* were linoleic acid (44.7%), palmitic acid

Table 2. Total fatty acid content of cultivated *P. ostreatus* in medium enriched by $ZnSO_4$, ZnO, $FeSO_4$ and Fe_2O_3.

Treatments	Lipid (mg/100g)
Control	5660 ± 10
$ZnSO_4$	6820 ± 12
ZnO	5240 ± 11
$FeSO_4$	5840 ± 14
Fe_2O_3	5120 ± 12

Values are means with triplicate determination. Means sharing the same superscript across column are not significantly different at P< 0.05.

(7.5%), oleic acid (7.35%), pentadecanoic acid (4.2%), heptadecanoic acid (2.8%), and stearic acid (1.8%) (Table 3). The most prominent fatty acids in *P. ostreatus* enriched with ZnO were linoleic acid (25%), oleic acid (14.45%), palmitic acid (12.4%), palmitoleic acid (3.95%), and stearic acid (2%) (Table 3). The most prominent fatty acid in *P. ostreatus* enriched with $FeSO_4$ were linoleic acid (38%), palmitic acid (9.6%), oleic acid (8.85%), pentadecanoic acid (5.4%), myristic acid (3.6), heptadecanoic acid (2.95%), and stearic acid (1.85%) (Table 3). The most prominent fatty acid in *P. ostreatus* nriched with Fe_2O_3 were linoleic acid (35.85%), palmitic acid (9.93%), oleic acid (8.85%), palmitoleic acid (3.25%) and stearic acid (2.4%) (Table 3).

Yilmaz et al. (2006) reported that the main fatty acid composition of *P. ostreatus* were linoleic acid (44%), oleic acid (20%), palmitic acid (12%), and stearic acid (5%). Woldegiorgis et al. (2015) reported that the main fatty acid composition of *P. ostreatus* were linoleic acid (1663 mg/g), oleic acid (323 mg/g), palmitic acid (310 mg/g), and stearic acid (39 mg/g). Pedneault et al. (2007) reported that the main fatty acid composition of *P. ostreatus* were linoleic acid (79%), palmitic acid (11%) and oleic acid (5.6%). Ergonul, et al. (2013) reported that the main fatty acid composition of *P. ostreatus* were linoleic acid (65.3%), palmitic acid (12.4%), oleic acid (10.4%) and stearic acid (3.7%). Based on the above-mentioned studies, the proportion of unsaturated fatty acids were higher than saturated fatty acids in *P. ostreatus* which is consistent with our data.

The results of individual fatty acids including saturated fatty acids (SFA), unsaturated fatty acids (UFA), monounsaturated fatty acids (MUFA) and polyunsaturated fatty acids (PUFA), as well as omega-6 fatty acids, omega-7 fatty acids, and omega-9 fatty acids have shown in Table 4. PUFA especially omega-6 fatty acid constitute the most proportion of fatty acids of *P. ostreatus.* ZnO strongly and Fe_2O_3 slightly lead a decrease in UFA, PUFA and omega-6 and an increase in the MUFA, omega-7 and omega-9 content that were close to the values already reported by Pedneault, et al., (2008), Ogwok, et al., (2017) and Warude, et al., (2006).

Linoleic acid (C18:2n6) as an omega-6 fatty acid, is the precursor of 1-octen-3-ol, known as the alcohol of fungi. Aromatic compounds which exist in most fungi and might contribute to mushroom flavor originates from 1-octen-3-ol (Ribeiro et al., 2009). Palmitic acid (16:0) is the most common saturated fatty in human food. This saturated fatty acid is the precursor of long fatty acids like oleic acid (18:1) (Ohlsson, 2010). Oleic acid (C18:1n9) is a bioactive compound that decreases cholesterol serum level. This fatty acid is a good substrate for the liver enzyme known as Acyl CoA:cholesterol acyltransferase (ACAT), a liver enzyme. ACAT transfer a fatty acid (such as oleic acid) from coenzyme A to the hydroxyl group of cholesterol and convert it to cholesterol ester (the hydrophobic form of cholesterol) (Won et al., 2007). Stearic acid (C18:0) as compared to cholesterol-raising SFAs decreases LDL while raises LDL as compared with unsaturated fatty acids (Mensink, 2005). Pentadecanoic acid (15:0) is the member of odd chain saturated fatty acids (OCS-FA). It has been shown that consumption of OCS-FAs rich foods, such as dairy fats, could reduce the risk of developing metabolic diseases (Jenkins et al., 2015). Accordingly, the biological action of *P. ostreatus* fatty acid extract on the above-mentioned activities must be investigated.

Desaturase Gene Transcription

Fatty acid desaturases play a critical role in the biosynthesis of PUFA by catalyzing the addition of double bond in specific positions of fatty acid chain. The most predominant fatty acids analyzed

Table 3. Fatty acid composition (percent of total fatty acid) of cultivated *P. ostreatus* in medium enriched by $ZnSO_4$, ZnO, $FeSO_4$ and Fe_2O_3.

Fatty acid	Control	$ZnSO_4$	ZnO	$FeSO_4$	Fe_2O_3
Dodecanoic acid (C12:0)	1.00	1.00	1.00	1.00	1.85
Tridecanoic acid (C13:0)	0.01	0.01	0.01	0.01	0.01
Tetradecanoic acid (C14:0)	0.20	0.15	1.50	3.60	0.50
9-Tetradecenoic acid (C14:1n5)	0.02	0.02	0.02	0.02	0.02
Pentadecanoic acid (C15:0)	2.60	4.19	1.23	5.42	0.96
Hexadecanoic acid (C16:0)	8.60	7.55	12.40	9.60	9.93
9-Hexadecenoic acid (C16:1n7)	1.28	1.20	4.00	1.60	3.25
7,10-Hexadecadienoic acid (C16:2n6)	0.03	0.03	0.03	0.03	0.03
7,10,13-Hexadecatrienoic acid (C16:3n3)	0.04	0.04	0.04	0.04	0.04
Heptadecanoic acid (C17:0)	2.26	2.80	0.60	2.95	0.35
Octadecanoic acid (C18:0)	2.90	1.79	1.95	1.85	2.40
9-Octadecenoic acid (C18:1n9 Trans)	0.04	0.04	0.04	0.04	0.04
9-Octadecenoic acid (C18:1n9 Cis)	8.50	7.35	14.45	8.85	8.85
10,13-Octadecadienoic acid (C18:2n5)	0.02	0.02	0.02	0.02	0.02
9,12-Octadecadienoic acid (C18:2n6 Trans)	0.03	0.03	0.03	0.03	0.03
9,12-Octadecadienoic acid (C18:2n6 Cis)	44.70	44.65	25.00	37.90	35.85
9,12,15-Octadecatrienoic acid (C18:3n3)	0.03	0.03	0.03	0.03	0.03
6,9,12-Octadecatrienoic acid (C18:3n6)	0.20	0.45	0.37	1.20	0.35
Docosanoic acid (C22:0)	0.40	0.35	0.10	0.20	0.08
Total lipid	**72.86**	**71.70**	**62.81**	**74.39**	**64.58**

The most prominent fatty acids are linoleic acid > palmitic acid > oleic acid.

Table 4. Saturated and unsaturated fatty acid composition (percent of total fatty acid) of cultivated *P. ostreatus* in medium enriched by ZnSO4, ZnO, $FeSO_4$ and Fe_2O_3.

Fatty acid	Control	$ZnSO_4$	ZnO	$FeSO_4$	Fe_2O_3
Saturated fatty acid (SFA)	17.77	17.69	17.29	21.03	15.57
Unsaturated fatty acid (UFA)	54.89	53.86	44.03	49.76	48.51
Monounsaturated fatty acid (MUFA)	9.84	8.61	18.51	10.51	12.16
Polyunsaturated fatty acid (PUFA)	45.05	45.25	25.52	39.25	36.35
Omega-3 fatty	0.07	0.07	0.07	0.07	0.07
Omega-5 fatty	0.02	0.02	0.02	0.02	0.02
Omega-6 fatty	44.96	45.16	25.43	39.16	36.26
Omega-7 fatty	1.28	1.20	4.00	1.60	3.25
Omega-9 fatty	8.54	7.39	14.49	8.89	8.89

The most prominent UFA are PUFA especially omega-6.

in this study were palmitic acid (16:0), stearic acid (18:0), oleic acid (18:1n9) and linoleic acid (18:2n6). The conversion of palmitic acid to stearic acid catalyzed by elongase. Δ9-desaturase catalyzes the conversion of stearic acid to oleic acid, an omega-9 fatty acid. Oleic acid then converted to, linoleic acid (an omega-6 fatty acid) by the action of Δ12-desaturase. Δ15-desaturase then converts linoleic acid to α-linolenic acid (18:3n3), an omega-3 fatty acid. Δ12-desaturase and Δ15-desaturase was not found in animals but present in plants, algae and fungi. Accordingly, linoleic and linolenic acid are essential fatty acids and must be obtained from diet. Our experimental results showed ZnO and Fe_2O_3 upregulated Δ9-desaturase but $FeSO_4$ and $ZnSO_4$ did not significant effects on the upregulation of these genes (Figure 1). *P. ostreatus* has the potential to be a strain for production of omega-6 and omega-3 polyunsaturated fatty acid. The biosynthesis of the omega-6 and omega-3 fatty acid is catalyzed by

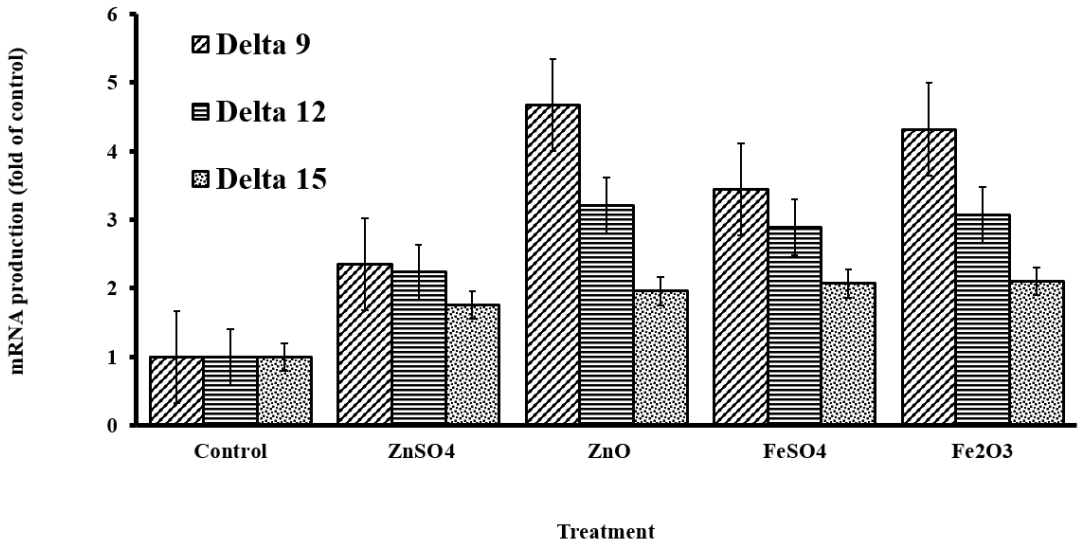

Figure 1. Stimulatory effect of $ZnSO_4$, $FeSO_4$, ZnO and Fe_2O_3 at concentration of 80 µM on the expression of delta 9 desaturase, delta 12 desaturase and delta 15 desaturase in cultivated *P. ostreatus*.

desaturase enzymes, including Δ9-desaturase, Δ12-desaturase, Δ15-desaturase, and Δ6-desaturase. The 5′ upstream flanking sequence of desaturase genes contain regulatory elements, including metal-responsive element. The presence of this special cis-acting response elements in the promoter region of desaturase genes implies that their transcription is regulated by metal ions (Lee, et al., 2016). Tan et al. (2017) reported that metal ions such as $ZnSO_4$ and $FeCl_3$ could stimulate polyunsaturated fatty acid production and upregulate Δ9-desaturase, Δ12-desaturase, Δ5-desaturase and Δ6-desaturase gene transcription in Mortierella sp.

Conclusion

Our results clearly revealed that the most predominant fatty acids in *P. ostreatus* were linoleic acid, palmitic acid, oleic acid and stearic acid. This mushroom also can be considered as an edible source of PUFA and omega-6 fatty acid content. ZnO strongly and Fe_2O_3 slightly lead to a decrease in UFA, PUFA and omega-6 and an increase in the MUFA, omega-7, and omega-9 content. Our results considerably revealed differential effects of $FeSO_4$, $ZnSO_4$, ZnO, and Fe_2O_3 on fatty acid content of the mushroom that may be attributed to differential co-factor activity of zinc and iron on the biochemical pathway for fatty acid synthesis.

References

1. Dyal, S.D., Bouzidi, L., Narine, S.S. (2005). Maximizing the production of γ-linolenic acid in Mortierella ramanniana var. ramanniana as a function of pH, temperature and carbon source, nitrogen source, metal ions and oil supplementation. Food Research International, 38: 815-829.
2. Ergonul, P.G., Akata, I., Kalyoncu, F., Ergonul, B. (2013). Fatty acid compositions of six wild edible mushroom species. The Scientific World Journal. Doi.10.1155/2013/163964.
3. Freitas, H.R., Isaac, A.R., Malcher-Lopes, R., Diaz, B.L., Trevenzoli, I.H., De Melo Reis, R.A. (2017). Polyunsaturated fatty acids and endocannabinoids in health and disease. Nutritional Neuroscience. doi.org/10.1080/1028415X.2017.1347373.
4. Gasecka, M., Mleczek, M., Siwulski, M., Niedzielski, P. (2016). Phenolic composition and antioxidant properties of *Pleurotus ostreatus* and *Pleurotus eryngii* enriched with selenium and zinc. European Food Research and Technology, 242: 723-732.
5. Hansson, L., Dostálek, M. (1988). Effect of culture conditions on mycelial growth and production of γ-linolenic acid by the fungus *Mortierella ramanniana*. Applied Microbiology and Biotechnology, 28: 240-246.
6. Jenkins B., West J.A., Koulman A. (2015). A review of odd-chain fatty acid metabolism and the role of pentadecanoic acid (C15:0) and heptadecanoic acid (C17:0) in health and disease. Molecules, 20: 2425-2444.
7. Lee, J.M., Lee, H., Kang, S., Park, W.J.

(2016). Fatty acid desaturases, polyunsaturated fatty acid regulation, and biotechnological advances. Nutrients, 8: 23-28.
8. Livak, K.J., Schmittgen, T.D. (2001). Analysis of relative gene expression data using real-time quantitative PCR and the 2−ΔΔCT method. Methods, 25: 402-408.
9. Mensink R.P. (2005) Effects of stearic acid on plasma lipid and lipoproteins in humans. Lipids, 40: 1201-1205.
10. Mishra, S.K., Suh, W.I., Farooq, W., Moon, M., Shrivastav, A., Park, M.S., Yang, J.W. (2014). Rapid quantification of microalgal lipids in aqueous medium by a simple colorimetric method. Bioresource Technology, 155: 330-333.
11. Ogwok, P., Ogwok, P., Muyinda, R., Muyinda, R., Nakisozi, H., Nakisozi, H., Bamuwamye, M., Bamuwamye, M. (2017). Fatty acid profile of wild edible and cultivated mushrooms (*Pleurotus ostreatus*, Amanita spp and *Termitomyces microcarpus*). Nutrition & Food Science, 47: 357-368.
12. Ohlsson L., (2010). Dairy products and plasma cholesterol levels. Food & Nutrition Research, 54: 5124-5128.
13. Pedneault, K., Angers, P., Gosselin, A., Tweddell, R.J. (2008). Fatty acid profiles of polar and neutral lipids of ten species of higher basidiomycetes indigenous to eastern Canada. Mycological Research, 112: 1428-1434.
14. Poniedziałek, B., Mleczek, M., Niedzielski, P., Siwulski, M., Gąsecka, M., Kozak, L., Komosa, A., Rzymski, P. (2017). Bio-enriched Pleurotus mushrooms for deficiency control and improved antioxidative protection of human platelets?. European Food Research and Technology, 243: 2187-2198.
15. Poursaeid, N., Azadbakht, A., Balali, G.R. (2015). Improvement of zinc bioaccumulation and biomass yield in the mycelia and fruiting bodies of *Pleurotus florida* cultured on liquid media. Applied Biochemistry and Biotechnology, 175: 3387-3396.
16. Rathore, H., Prasad, S., Sharma, S. (2017). Mushroom nutraceuticals for improved nutrition and better human health: a review. Pharma Nutrition, 5: 35-46.
17. Ribeiro, B., Pinho, P.G., Andrade, P.B., Baptista, P., Valentao, P. (2009). Fatty acid composition of wild edible mushrooms species: A comparative study. Microchemical Journal, 93: 29-35.
18. Roncero-Ramos, I., Delgado-Andrade, C. (2017). The beneficial role of edible mushrooms in human health. Current Opinion in Food Science, 14: 122-128.
19. Sajbidor, J., Kozelouhov, D., Certik, M. (1992). Influence of some metal ions on the lipid content and arachidonic acid production by Mortierella sp. Folia Microbiologica, 37: 404-406.
20. Stephan, A., Ahlborn, J., Zajul, M., Zorn, H. (2018). Edible mushroom mycelia of *Pleurotus sapidus* as novel protein sources in a vegan boiled sausage analog system: functionality and sensory tests in comparison to commercial proteins and meat sausages. European Food Research and Technology, 244: 913-924.
21. Tan, L., Zhuo, R., Li, S., Ma, F., Zhang, X. (2017). Differential expression of desaturase genes and changes in fatty acid composition of Mortierella sp. AGED in response to environmental factors. Journal of the Science of Food and Agriculture. 97: 1876-1884.
22. Turlo, J., Gutkowska, B., Herold, F., Klimaszewska, M., Suchocki, P. (2010). Optimization of selenium-enriched mycelium of *Lentinula edodes* (berk.) pegler as a food supplement. Food Biotechnology, 24: 180-196.
23. Warude, D., Joshi, K., Harsulkar, A. (2006). Polyunsaturated fatty acids: Biotechnology. Critical Review in Biotechnology, 26: 83-93.
24. Woldegiorgis, A.Z., Abate, D., Haki, G.D., Ziegler, G.R., Harvatine, K.J. (2015). Fatty acid profile of wild and cultivated edible mushrooms collected from Ethiopia. Journal of Nutrition & Food Sciences, 5: 1-10.
25. Won, S.R., Hong, M.J., Kim, Y.M., Li, C.Y., Kim, J.W., Rhee, H.I. (2007). Oleic acid: an efficient inhibitor of glucosyltransferase. FEBS Letters, 581: 4999-5002.
26. Yang, J.H., Lin, H.C., Mau, J.L. (2001). Non-volatile taste components of several commercial mushrooms. Food Chemistry, 72: 465-471.
27. Yilmaz, N., Solmaz, M., Turkekul, I., Elmastas, M. (2006). Fatty acid composition in some wild edible mushrooms growing in the middle Black Sea region of Turkey.

Food Chemistry. 99: 168-174.
28. Zarate, R., el Jaber-Vazdekis, N., Tejera, N., Pérez, J.A., Rodríguez, C. (2017). Significance of long chain polyunsaturated fatty acids in human health. Clinical and Translational Medicine, 6: 25-32.
29. Zhang, L., Li, C. G., Liang, H., Reddy, N. (2017). Bioactive mushroom polysaccharides: immunoceuticals to anticancer agents. Journal of Nutraceuticals and Food Science, 2: 6-11.

Journal of Cell and Molecular Research (2018) 10 (1), 40-46 DOI: 10.22067/jcmr.v10i1.70766

Review Article

MicroRNA-mediated Resistance to Plant Viruses

Amir Ghaffar Shahriari[1,*], Aminallah Tahmasebi[2]

[1] *Department of Agriculture and Natural Resources, Higher Education Center of Eghlid, Eghlid, Iran*
[2] *Plant Virology Research Center, Shiraz University, Shiraz, Iran*

Received 4 February 2018 Accepted 19 September 2018

Abstract

MicroRNAs (miRNAs) are 20-24 nucleotide small RNAs which are processed from nuclear-encoded transcripts. miRNAs control the expression of target transcripts by cleaving or translational inhibition of the target RNAs. Artificial microRNAs (amiRNAs) are modified endogenous miRNA precursors in which the miRNA: miRNA duplex is replaced with sequences to silence a target gene. amiRNAs are used as new transformation techniques in eukaryotes and have been proven to be more effective in specificity and stability than other RNA-mediated gene silencing methods. amiRNA-based antiviral defense is an effective and new approach to engineer resistance to plant viruses. Here, we summarize the role of miRNAs in resistance to plant viruses.

***Keywords*:** amiRNA, Gene silencing, miRNA, Plant viruses, Resistance

miRNA History

The first report on microRNAs (miRNAs) dates back to 19 years ago when Lee et al., screened the *Caenorhabditis elegans* genes to study the development of its larvae. *lin-4* gene was shown to control the timing of larval development. Further studies indicated that *lin-4* RNA binds to 3' untranslated region of *lin-14* mRNA and blocks its translation. This function of lin-4 is part of the regulatory pathway which triggers a transition from L1 (larval stage 1) to the L2 stage (Lee et al., 1993; Wightman et al., 1993). miRNA genes have been found in mammals, fish, worms, flies, plants and many other eukaryotic organisms (Bartel, 2004).

Pre-miRNA Transcription

miRNA encoding genes are located on non-coding parts of the genome. Plant miRNA genes are gathered together in the form of gene families.

miRNAs are long strands (sometimes even longer than 1000 nucleotides), which are bending on themselves and forming stem-loop structures. They are capped and polyadenylated at 5' and 3' ends, respectively. These features indicate that plant miRNA genes are probably transcribed by RNA Polymerase II (Devers et al., 2011; Tanzer et al., 2008).

miRNA Processing

Plants and animals differ in miRNA synthesis at the post-transcriptional stage. The main step in miRNA maturation process is cleaving the mature miRNA from its precursor. In animals, this is performed by Drosha and Dicer enzymes. Plants have a 'Dicer-like' protein, DCL1, analogous to Dicer and Drosha, that generates the double-stranded miRNA: miRNA (Tanzer et al., 2008; Bazin et al., 2012; Wang et al., 2007). HYPONASTIC LEAVES1 (HYL1) protein also appears to contribute to DCL1 in plants. The HYL1 protein helps DCL1 to recognize cleavage site. The next step in the maturation process of plant miRNAs is methylation of the 3' end of "miRNA: miRNA" double-stranded molecules by HUA ENHANCER1 (HEN1) in the nucleus. Methylation of this molecule prevents its degradation (Kai and Pasquinelli, 2010). After cleaving by DCL1 and methylation by HEN1, "miRNA: miRNA" double strands are transferred from the nucleus into cytoplasm via a Ran-GTP-dependent mechanism, by HASTY (HST), a member of importin β family of nucleocytoplasmic transport receptors (Figure 1) (Jones-Rhoades et al., 2006; Mendes et al., 2009).

RNA-induced Silencing Complex (RISC)

The synthesis stage is the formation of double-stranded "miRNA:miRNA" molecules in the cytoplasm. A helicase breaks the bonds between the two strands of the molecule and separates them. The "guide strand" of a miRNA is incorporated into silencing complex and enables target recognition via complementary base pairing (Wang et al., 2007; Kai

*Corresponding author E-mail: *shahriari.ag@eghlid.ac.ir*

and Pasquinelli, 2010; Jones-Rhoades et al., 2006; Mendes et al., 2009; Hammond et al., 2007). RISC has an affinity for strands with a less stable 5' end. "Passenger strands" are often degraded (Thomas et al., 2010; Winter et al., 2009), although recent findings indicate that some of them may play an important role in regulating gene expression or triggering silencing mechanisms (Fullaondo and Lee, 2012).

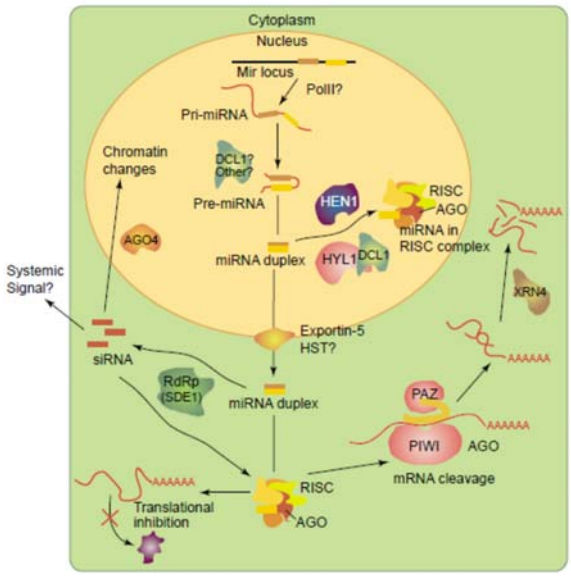

Figure 1. miRNA biogenesis and its regulation mechanisms in plants. Transcription of miRNA by RNA polymerase II produces a pri-miRNA of about 1 kb. This pri-miRNA is cleaved into pre-miRNA by DCL1 and other proteins to yield the fold-back precursor pre-miRNA. Duplex miRNAs are exported to the cytoplasm out of the nucleus by HST (Exportin-5). These proteins process the pre-miRNA to form a miRNA–miRNA duplex, which is loaded on the RISC. The RISC complex is guided by the miRNA to target mRNAs. The cleaved target mRNAs are degraded by XRN4 protein. Secondary small interfering RNAs (siRNAs) are generated from the action of RNA-dependent RNA polymerase (RdRP). The RISC can also cause translational inhibition (Kidner and Martienssen, 2005).

Translation Repression

The RISC-miRNA complex can repress translation of the target RNA in two ways. In animals, miRNAs often repress translation of their target RNAs by an imperfect sequence which is matched with 3' untranslated region (UTR) (Sontheimer and Carthew, 2005). After binding to 3' UTR, miRNAs can prevent translation of mRNAs by interfering with translation initiation factors or disrupting poly(A) tail's function (Gu and Kay, 2010). It has also been shown that RISC may form a stable complex with polyribosomes and prevent translation, even after its initiation and at the elongation phase (Bartel, 2004).

mRNA Degradation

Whether a miRNA represses translation or degrades its target RNA, depends on the degree of complementarity between their sequences (Lu et al., 2008). It has been observed in plants and mammals that a nearly perfect base complementarity between miRNA and its target RNA leads to degradation of the target rather than repressing its translation (Bartel, 2004; Kadotani et al., 2004; Nakayashiki, 2005). A perfect base complementarity appears to be required for effective mRNA cleavage by miRNAs (Wang et al., 2007). MiR-172 has been shown to act as a translation repressor in *Arabidopsis* (Sontheimer and Carthew, 2005). As soon as the target is effectively cleaved, the miRNA molecule is able to cleave other target RNAs or direct them toward mRNA processing bodies to be subsequently degraded (Bartel, 2004).

Transcriptional Gene Silencing

miRNAs turn off genes at transcription level by methylation of chromatin in plants. The effects of the level of sequence complementarity between miRNAs and its target RNA on the degree of RNA methylation is not yet clear (Jones-Rhoades et al., 2006).

RNA silencing mechanism to induce resistance against plant viruses

RNA silencing is a powerful antiviral defense, although viruses have also evolved suppressor proteins to counteract RNA silencing (Tahmasebi and Zangeneh, 2010). Post-transcriptional gene silencing (PTGS) has been developed to induce resistance in plants against viruses. Various constructs have been introduced for enhancing the efficiency of this mechanism (Kavosipour et al., 2012). Hairpins with sense and antisense strands have been used to develop resistance to Barley yellow dwarf virus (BYDV-PAV) in bread wheat (Yasaie et al., 2011). Hairpins of the *b2* gene have also induced resistance to Cucumber mosaic virus (Kavosipour et al., 2012).

RNA interference (RNAi) can be used to degrade the target RNA sequences or prevent their translation through the PTGS process (Kavosipour et al., 2012). Application of RNAi against two subunits of Vacuolar-ATPase enzyme in the insect vector *Peregrinus maidis* showed that targeting vector genes can be a novel strategy for insect control and also for studying the genes involved in controlling

interactions of *Peregrinus maidis* and Maize mosaic virus (Yao et al., 2013). Gene silencing can be used as an effective tool against plant viruses and their vectors.

The role of miRNAs in plants

Plant miRNAs play a role in development, adaptive responses to nutritional stress and biotic and abiotic stresses, metabolism, suppression of plant defenses in order to enable symbiosis with nitrogen-fixing bacteria, nodule formation and symbiosis with rhizo-fungi (Lu et al., 2008; Jones-Rhoades et al., 2006).

miRNAs in antiviral defense

miRNAs have been shown to play an important role in defense against viruses (Lu et al., 2008). In fact, many viruses have the ability to escape the host's RNA silencing pathway. Human adenovirus can stop the synthesis of host miRNAs which would prevent its replication; tissue culture experiments have shown that primate foamy virus type I (PFV-1) can escape RNA silencing mechanism mediated by miR-32 using a silencing suppressor protein known as Tas. miRNA-based defense is not always able to overcome viral attacks (Wang et al., 2007). It has been proposed that plant miRNAs-based RNA silencing plays two main roles in an antiviral defense response: targeting viral RNAs and triggering the biogenesis of siRNA responsible for the antiviral defense.

Antiviral function of endogenous miRNAs has been described in animal systems (Qu and Fang, 2007).

Interaction of viral suppressors and miRNAs in plants

Many viruses encode silencing suppressors which directly interfere with the miRNA pathway. HEN1-dependent methylation of 3'-terminal nucleotides is an important step in the formation of plant miRNAs. Several viral suppressors of RNA silencing (P1/HC-Pro, p21, p19) prevent methylation of miRNAs by HUA ENHANCER1 (HEN1) methyl transferase. The 21 kDa protein p21 of Beet yellows virus, the 19 kDa protein p19 of Tomato bushy stunt virus and P1/HC-Pro silencing suppressor of Turnip mosaic virus all inhibit the miRNA pathway (Yu et al., 2006). Some viral suppressors of RNA silencing inhibit the function of AGO proteins that have a pivotal role in the antiviral RNA silencing (Carbonell and Carrington, 2015). Taken together, viral suppressors of RNA silencing cause major changes in the plant miRNA-mediated gene silencing pathway.

miRNA targets

miRNAs act as molecules to direct the silencing complex toward target mRNAs, and it is necessary to understand the mechanisms by which miRNAs recognize the target RNA and target mRNAs can be predicted for a miRNA sequence (Tanzer et al., 2008). A few interactions between miRNAs and mRNAs have been characterized and confirmed that they are available in 'Tarbase' database. Perfect complementarity between miRNA and its target is not necessary, most miRNA-mRNA pairs form imperfect double strands. miRNA-mRNA double strands are asymmetric, with the bond between 5' end of miRNA and 3' end of the target molecule. The average number of targets per miRNA is low in plants and is often limited only to closely related genes (Tanzer et al., 2008).

Detection and prediction of miRNAs and their target sites

There are numerous methods (e.g. PCR, cloning and sequencing and computer-based predictions) for detecting miRNAs and their targets in various organisms. Most miRNAs have been identified using bioinformatic approaches, homology search against known miRNAs and thermodynamic stability analysis of the stem-loop structures of miRNA precursors.

In closely related species, phylogenetic data can also be used to find conserved sequences in stem-loops. Several software packages including RNAmicro, miralign, miRseeker, miRscan, PicTar and Target Scan are available for detecting miRNAs in genomes of various organisms (Meziere and Enright, 2007). PicTar and Target Scan showed better results for detecting miRNAs in the genome (Thomas et al., 2010).

Trans-acting (ta) siRNAs

miRNAs and trans-acting (ta) siRNAs are generated through different pathways in plants, although both lead to degradation of their target mRNAs. miR173 and miR390 regulate the ta-siRNA precursor processing. The generation of pre-ta-siRNA transcripts is accompanied with the help of miRNAs by RDR6 and Dicer. ta-siRNAs regulate expression of target genes (Allen et al., 2005).

Artificial miRNA

Artificial miRNAs (amiRNAs) are produced using endogenous miRNA precursors in which the mature miRNA region is replaced with the target viral genome (Table 1). This method was first used in animals and then in plants. The precursor can be altered without affecting its normal processing and

Table 1. Plant miRNA precursors and target viral regions for resistance against plant viruses

Plant species	MiRNA backbone	Virus	Target viral region
Arabidopsis thaliana	*Arabidopsis* pre-miR159	TYMV, TUMV	P69, HC-Pro
Nicotiana benthamiana	*Arabidopsis* miR159a, miR167b and miR171a	PPV	P1/HC-Pro
Nicotiana benthamiana	*Arabidopsis* pre-miR171a	CMV	2b
Arabidopsis thaliana	*Arabidopsis* pre-miR159	CMV	3'-UTR
Arabidopsis thaliana, Nicotiana benthamiana	*Arabidopsis* pre-miR159	TuMV	P69
Nicotiana tabacum	*Arabidopsis* miR159a, miR167b, and miR171a	PVY, PVX	HC-Pro, TGBp1/p25 (p25)
Solanum lycopersicum	*Arabidopsis* pre-miR159a	CMV	2a and 2b viral genes, 3'-UTR
Nicotiana benthamiana	*Arabidopsis* pre-miR159a	WSMoV	Conserved motifs of L (replicase) gene
Triticum	Rice miR395	WSMV	Conserved region
Vitis vinifera	*Arabidopsis* pre-miR319a	GFLV	Coat protein (CP)
Nicotiana benthamiana	Cotton pre-miR169a	CLCuBuV	V2
Solanum lycopersicum	*Arabidopsis* premiR319a, Tomato pre-miR319a and pre-miR168a	ToLCV	The middle region of the AV1 (coat protein), the overlapping region of the AV1 and AV2 (pre-coat protein)
Nicotiana benthamiana	*Arabidopsis* pre-miR319a	PVY	CI, NIa, NIb, CP
Zea mays	Maize pre-miR159a	RBSDV	Conserved region
Nicotiana benthamiana	Barley pre-miR171	WDV	Conserved region
Oryza sativa	Rice pre-miR528	RSV, RBSDV	Middle segment, 3' end and 3'-UTR region of the CP gene
Nicotiana benthamiana	*Arabidopsis* pre-miR159a	CBSV, UCBSV	P1, P3, CI, Nib and CP
Nicotiana benthamiana	*Arabidopsis* pre-miR159a	TSWV	N, NSs
Nicotiana benthamiana	Six amiRNAs	PSTVd	Structural domains

TYMV, Turnip yellow mosaic virus (Potyviridae); TuMV, Turnip mosaic virus (Potyviridae); CMV, Cucumber mosaic virus (Bromoviridae); PPV, Plum pox virus (Potyviridae); PVY, Potato virus Y (Potyviridae); PVX, Potato virus X (Alphaflexiviridae); WSMoV, Watermelon silver mottle virus (Bunyaviridae); WSMV, Wheat streak mosaic virus (Potyviridae); GFLV, Grapevine fan leaf virus (Secoviridae); CLCuBuV, Cotton leaf curl Burewala virus (Geminiviridae); WDV, Wheat dwarf virus (Geminiviridae); RSV, Rice stripe virus (unassigned); RBSDV, Rice black streaked dwarf virus (Reoviridae); CBSV, Cassava brown streak virus (Potyviridae); UCBSV, Ugandan cassava brown streak virus (Potyviridae); TSWV, Tomato spotted wilt virus (Bunyaviridae); PSTVd, Potato spindle tuber viroid (Pospiviroidae); ToLCV, Tomato leaf curl virus (Geminiviridae) (Liu et al., 2017).

secondary structure. amiRNAs should not have any sequence complementarity with other parts of the host's genome. Another point is that they should have the minimum hybridization energy with their targets (less than -30 kcal/mole).

A convenient and fast way to design amiRNAs is using the Web miRNA designer service. The 21-nt amiRNA sequence should not have mismatches at nucleotides 10 or 11, as these regions are binding sites of miRNA with its target. Preferably, there should also be no mismatches at 5' end. Some of the precursors including *Arabidopsis* MIR319a, rice MIR528 and *Chlamydomonas* MIR1157 are used to design amiRNAs (Table 1). Constructs with strong promoters (e.g. CaMV 35S) are highly expressed in plants. Overlapping PCR is used for mutagenesis and introduction of the viral sequence into a pRS300 vector harboring miRNA precursor. A 20 bp part of MIR319a is replaced with the 21 bp viral sequence. The pRS300 plasmid is derived from pBluescript. The 21-nt viral sequence is inserted into pRS300 by overlapping PCR method. amiRNA is inserted into the pBI221 vector and then introduced into pCAMBIA 1300 binary vector for cloning and expression of the p35S-miRNA construct. The binary vector is finally transformed into *Agrobacterium tumefaciens* for the production of transgenic plants. Tissue-specific or inducible promoters can also be used to control the expression of amiRNAs. amiRNA-directed degradation of the target is confirmed by RACE-PCR which amplifies degraded segments. Sensitive and resistant plants can be checked using ELISA and PCR methods and symptoms of viral infection (Qu and Fang, 2007; Pérez-Quintero and López, 2010).

amiRNAs-mediated resistance to plant viruses

Plant miRNAs have the potential to trigger antiviral defense, this theory is supported by bioinformatic analyses. Transgenic *Arabidopsis* and tobacco plants with amiRNAs containing sequences from Turnip mosaic virus, Turnip yellow mosaic virus and Cucumber mosaic virus have shown resistance to these viruses. The precursor of grapevine miR166f has been used to produce amiRNAs by replacing 21 nucleotides of Grapevine virus A with 21 nucleotides of the precursor. The viral sequences used in that study were ORF1 (replicase) and ORF5 (RNA silencing suppressor). amiRNAs induced resistance to Grapevine virus A in tobacco (Roumi et al., 2012). amiRNAs could also prevent replication, movement and transmission of the virus. Using viral suppressors of RNA silencing sequences in amiRNAs will therefore enhance plant resistance against viruses (Pérez-Quintero and López, 2010).

Advantages and disadvantages of amiRNAs

Advantages

The amiRNA method can be used to simultaneously silence a group of associated genes or selectively silence a gene in an inducible or tissue-specific manner. amiRNAs have been successfully applied to silence genes in dicotyledons (*Arabidopsis*, tomato and tobacco), monocotyledons (rice), mosses and algae. Precursors from a plant species can be expressed in other plant species and effectively induce gene silencing. amiRNAs have the ability to silence a specific viral sequence. It was shown in a study that the majority of tobacco plants transformed with miR2b showed no abnormal phenotypes; and the plants expressed the highest miR2b indicated no viral symptoms and accumulation of Cucumber mosaic virus. On the contrary, plants with low miR2b levels were highly susceptible. It is speculated that miR2b copies were not sufficient to activate the host's RNA silencing and suppress the viral infection (Qu and Fang, 2007; Pérez-Quintero and López, 2010). Compared to other methods, amiRNA-based silencing shows fewer environmental problems. The size of the transgene is relatively small and the risk of horizontal transfer of viral genes is therefore reduced. Production of new allergens or toxic proteins in transgenic plants is probably less (Pérez-Quintero and López, 2010). amiRNA transgenes are often stable and remain active in the offsprings. amiRNAs have retained their activity up to 6 months and 500 generations in *Chlamydomonas*. Such advantages can make the amiRNAs as the best choice to produce transgenic resistant plants against viruses. amiRNAs can be designed for selectively silencing an allele or a certain form of a gene. The target sequence should be chosen from conserved parts of viral genomes, so that it can induce resistance to various viral strains. miRNA expression level is independent of temperature in *Arabidopsis*, but a number of reports suggest that miR2b expression in tobacco is lower at 15°C than 25°C. The difference between *Arabidopsis* and tobacco may be due to the fact that *Arabidopsis* normally grows at 15°C, whereas this is different for tobacco.

Expression of amiRNAs in plants will probably result in better protection against viral infections (Qu and Fang, 2007; Pérez-Quintero and López, 2010).

Disadvantages

Virus variants with minor differences in the target sequence are difficult to escape this type of silencing mechanism. Viral genomes evolve faster than plant miRNAs and viruses will be able to escape amiRNAs by mutations or deletions in target sequences. This is a barrier to the development of gene therapies for diseases. Point mutagenesis in viral target sequences has been occurred to escape this phenomenon in plant viruses (Plum pox potyvirus and Turnip mosaic virus). amiRNAs from several different sequences of a virus or even from multiple viruses, and preferably using highly conserved sequences might serve as a solution to overcome these problems.

Conclusion

amiRNA is a novel and effective technique to produce transgenic plants. This method can be applied to determine gene function with a very high speed and without the need for large populations or fully sequenced genomes. Advantages of this method include high specificity and lack of recombination with viral genomes (which significantly reduces biosafety risks). Another point is that amiRNA-mediated silencing can be stable at lower temperatures. Research on amiRNAs has also helped the development of other related methods, including ta-siRNA. amiRNAs can also be widely used in plant genetic engineering and provide an efficient mechanism with advantages such as stability, environmental safety and high specificity.

References

1. Allen E., Xie Z., Gustafson A. M. and Carrington J. C. (2005) miRNA -directed

phasing during transacting siRNA biogenesis in plants. Cell 121: 207–221.
2. Bartel D. P. (2004) MiRNA s: Genomics, Biogenesis, Mechanism, and Function. Cell 116: 281-297.
3. Bazin J., Bustos-Sanmamed P., Hartmann C., Lelandais-Brière C. and Crespi M. (2012) Complexity of miRNA-dependent regulation in root symbiosis. Philosophical Transactions of Research Society 367: 1570-1579.
4. Carbonell A. and Carrington J. C. (2015) Antiviral roles of plant ARGONAUTES. Current Opinion in Plant Biology 27: 111-117.
5. Devers E. A., Branscheid A., May P. and Krajinski F. (2011) Stars and Symbiosis: MiRNA - and MiRNA *-Mediated Transcript Cleavage Involved in Arbuscular Mycorrhizal Symbiosis. Plant Physiology 156: 1990-2010.
6. Fullaondo A. and Lee S. Y. (2012) Identification of putative miRNA involved in Drosophila melanogaster immune response. Developmental and Comparative Immunology 36: 267-273.
7. Gu S. and Kay M. A. (2010) How do miRNA mediate translational repression. Silence Journal 1: 1-5.
8. Hammond T. M., Bok J. W., Andrewski M. D., Reyes-Domı´nguez Y., Scazzocchio C. and Keller N. P. (2007) RNA Silencing Gene Truncation in the Filamentous Fungus Aspergillus nidulans. Eukaryotic Cell 7:2, 339-349.
9. Jones-Rhoades M. W., Bartel D. P. and Bartel B. (2006) MiRNA s and Their Regulatory Roles in Plants. Annual Review of Plant Biology 57: 19-53.
10. Kadotani N., Nakayashiki H., Tosa Y. and Mayama S. (2004) One of the Two Dicer-like Proteins in the Filamentous Fungi Magnaporthe oryzae Genome Is Responsible for Hairpin RNA-triggered RNA Silencing and Related Small Interfering RNA Accumulation. The Journal of Biological Chemistry 279: 44467-44474.
11. Kai Z. and Pasquinelli A. E. (2010) MiRNA assassins: factors that regulate the disappearance of miRNAs. Nature Structural and Molecular Biology 17: 5-10.
12. Kavosipour S., Niazi A., Izadpanah K., Afsharifar A. and Yasaie M. (2012) Induction of resistance to cucumber mosaic virus (CMV) using hairpain construct of 2b gene. Iranian Journal of Plant Pathology 48:2, 209-219.
13. Kidner C. A. and Martienssen R. A. (2005) The developmental role of microRNA in plants. Current Opinion in Plant Biology 8(1): 38-44.
14. Lee R. C., Feinbaum R. L. and Ambros V. (1993) The C. elegans Heterochronic Gene lin-4 Encodes Small RNAs with Antisense Complementarity to lin-14. Cell 75: 843-854.
15. Lennefors B. L., Savenkov E. I., Bensefelt J., Wremerth-Weich E., van Roggen P., Tuvesson S., Valkonen J. P. T. and Gielen J. (2006) dsRNA-mediated resistance to Beet Necrotic Yellow Vein Virus infections in sugar beet (Beta vulgaris L. ssp. vulgaris). Molecular breeding 18:4, 313-325.
16. Liu S. R., Zhou J. J., Hu C. G., Wei C. L. and Zhang J. Z. (2017) MicroRNA-mediated gene silencing in plant defense and viral counter-defense. Frontiers in microbiology, 8: 1801.
17. Lu Y., Gan Q., Chi X. and Qin S. (2008) Roles of miRNA in plant defense and virus offense interaction. Plant Cell Reports 27: 1571-1579.
18. Mendes N. D., Freitas, A. T. and Sagot M. F. (2009) Current tools for the identification of miRNA genes and their targets. Nucleic Acids Research 37:8, 2419-2433.
19. Meziere P. and Enright A. J. (2007) Prediction of miRNA targets. Drug Discovery Today 12: 452-457.
20. Nakayashiki H. (2005) RNA silencing in fungi: Mechanisms and applications. FEBS Letters 579: 5950-5957.
21. Pérez-Quintero A. L. and López C. (2010) Artificial miRNA s and their applications in plant molecular biology. Agronomía Colombiana 28: 373-381.
22. Qu J. Y. J. and Fang R. (2007) AmiRNA - Mediated Virus Resistance in Plants. Journal of Virology 81: 6690–6699.
23. Roumi V., Afsharifar A., Saldarelli P., Niazi A., Martelli G. P. and Izadpanah K. (2012) Transient expression of artificial miRNA s confers resistance to Grapevine Virus A in Nicotiana benthamiana. Journal of Plant Pathology 94: 643-649.
24. Sontheimer E. J. and Carthew R. W. (2005) Silence from within: Endogenous siRNAs and miRNAs. Cell 122: 9-12.
25. Tahmasebi A. and Zangeneh M. (2010) Interaction of RNA silencing with plant

viruses in plants. Genetics in the 3rd Millennium 8:3, 2095-2105.
26. Tanzer A., Riester M., Hertel J., Bermudez-Santana C. I., Gorodkin J., Hofacker I. L. and Stadler P. F. (2008) Evolutionary Genomics of miRNA s and Their Relatives. John Wiley and Sons, Inc., 1-35 pp.
27. Thomas M., Lieberman J. and Lal A. (2010) Desperately seeking miRNA targets. Nature Structural and Molecular Biology 17: 1169-1174.
28. Wang Y., Stricker H. M., Gou D. and Liu L. (2007) MiRNA : past and present. Frontiers in Bioscience 12: 2316-2329.
29. Wightman B., Ha I. and Ruvkun G. (1993) Posttranscriptional Regulation of the Heterochronic Gene lin-14 by lin-4 Mediates Temporal Pattern Formation in C. elegans. Cell 75: 855-862.
30. Winter J., Jung S., Keller S., Gregory R. I. and Diederichs S. (2009) Many roads to maturity: micriRNA biogenesis pathways and their regulation. Nature Cell Biology 11: 228-233.
31. Yao J., Rotenberg D., Afsharifar A., Barandoc-Alviar K. and Whitfield A. E. (2013) Development of RNAi methods for Peregrinus maidis, the corn planthopper. PloS one 8:8, e70243.
32. Yasaie M., Afsharifar A., Niazi A., Salehzadeh S. and Izadpanah K. (2011) Induction of resistance to barley yellow dwarf virus in bread wheat using post transcriptional gene silencing (PTGS). Iranian Journal of Plant Pathology 47:1, 67-82.
33. Yu B., Chapman E. J., Yang Z., Carrington J. C. and Chen X. (2006) Transgenically expressed viral RNA silencing suppressors interfere with miRNA methylation in Arabidopsis. FEBS Letters 580: 3117–3120.

Scientific Reports

A Novel Signal Peptide Derived from *Bacillus Licheniformis* α-Amylase Efficiently Targets Recombinant Human Activin A to the Periplasm of *Escherichia coli*

Zahra Hajihassan[1*], Seyed kazem Hosseini[1], Alireza Zomorodipour[2]

[1] *Department of Life Science Engineering, Faculty of New Sciences and Technologies, University of Tehran, Tehran, Iran.*
[2] *Molecular Biotechnology Department, National institute of Genetic Engineering and Biotechnology, Tehran, Iran.*

Received 24 May 2017 Accepted 2 June 2018

Abstract

Human activin A is a member of the transforming growth factor-β superfamily consists of two similar beta subunits. Activin A is expressed by different cells and displays numerous biological activities such as control of neuronal cell proliferation and differentiation, promotion of neuronal survival in the body. Therefore, recombinant production of activin A is beneficial because it can be used to treat many neurodegenerative diseases such as Alzheimer's and Parkinson diseases. In this study *E. coli* as a cheap and fast-growing host was selected to produce recombinant human activin A. As cytoplasmic expression of human activin A with complex structure and disulfide bonds produces inclusion bodies, so periplasmic expression of it can be beneficial. Therefore, we used modified Iranian *B. licheniformis* α-amylase signal peptide as a new signal peptide in order to translocate the recombinant activin A through the inner membrane. In this study human pro-activin A cDNA and signal sequence were cloned in pET21b vector and resulting vector transformed into the two strains of *E. coli* BL21. SDS-PAGE and western blot techniques were used to confirm recombinant activin A expression. Finally, our results indicated that the signal peptide used in this study was effective for secretion of activin A into the periplasmic space of *E. coli*.

***Keywords*:** Activin A, modified α-amylase signal peptide, periplasmic expression

Introduction

Activins are members of the transforming growth factor β (TGF) super family. They are biologically active as dimmers. In mammalians, four isoforms of the activin β-subunit have been identified: βA, βB, βC and βE. Activin A is dimmer of A subunits (βAβA) that are linked together by disulfide bond. (Walton et al., 2012; Weiss and Attisano, 2013). Activin A participates in numerous physiological processes in the body, including cellular differentiation, apoptosis, metabolism, wound repair, maintenance and survival of the neurons, immune response; so, it can be used as a therapeutic agent besides many other growth factors (Chen et al., 2006; Sulyok et al., 2004; Schubert et al., 1990). Because of its extensive biological roles, several mammalian cell line expression systems have been used in order to produce it as a recombinant protein (Cronin et al., 1998; Pangas and Woodruff, 2002). As these systems have several disadvantages, including cost, technical difficulties in maintenance of the transfected cell lines and relatively low yields, some have used other eukaryotic hosts such as *pichia pastoris* in order to produce activins (Papakonstantinou et al., 2009).

Escherichia coli (E. coli) is the most appropriate expression host for expression of many recombinant proteins because it has several advantages such as fast growth, cheap culture media, well-known genetics and many available commercial vectors. Therefore, in this work we used *E. coli* for expression of recombinant human activin A. The oxidative environment of periplasm of *E. coli* is suitable for expression of proteins with disulfide bonds because it contains chaperones and at least four enzymes called Dsb (disulfide bond formation) proteins which are involved in protein folding and disulfide bond formation (Choi and Lee, 2004; Berkmen, 2012). Generally, bacteria use different secretion systems to transport proteins to the periplasm. There are three main pathways for extracting protein from the cytoplasmic space in bacteria, Sec pathway, SRP dependent pathway and Tat pathway. Secretion in each of these pathways depends on the signal peptides, which are mainly located at the N-terminal of the protein (Natale et al., 2008). In this study, we investigated the efficiency

*Corresponding author E-mail: hajihasan@ut.ac.ir

of modified Iranian *Bacillus Licheniformis* α-amylase signal peptide (m.I.B.L.α-amylase signal p) to secrete recombinant human activin A protein into the periplasmic space of *E. coli*. To do this, we cloned the signal sequence and cDNA of pro-activin A into the pET21b (+) expression vector and investigated the expression level.

Materials and Methods

Unless otherwise specified, all reagents were purchased from Merck Company (Germany).

Bacterial strains, culture conditions and recombinant DNA technology

The BL21(DE3) and BL21(DE3) plysS strains were used as the expression hosts and pET21b (+) (Novagene-USA) plasmid was used as expression vector throughout the experiments. The cDNA of human pro-activin A β subunit (Accession No. NM_002192) and Iranian *B. licheniformis* α-amylase signal sequence (Accession No. AY842512) were obtained from NCBI gene bank. In order to increase the hydrophobicity of the signal peptide, one Met codon (ATG) was inserted between bases 39 and 40. The TopPred software was used to survey the hydrophobicity of the modified signal peptide. Then the fusion of modified signal sequence and pro-Activin A cDNA was synthesized by ShineGene company (China) and cloned using NdeI and EcoRI restriction enzymes (Fermentas-USA) into the pET21b (+) vector (Sambrook and Russel, 2001). The resulting vector was individually transformed in *E. coli* host strains using heat shock procedure (Sambrook and Russel, 2001). The bacterial cells were grown in Luria-Bertani (LB) medium supplemented with 100 $\mu g.ml^{-1}$ampicillin at 37°C.

In order to detect the colonies with h-pro-activin A coding sequence, after isolating recombinant clones on selective media, the plasmid DNA from each clone was extracted and analyzed by restriction mapping and sequence analysis. For the purification of plasmid DNA, alkaline lysate method was used (Sambrook and Russel, 2001). Double digestion of purified plasmid using appropriate restriction enzymes was used; in addition, recombinant clones were sequenced to confirm the insertion of the h-pro-activin A gene into the vectors without any base deletion or substitution.

Protein expression; Preparation of cytoplasmic and periplasmic proteins

For gene expression, 1% dilution of an overnight culture of transformants was transferred into fresh LB medium and incubated at 30°C to an OD_{600nm} of 0.6-0.8. Gene expression was induced by addition of 1 mM of isopropyl thio-β-D-galactoside (IPTG) to the bacterial media. The negative control test was carried out with the recombinant strain without adding inducer. The cells were grown for additional 4 hours and harvested by centrifugation at 5000 g. To obtain periplasmic proteins, osmotic shock procedure with some modifications was used (Libby et al., 1987). Cytoplasmic proteins were obtained using urea 8M (Hajihassan et al., 2016).

SDS-PAGE and immunoblot analysis

Proteins were separated by 15% (w/v) sodium dodecyl sulfate polyacrylamide gel electrophoresis (SDS-PAGE) under denaturing and reducing conditions (Laemmli, 1970). For western blotting, the proteins from gel were transferred onto a nitrocellulose membrane (Millipore-USA) (Demaio, 1996) and membrane subsequently was treated with anti-human activin A monoclonal antibody (Abcam-UK; ab89307) with 1:1000 dilution in blocking buffer (PBS; 3% W/V skimmed milk). Peroxidase conjugated anti-mouse IgG (Sigma-USA; A9044) was added as a secondary antibody.

Results and Discussion

Construction of the pET21b::pro-Activin A expression vector

Several working groups produce activin A in eukaryotic hosts such as insect cell lines (Cronin et al., 1998), CHO (Pangas and Woodruff, 2002) and *Pichia pastoris* (Papakonstantinou et al., 2009). In this work two strains of *E. coli* were used in order to produce activin A. As production of complex eukaryotic proteins such as activin A with multiple disulfide bonds in the oxidative environment of the periplasmic space where suitable chaperons are present is beneficial (Berkmen, 2012; Rosano and Ceccarelli, 2014), we produced activin A in the periplasm of *E. coli*. For effective translocation of the protein across plasma membrane, appropriate signal peptide is usually located at the N-terminal of the target protein. In this study with the aim of addressing the recombinant human pro-Activin A in the periplasmic space of *E. coli* a novel signal peptide, Iranian *B. licheniformis* α-amylase signal peptide, was used. Usually, signal peptides contain three general domains: N-terminal domain with a net positive charge, a central hydrophobic region and a C-terminal region with the signal cleavage site. The data revealed that even natural signal peptides differ in production levels, depending on the type of recombinant protein fused to them (Low et al.,

2013). Even more efficient signal peptides need to be developed. As increasing the hydrophobicity of the center region of the signal peptide improve translocation of recombinant protein towards the membrane and into the periplasmic space, in this study a methionine residue was inserted between proline and leucine residues in the I.B.l.α-amylase signal peptide (Sahdev, 2008). Figure 1 shows the coding sequence and amino acid composition of I.B.l.α-amylase signal peptide and m.I.B.l.α-amylase signal peptide in comparison. The inserted Met residue is obvious in the figure.

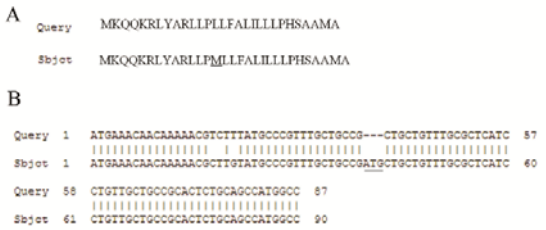

Figure 1. Amino acid composition (A) and sequence (B) of I.B.l.α-amylase signal peptide (Query) and m.I.B.l.α-amylase signal peptide (sbjct) in comparison. One inserted Met (ATG) is underlined. The alignment was done using NCBI BLAST.

After constructing the recombinant plasmid, it was moved into the BL21(DE3) and BL21(DE3) plysS strains of *E.coli* and a number of colonies in each case were isolated from selected media containing antibiotic. Plasmid DNA was isolated from the bacteria and restriction enzyme (RE) analysis was performed in order to release the signal p-pro-activin A insert with the size of 1320 bp (Figure 2). As shown in the figure (lane 2) double digestion with NdeI and EcoRI enzymes results two bands; one corresponds to the signal p-pro-activin A insert and the other corresponds to vector without insert. Also sequencing analysis using T7 terminator primer indicates the complete and correct insertion of the insert into the vector (data not shown here). The confirmed recombinant bacteria were subjected for subsequent expression analysis.

Effects of modified Iranian *B. licheniformis* α-amylase signal peptide on localization of Activin A

Total protein patterns from the bacteria carrying recombinant plasmid after induction with IPTG were analyzed by dot blotting using specific anti-human activin A monoclonal antibody to evaluate the production of rhpro-activin A. The results revealed that proteins obtained from both strains of bacteria were reactive to anti-human activin A antibody; a strong dark color dot indicates reactivity with antibody (Figure 3A). Uninduced bacterial extracts (protein expression without induction with IPTG) in DE3 strain was also reactive to the antibody because of basal transcription (promoter leakage) (Tegel et al., 2011).

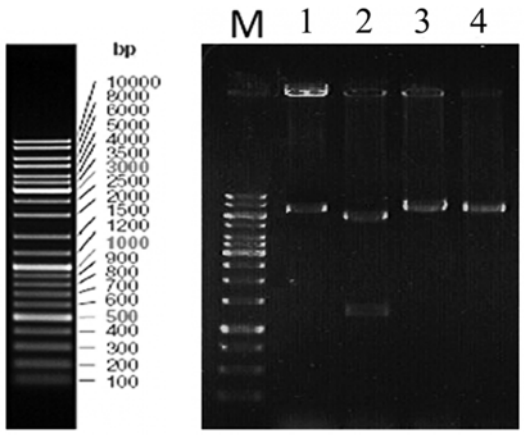

Figure 2. Restriction enzyme analysis of h-activin A construct by agarose gel (1% W/V) electrophoresis. M: DNA Ladder (Fermentas-USA). Lane 1: recombinant pET21b::h-pro-activin A DNA without digestion. Lane 2: digestion of recombinant pET21b::pro-activin A with NdeI and EcoRI restriction enzymes. Lane 3 and 4 are digestion of recombinant pET21b::pro-activin A with NdeI or EcoRI.

To analyze the efficiency of the signal peptide used in this study to secrete the pro-activin A into the periplasmic space, cellular fractionation (cytoplasm and periplasm) was carried out. SDS-PAGE and western blot experiments using anti-human activin A monoclonal antibody were done to analyze the protein patterns (Figure. 3B and C). Comparison of the periplasmic and cytoplasmic protein patterns in Figure 3 showed that both strains of bacteria harboring recombinant vectors secreted detectable amount of pro-activin A in their periplasms. It has to be noted that the two bands revealed in the western blot analysis are considered as processed and unprocessed forms of m.I.B.L.α-amylase signal p-hpro-activin A protein (48 and 45 KDa). Results obtained in this study indicated the periplasmic production of activin A in BL21(DE3) and BL21(DE3) plysS strains of *E. coli*. However western blot results showed that the detectable amount of activin A is yet present in the cytoplasm of *E. coli*; so to improve the secretary efficiency, it is suggested that some other modifications are necessary for developing a better signal peptide.

It is worth noting that the results of this study confirm the results presented by others about the

importance of the role of signal peptides in directing the target protein to the secretary machines in bacteria. Also, the results of this research and the results obtained by others indicated that the signal peptide optimization is usually necessary to achieve a high level of protein secretion (Han et al., 2017; Zamani et al., 2015; Low et al., 2013). There are many studies in this field. For example, Hajihassan and their coworkers showed that for periplasmic secretion of β.NGF in *E. coli*, DsbA signal peptide is the best choice (Hajihassan et al., 2016). In another study, Han and their coworkers used different natural and modified signal peptides to secrete the Alpha toxin$_{H35L}$ in *E. coli*. They showed that some modified signal peptide improved the yield of secreted Alpha toxin$_{H35L}$ by 3.5-fold (Han et al., 2017).

In conclusion, we introduce a novel and effective signal peptide to secrete the recombinant proteins to the periplasmic space of *E. coli*.

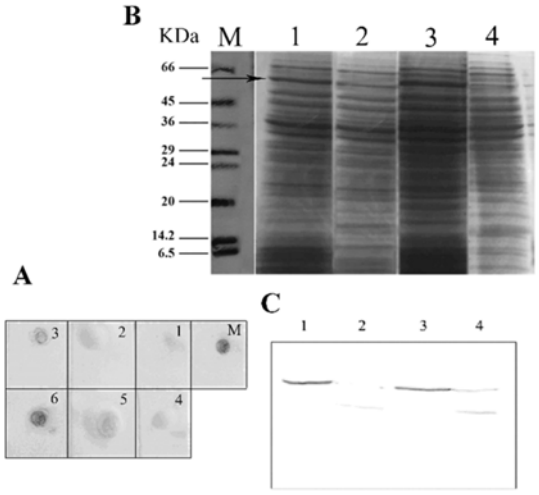

Figure 3. Dot blot assay of total proteins extracted from recombinant bacteria using anti-human activin A monoclonal antibody (A). Dots 1-3 are total proteins extracted from (DE3) plysS bacteria. 1-3 are proteins of bacteria lacking recombinant pET21b plasmid, proteins of bacteria carrying pET21b plasmid but without induction with IPTG, proteins of bacteria carrying pET21b plasmid after 4 h induction with 1 mM of IPTG respectively. Dots 4-6 are total proteins extracted from DE3 bacteria. 4-6 are proteins of bacteria lacking recombinant pET21b plasmid, proteins of bacteria carrying pET21b plasmid but without induction with IPTG, proteins of bacteria carrying pET21b plasmid after 4 h induction with 1 mM of IPTG respectively. M is commercial standard human activin A (Abcam- UK). SDS-PAGE (B) and western blot (C) analysis of the cytoplasmic and periplasmic protein patterns of recombinant bacteria carrying the pET21b::h-activin A plasmid. Lanes 1 and 2 are the cytoplasmic and periplasmic proteins of (DE3) plysS bacteria; lanes 3 and 4 are the cytoplasmic and periplasmic proteins of DE3 bacteria respectively. M shows the protein size marker (Sigma-USA). Recombinant activin A (48 KDa) has been shown with arrow.

Acknowledgements

The authors would like to acknowledge the financial support of University of Tehran and scientific and technological department of presidential office (Iran National Science Foundation) for this research under grant numbers 28669/06/03 and 91000470 respectively.

References

1. Berkmen M. (2012) Production of disulfide-bonded proteins in Escherichia coli. Protein Expr Purif. 82(1): 240-251.
2. Chen YG., Wang Q., Lin SL., Chang CD., Chuang J. and Ying SY. (2006) Activin signaling and its role in regulation of cell proliferation, apoptosis, and carcinogenesis. Exp Biol Med. 231(5): 534-44.
3. Choi JH. and Lee SY. (2004) Secretory and extracellular production of recombinant proteins using Escherichia coli. Appl Microbiol Biotechnol. 64(5): 625-635.
4. Cronin CN., Thompson DA. and Martin F. (1998) Expression of bovine activin-A and inhibin-A in recombinant baculovirus-infected Spodoptera frugiperda Sf 21 insect cells. Int J Biochem Cell Biol. 30(10): 1129-45.
5. Demaio A. (1996) Protein blotting and immunoblotting using nitrocellulose membranes. In protein blotting. Oxford University Press. Oxford. Pp. 11-30.
6. Hajihassan Z., Sohrabi M., Rajabi Bazl M. and Eftekhary HS. (2016) Expression of Human Nerve Growth Factor beta and Bacterial Protein Disulfide Isomerase (DsbA) as a Fusion Protein (DsbA:: hNGF) Significantly Enhances Periplasmic Production of hNGF beta in Escherichia coli. Romanian Biotechnological Letters. 21(5): 11850-11856.
7. Han S., Machhi S., Berge M., Xi G., Linke T. and Schoner R. (2017) Novel signal peptides improve the secretion of recombinant Staphylococcus aureus Alpha toxinH35L in Escherichia coli. AMB Express. 7(1):93.
8. Laemmli UK. (1970) Cleavage of structural proteins during the assembly of the head of bacteriophage T4. Nature. 227 (5259): 680-

685.
9. Libby RT., Braedt G., Kronheim SR., et al. (1987) Expression and purification of native human granulocyte-macrophage colony-stimulating factor from an Escherichia coli secretion vector. DNA. 6(3): 221-229.
10. Low KO., Muhammad Mahadi N. and Md Illias R. (2013) Optimisation of signal peptide for recombinant protein secretion in bacterial hosts. Appl Microbiol Biotechnol. 97(9): 3811-26.
11. Low KO., Muhammad Mahadi N. and Md Illias R. (2013) Optimisation of signal peptide for recombinant protein secretion in bacterial hosts. Appl Microbiol Biotechnol. 97(9): 3811-26.
12. Natale P., Brüser T. and Driessen AJ. (2008) Sec-and Tat-mediated protein secretion across the bacterial cytoplasmic membrane-distinct translocases and mechanisms. Biochim Biophys Acta. 1778(9): 1735-1756.
13. Pangas SA. and Woodruff TK. (2002) Production and purification of recombinant human inhibin and activin. J Endocrinol. 172: 199–210.
14. Papakonstantinou T., Harris SJ., Fredericks D., Harrison C., Wallace EM. and Hearn MT. (2009) Synthesis, purification and bioactivity of recombinant human activin A expressed in the yeast Pichia pastoris. Protein Expr Purif. 64(2): 131-138.
15. Rosano GL. and Ceccarelli EA. (2014) Recombinant protein expression in Escherichia coli: advances and challenges. Front Microbiol. 5: 172.
16. Sahdev S., Khattar SK. and Saini KS. (2008) Production of active eukaryotic proteins through bacterial expression systems: a review of the existing biotechnology strategies. Mol Cell Biochem. 307: 249-264.
17. Sambrook J. and Russel DW. (2001) Molecular cloning: A laboratory manual. 4th edition. New York, USA. Cold spring harbor laboratory press.
18. Schubert D., Kimura H., LaCorbiere M., Vaughan J., Karr D. and Fischer WH. (1990) Activin is a nerve cell survival molecule. Nature. 344: 868-870.
19. Sulyok S., Wankell M., Alzheimer C. and Werner S. (2004) Activin: an important regulator of wound repair, fibrosis, and neuroprotection. Mol Cell Endocrinol. 225(1–2): 127–32.
20. Tegel H., Ottoson J. and Hober S. (2011) Enhancing the protein production levels in Escherichia coli with a strong promoter. The FEBS J. 278 (5): 729-739.
21. Walton KL., Makanji Y. and Harrison CA. (2012) New insights into the mechanisms of activin action and inhibition. Mol Cell Endocrinol. 359(1-2): 2-12.
22. Weiss A. and Attisano L. (2013) The TGFbeta superfamily signaling pathway. Wiley Interdiscip Rev Dev Biol. 2(1):47-63.
23. Zamani M., Nezafat N., Negahdaripour M., Dabbagh F. and Ghasemi Y. (2015) In Silico Evaluation of Different Signal Peptides for the Secretory Production of Human Growth Hormone in E. coli. INT J PEPT RES THER. 21(3): 261-268.

Scientific Reviewers

Ariane Sadr-Nabavi, Ph.D., (Associate Professor of Genetics), Iranian Academic Center for Education, Culture and Research (ACECR)-Mashhad Branch, Mashhad, Iran

Ahmad Sharifi, Ph.D., (Assistant Professor of Agricultural Biotechnology), Iranian Academic Center for Education, Culture and Research (ACECR)-Mashhad Branch, Mashhad, Iran

MANUSCRIPT PREPARATION

Manuscripts should be prepared in accordance with the uniform requirements for Manuscript's Submission to **"Journal of Cell and Molecular Research".**

Language: Papers should be in English (either British or American spelling). The past tense should be used throughout the results description, and the present tense in referring to previously established and generally accepted results. Authors who are unsure of correct English usage should have their manuscript checked by somebody who is proficient in the language; manuscripts that are deficient in this respect may be returned to the author for revision before scientific review.

Typing: Manuscripts must be typewritten in a font size of at least 12 points, double-spaced (including References, Tables and Figure legends) with wide margins (2.5 cm from all sides) on one side of the paper. The beginning of each new paragraph must be clearly indicated by indentation. All pages should be numbered consecutively at the bottom starting with the title page.

Length: The length of research articles should be restricted to ten printed pages. Short communication should not exceed five pages of manuscript, including references, figures and tables. Letters should be 400-500 words having 7-10 references, one figure or table if necessary. Commentaries and news should also be 800-1000 words having 7-10 references and one figure or table if necessary.

Types of Manuscript: JCMR is accepting original research paper, short communication reports, invited reviews, letters to editor, biographies of scientific reviewers, commentaries and news.

Statement of Human and Animal Rights: Author's should declare regulatory statement regarding the experiments using animals, human cells/tissues that all in vivo experiments have been performed according to the guidelines (explained by WHO, international animal rights federations or your respective institute) to use animals in their research work.

Conflict of Interest Statement: Authors or corresponding author should declare statement of conflict of interest at the last of manuscript.

Manuscript Evaluation Time: All submitted manuscripts will be evaluated and reviewed according to following evaluation schedule.
Pre-Editorial Evaluation: All submitted manuscripts, right after their submission to JCMR will be evaluation by Editors for being according to the journal scope and format. This evaluation can take 2-7 days of submission.
Reviewer's Evaluation: Selected manuscripts after pre-editorial evaluation will be sent to minimum two blind reviewers assigned by Editor-in-Chief. This process may take 21-27 days.
Post Editorial Evaluation: After receiving reviewer's comments, editors evaluate the manuscripts considering the comments and decide their first decision. This process takes 3-5 days and then authors are informed regarding the editorial decision.

GENERAL ARRANGEMENT OF PAPERS

Title: In the first page, papers should be headed by a concise and informative title. The title should be followed by the authors' full first names, middle initials and last names and by names and addresses of laboratories where the work was carried out. Identify the affiliations of all authors and their institutions, departments or organization by use of Arabic numbers (1, 2, 3, etc.).

Footnotes: The name and full postal address, telephone, fax and E-mail number of corresponding author should be provided in a footnote.

Abbreviations: The Journal publishes a standard abbreviation list at the front of every issue. These standard abbreviations do not need to be spelled out within paper. However, non-standard and undefined abbreviations used five or more times should be listed in the footnote. Abbreviations should be defined where first mentioned in the text. Do not use abbreviations in the title or in the Abstract. However, they can be used in Figures and Tables with explanation in the Figure legend or in a footnote to the Table.

Abstract: In second page, abstract should follow the title (no authors' name) in structured format of not more than 250 words and must be able to stand independently and should state the Background, Methods, Results and Conclusion. Write the abstract in third person. References should not be cited and abbreviations should be avoided.

Keywords: A list of three to five keywords for indexing should be included at bottom of the abstract. Introduction should contain a description of the problem under investigation and a brief survey of the existing literature on the subject.

Materials and Methods: Sufficient details must be provided to allow the work to be repeated. Correct chemical names should be given and strains of organisms should be specified. Suppliers of materials need only be mentioned if this may affect the results. Use System International (SI) units and symbols.

Results: This section should describe concisely the rationale of the investigation and its outcomes. Data should not be repeated in both a Table and a Figure. Tables and Figures should be selected to illustrate specific points. Do not tabulate or illustrate points that can be adequately and concisely described in the text.

Discussion: This should not simply recapitulate the Results. It should relate results to previous work and interpret them. Combined Results and Discussion sections are encouraged when appropriate.

Acknowledgments: This optional part should include a statement thanking those who assisted substantially with work relevant to the study. Grant support should be included in this section.

References: References should be numbered and written in alphabetical order. Only published, "in press" papers, and books may be cited in the reference list (see the examples below). References to work "in press" must be accompanied by a copy of acceptance letter from the journal. References should not be given to personal communications, unpublished data, manuscripts in preparation, letters, company publications, patents pending, and URLs for websites. Abstracts of papers presented at meetings are not permissible. These references should appear as parenthetical expressions in the text, e.g. (unpublished data). Few example of referencing patterns are given as follows:

Bongso A., Lee E. H. and Brenner S. (2005) Stem cells from bench to bed side. World Scientific Publishing Co. Singapore, 38-55 pp.

Irfan-Maqsood M. (2013) Stem Cells of Epidermis: A Critical Introduction. Journal of Cell and Molecular Research 5(1): 1-2.

Note: All the reference should be in EndNote format (JCMR EndNote Style is available on JCMR's web site, Author's Guideline)

Tables and Figures: Tables and Figures should be numbered (1, 2, 3, etc.) as they appear in the text. Figures

should preferably be the size intended for publication. Tables and Figures should be carefully marked. Legends should be typed single-spaced separately from the figures. Photographs must be originals of high quality. Photocopies are not acceptable. Those wishing to submit color photographs should contact the Editor regarding charges.

Black Page Charges: There is no black page charges for publication in the Journal of Cell and Molecular Research.

Color Page Charges: All color pages being printed in color will cost 1,000,000 Iranian Rials/page.

JCMR Open Access Policy: Journal of Cell and Molecular Research follows the terms outlined by the Creative Common's Attribution-Only license (CC-BY) to be the standard terms for Open Access. Creative Commons License.

Note: All manuscripts submitted to JCMR are tracked by using "Plagiarism Tracker X" for possible plagiarism before acceptance to jcmr

Table of Contents

Evaluating the Effect of Eugenol on the Expression of Genes Involved in the Immunomodulatoty Potency of Mouse Mesenchymal Stem Cells In Vitro 1
Maryam Yazdani, Ali Bidmeshkipour, Sajjad Sisakhtnezhad

Polyurethane/Hydroxyapatite Induces MSCs towards Osteo-like Cells in a Similar Fashion to Demineralized Bone Matrix 11
Mostafa Shahrezaei, Mohamad Moosaee

Global Analysis of Gene Expression and Identification of Modules in Echinacea purpurea Using Systems Biology Approach 18
Ahmad Tahmasebi, Farzaneh Aram, Hassan Pakniyat, Ali Niazi, Elahe Tavakol, Esmaeil Ebrahimie

Investigation of coa Gene Polymorphism in Clinical Isolates of Staphylococcus aureus in North of Iran 27
Mohammad Reza Izadpanah, Leila Asadpour

Desaturase Genes Expression and Fatty Acid Composition of Pleurotus ostreatus in Response to Zinc and Iron 32
Kamran Safavi, Gholamreza Kavoosi, Roghayeh Siahbalaei

MicroRNA-mediated Resistance to Plant Viruses 40
Amir Ghaffar Shahriari, Aminallah Tahmasebi

A Novel Signal Peptide Derived from Bacillus Licheniformis α-Amylase Efficiently Targets Recombinant Human Activin A to the Periplasm of Escherichia coli 47
Zahra Hajihassan, Seyed kazem Hosseini, Alireza Zomorodipour

Journal of Cell and Molecular Research

Volume 10, Number 1, Summer 2018